Phase Behavior Modeling of Asymmetric n-Alkane + Aromatic and Naphthenic Hydrocarbon Mixtures

by

Sourabh Ahitan

A thesis submitted in partial fulfillment of the requirements for the degree of

Master of Science

in

CHEMICAL ENGINEERING

Department of Chemical and Materials Engineering
University of Alberta

© Sourabh Ahitan, 2016

Abstract

Global phase behavior calculations based on 150 n-alkane + aromatic and n-alkane + naphthenic hydrocarbon binary mixtures were performed. These calculations were compared with experimental measurements whenever possible, and additional measurements were made as part of this work. The widely used Peng-Robinson (PR) and Soave-Redlich-Kwong (SRK) equations of state are shown to predict non-physical liquid-liquid phase behavior for long chain n-alkane + aromatic and long chain n-alkane + naphthenic hydrocarbon binary mixtures with standard pure component parameters (T_c, P_c, ω). Incorrect global phase behavior prediction is shown to be insensitive to the selection of correlations for estimating pure component properties for n-alkanes that are not available from experimental data. For cubic equations of state, correct phase behaviors are only obtained if negative binary interaction parameter (k_{ij}) values are used. For PC-SAFT, a non-cubic equation of state (with standard parameter values defining molecules and with binary interaction parameters set to zero), phase behaviors that are consistent with observed phase behaviors are obtained. However, below the melting temperature of at least one of the components, liquid-liquid phase behavior is predicted for some binary mixtures.

At higher temperatures (above the L_1=L_2 critical locus) correct phase behaviors (L, LV, V, L=V) are predicted by both cubic and PC-SAFT equations of state. To assess the quality of liquid/vapor phase equilibrium predictions in the miscible region, bubble pressures and L=V critical loci are evaluated for 13 binary n-alkane + benzene mixtures, including benzene + n-C_{20}, n-C_{24}, n-C_{28} and n-C_{36} binary mixtures for which new experimental bubble pressure data is obtained in this work. Computed bubble pressures for the Peng-Robinson (PR), Soave-Redlich-Kwong (SRK) and Perturbed-

Chain Statistical Associating Fluid Theory (PC-SAFT) equations of state are compared with one another and with experimental measurements. The PC-SAFT EOS, with pure component parameters rescaled to conform with critical temperatures and pressures, and interaction parameter values set to zero, yield accurate bubble pressures and critical loci for all benzene + n-alkane mixtures. By contrast, the PR and SRK EOS require mixture specific k_{ij} values in order to provide quantitative bubble pressure and critical loci estimates, and best-fit k_{ij} values exhibit significant temperature dependence. In the absence of experimental bubble pressures, options for estimating interaction parameters for cubic EOS for binary benzene + n-alkane mixtures, and for aromatic or naphthenic + alkane mixtures more broadly are discussed. While subject to further testing, selection of interaction paramater values for cubic EOS such that computed bubble pressures closely mimic bubble pressures predicted by the scaled PC-SAFT EOS is recommended.

Key words: phase behavior, bubble pressure, binary interaction parameter, prediction, PR, SRK, PC-SAFT, equation of state

Preface

(Mandatory due to collaborative work)

Chapter 3 was published as "Ahitan, S.; Satyro, M. A.; Shaw, J. M. Systematic Misprediction of n-Alkane + Aromatic and Naphthenic Hydrocarbon Phase Behavior Using Common Equations of State. *J. Chem. Eng. Data* **2015***, 60*, 3300-3318." Dr. Marco A. Satyro, a professor in Department of Chemical & Biomolecular Engineering, Clarkson University, Potsdam, New York 13699-5705, United States, was responsible for correlations shown in Figure 3.13 and provided suggestions and comments as the work developed. He also commented on the text. Dr. John M. Shaw was the supervisory author and was involved with concept formulation and manuscript editing. I was responsible for performing experiments, calculations and data compilation, and manuscript preparation.

Chapter 4 has been submitted to Fluid Phase Equilibria as "Ahitan, S.; Shaw, J. M. Quantitative Comparison Between Predicted and Experimental Binary n-Alkane + Benzene Phase Behaviors Using Cubic and PC-SAFT EOS." Dr. John M. Shaw was the supervisory author and was involved with concept formulation and manuscript composition. I was responsible for performing experiments, calculations and data compilation, and manuscript editing.

Acknowledgements

First and foremost, I would like to thank my mentor and supervisor, Dr. John M. Shaw for his continued help and support since the day I landed in Edmonton. More than two years of my masters passed like a breeze working under his guidance. He has a great sense of humor and a unique way of coaching that makes working with him a pleasure. I thank him for being patient with my countless questions, queries and sloppy manuscripts. I have learned a lot while working with him.

I thank Dr. Marco Satyro, for his help and guidance during my project. I would also like to thank Dr. Mohammad Javad Amani for his guidance on the X-ray view cell. He had been a constant source of information (even after his graduation) for all my x-ray view cell related queries. I would also like to express my gratitude to Mildred Becerra, for her help and expertise in the lab, and Linda Kaert, for the administrative support.

I would also like to acknowledge the sponsors of the NSERC Industrial Research Chair in Petroleum Thermodynamics: Natural Sciences and Engineering Research Council of Canada (NSERC), Alberta Innovates - Energy and Environmental Solutions, British Petroleum Canada Energy Corporation, ConocoPhillips Canada Resource Corporation, Nexen Energy ULC, Shell Canada Ltd., Total E&P Canada Ltd., Virtual Materials Group Incorporated.

Lastly, I would like to express my gratitude to my sister, mom and dad for their love and care. They have been a constant source of encouragement and support throughout my life.

Table of Contents

List of Tables

List of Figures

Chapter 1. Introduction

Thermodynamic data play a foundational role in the chemical and petroleum industries, especially in engineering design and operation optimization. For instance, during gas production from a gas-condensate reservoir, retrograde condensation phenomena can sometimes halve well productivity [1]. Such wells typically require expensive and complex well stimulation techniques in order to revive production. Maintaining the reservoir pressure higher than the dew point pressure of the well fluid, is a practical and simple solution for this kind of production problem, but requires phase behavior knowledge for the system ahead of time. This is just one example that demonstrates the importance of phase behavior knowledge for safe and smooth industrial process operation.

There are two ways of assessing phase equilibrium behavior: by experiment, or by implementing appropriate thermodynamic models. While experiments are the most reliable and accurate source of phase behavior information, they are generally time consuming, expensive and sometimes also sample constrained. Furthermore, intrinsic properties of mixtures or compounds can also limit the use of experimental techniques. For example, critical properties of heavy paraffins are hard to measure experimentally due to their thermal instability at higher temperatures. Thermodynamic models are often preferred over experimental approaches. However, models are not always

quantitative. For example, correct phase behaviors but incorrect phase compositions are obtained. Sometimes they provide qualitatively incorrect results, such as liquid instead of vapor behavior. Incorrect or inaccurate phase equilibrium predictions can lead to catastrophic technical failures of process designs and may introduce safety or sub-optimal process performance in the field. Such model shortcomings must be identified, brought to the attention of practitioners, and corrected where possible.

A brief introduction to some of the common thermodynamic models used in the petroleum industry is provided in this chapter. The classification of phase behavior types is also discussed along with common causes of phase behavior misprediction, the focus of this work.

1.1 Thermodynamic Models in the Petroleum Industry

The need for accurate and reliable phase equilibrium prediction has driven the development and modification of thermodynamic models. Better models have helped improve the overall quality of predictions over time, but they have also made model selection for specific applications more challenging for the end user. Selection of a model is dependent on a number of factors such as, type of operation, operating conditions, composition of the mixture, availability of thermophysical properties, the computational demands of the model, and desired accuracy of predictions. For example, models such as NRTL [2] and UNIQUAC [3] are generally preferred over Peng-Robinson [4] or PSRK [5] for polar mixtures when the operating pressure is less than 10 bar, while the latter are preferred at higher pressures and for non-polar components.

Selection of thermodynamic models in the petroleum industry is driven by the availability of thermodynamic properties more than any other factor. The physical

property data for crude oils is generally limited to boiling point curves and thus only average physical properties of pseudocomponents (representative components) are available as inputs for models.

1.1.1 Cubic Equations of State

Cubic equations of state are by far the most commonly used thermodynamic models in the petroleum industry. They build on the early work of van der Waals (vdW) [6], with subsequent contributions from Redlich-Kwong (RK) [7], Soave-Redlich-Kwong (SRK) [8] and Peng-Robinson (PR) [4] over the succeeding century. The SRK and PR EOS are heavily used due to their long history for successful application, and their simplicity. Parameters appearing in them are typically calculated using the critical properties and acentric factor of pure compounds. Mathematical expressions for some of the cubic EOS are shown in their simplest form in Table 1.1.

Table 1.1 Mathematical expressions for some cubic equations of state.

EOS	Equation
van der Waals	$P = \frac{RT}{v-b} - \frac{a}{v^2}$
Redlich-Kwong	$P = \frac{RT}{v-b} - \frac{a}{v(v+b)\sqrt{T}}$
Soave-Redlich-Kwong	$P = \frac{RT}{v-b} - \frac{a(T)}{v(v+b)}$
Peng-Robinson	$P = \frac{RT}{v-b} - \frac{a(T)}{v(v+b)+b(v-b)}$

The equations shown in Table 1.1 are for pure substances only. Mixing rules need to be used in order to extend these models to mixtures. A large number of universal and equation of state specific mixing rules are present in the literature. Some common

examples include the van der Waals (vdW), Huron-Vidal [9], linear combination of Vidal and Michelsen (LCVM) [10], modified Huron–Vidal second order (MHV2) [11], predictive Soave–Redlich–Kwong (PSRK) [5] and Wong-Sandler (WS) [12] mixing rules. Like thermodynamic models, the selection of mixing rules also depends on a number of factors. The van der Waals (vdW1) mixing rule, equations 1.1 and 1.2, is the most widely used mixing rule in the petroleum industry. In addition to composition (z_i) and pure component parameters (a_i, b_i), the mixing rule also requires binary interaction parameter (k_{ij}) between components *i* and *j*.

$$a = \sum_{i=1}^{N}\sum_{j=1}^{N} z_i z_j \sqrt{a_i a_j}\left(1 - k_{ij}\right) \qquad k_{ij} = k_{ji}\,; \quad k_{ii} = 0 \tag{1.1}$$

$$b = \sum_{i=1}^{N} z_i b_i \tag{1.2}$$

$$k_{ij} = 1 - \left[\frac{2(T_{C_i} T_{C_j})^{0.5}}{(T_{C_i} + T_{C_j})}\right]^{\left(\frac{Z_{C_i} + Z_{C_j}}{2}\right)} \tag{1.3}$$

The value of k_{ij} is generally fitted to experimental phase equilibrium data in order to improve the accuracy of predictions by the EOS and therefore it is equation of state specific. The k_{ij} for non-polar mixtures is typically close to zero and therefore it is often assumed to be zero for hydrocarbon mixtures. While for polar and asymmetric mixtures, non-zero values might be required in order to obtain accurate predictions. Numerous correlations have been developed to estimate k_{ij} values in the absence of experimental data. Correlations use pure component thermophysical properties or sometimes they are based on group contribution theory. A correlation developed by

Gao et al. [13] (equation 1.3) is an example of a correlation based on pure component thermophysical properties for binary hydrocarbon mixtures, in this case on pure component critical temperature and compressibility.

1.1.2 More Advanced Models: Statistical Associating Fluid Theory (SAFT)

Statistical Associating Fluid Theory (SAFT) EOS [14,15] comprises a relatively complex family of EOS that are more advanced than the cubic family of EOS. They are based on Wertheim's first-order perturbation theory [16-19]. The underlying notion of a fluid in SAFT is presented schematically in Figure 1.1. SAFT assumes a fluid is constituted of hard spheres. Dispersive forces (such as covalent bonds) between the hard spheres cause them to form segments. The segments as collective entities interact with other segments via association forces (such as hydrogen bonds). All these assumptions contribute to the residual Helmholtz energy and are reflected by their respective terms in residual Helmholtz energy (a^{res}) expression, shown in equation 1.4.

$$\frac{a^{\text{res}}}{RT} = \frac{a^{\text{hs}}}{RT} + \frac{a^{\text{disp}}}{RT} + \frac{a^{\text{chain}}}{RT} + \frac{a^{\text{assoc}}}{RT} \tag{1.4}$$

where, a^{hs} is the contribution from hard spheres, a^{disp} is the contribution from dispersion forces, a^{chain} is the contribution from chain (segment) formation and a^{assoc} is the contribution from association. Five pure component parameters are required for the SAFT EOS, when used for associating fluids: the segment number, the segment diameter, the segment energy parameter, the association volume and the association energy. These parameters except for association volume and association energy are generally estimated using experimental data for pure compounds, typically vapor pressures, and liquid densities. Estimation of association parameters is not very straightforward. They may need to be estimated from molecular orbital calculations or experimental values of the enthalpy and entropy of hydrogen bonding.

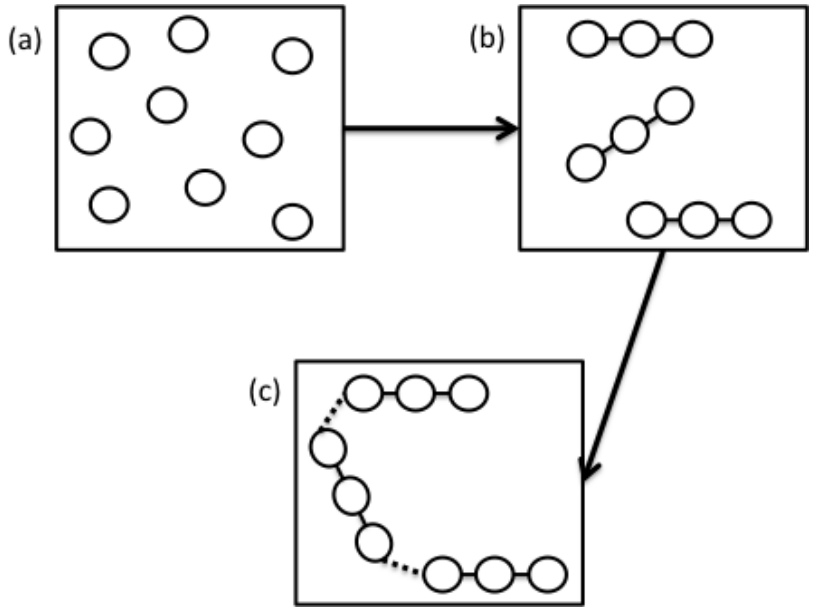

Figure 1.1 Schematic showing the underlying notion of a fluid in SAFT.

Computational advances and demand for better thermodynamic models to create new processes or for making existing processes more efficient, has motivated refinement and development of a host of SAFT EOS. Simplified SAFT [20], Lennard-Jones-SAFT (LJ-SAFT) [21], SAFT for variable range (SAFT-VR) [22], soft SAFT [23], perturbed chain-SAFT (PC-SAFT) [24] and simplified PC-SAFT [25] are some common variants. Like Cubic EOS, SAFT models also require mixing rules in order to be used for mixtures. van der Waals one-fluid mixing rule is commonly used to calculate parameters for mixtures. PC-SAFT, by Gross and Sadowski [24] has become one of the most promising SAFT models during the past decade. In addition to polar mixtures, PC-SAFT accurately represents asymmetric hydrocarbon mixtures, including mixtures of interest to the petroleum industry.

1.2 Phase Behavior Type Classification

Most thermodynamic models predict the six types of binary phase behaviors observed experimentally as per the van Konynenburg and Scott classification scheme [26]. van der

Waals model does not predict all six but other cubic EOS do. Some, drawn from the SAFT family of EOS predict additional non-physical phase behaviors [27]. Figure 1.2 illustrates PT projections for the six experimentally observed types of binary phase behavior. In Type I, there is a continuous liquid-vapor critical locus connecting the critical points of pure components in the P-T projection. Type II is similar to Type I. In addition to the critical locus joining the critical points of pure components, it has a liquid-liquid-vapor (LLV) line that ends at Upper Critical End Point (UCEP), at temperatures below the critical temperature of more volatile component. A liquid-liquid (LL) critical locus is also present that originates from UCEP and extends to high pressures. For some binary mixtures, the LL immiscibility zone overlaps the P-T-x region where solids are dominant and the discrimination of Type I and Type II phase behaviour is ambiguous from an experimental perspective.

Type III exhibits liquid-vapor (LV) critical locus; one is between the critical point of more volatile component and an UCEP, and the other starts at the critical point of the less volatile component extending to high pressures. Type IV is characterized by a gap in immiscibility. The lower LLV curve ends at an UCEP, remote from the critical temperature of the more volatile component, similar to that in Type II, and the upper LLV curve starts at a higher temperature - a Lower Critical End Point (LCEP), extending up to a second UCEP. A liquid-vapor critical locus originates from critical point of the more volatile and less volatile component to end at a UCEP and an LCEP of the second LLV line, respectively. Type V phase behavior is similar to Type IV, in the critical region but the components are miscible at lower temperatures. For Type VI phase behavior, the LV critical locus connects the critical points of the two components, like in Type I and there is an immiscible region, which is depicted by an

LLV coexistence curve confined by LCEP and UCEP points connected by a LL critical curve at lower temperatures.

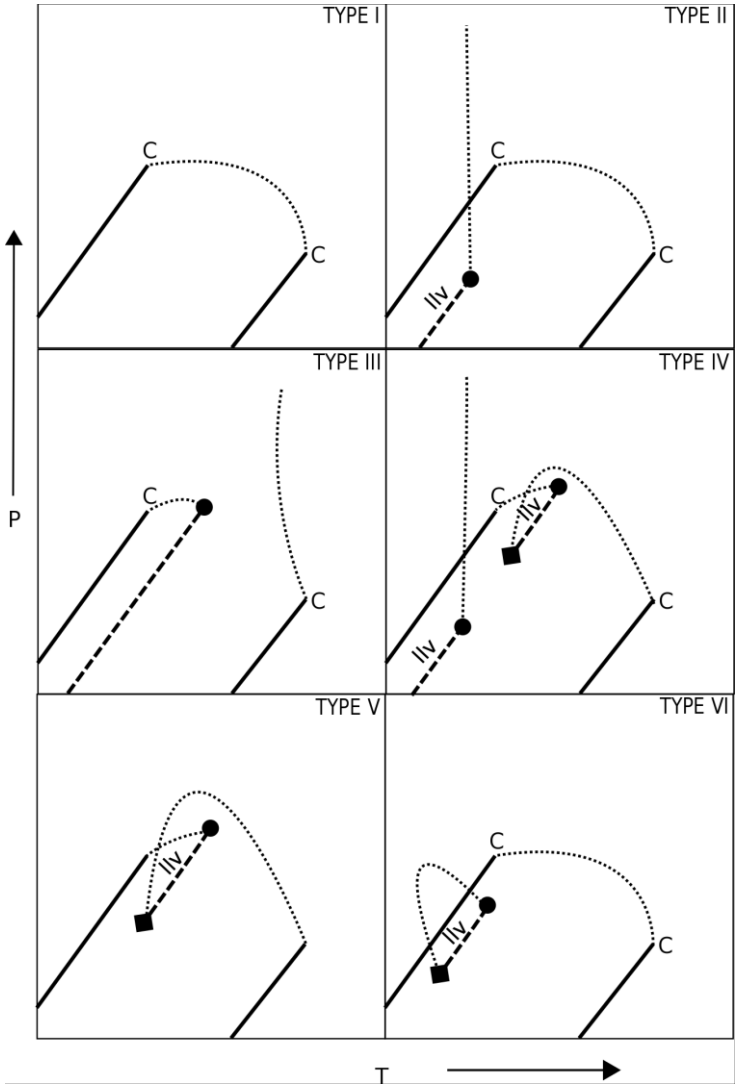

Figure 1.2 Pressure-temperature projections of the six binary phase behavior types, based on the van Konynenburg and Scott classification scheme [26]: (a) Type I, (b) Type II, (c) Type III, (d) Type IV, (e) Type V and (f) Type VI. (—) pure component vapor pressure curve, (·····) critical line, (– – –) liquid-liquid-vapor line, (■) lower critical end point, (●) upper critical end point.

1.3 Reliability of Thermodynamic Models

The focus of this study is the correctness of the number and to a lesser extent the composition of phases predicted by equations of state. A phase equilibrium calculation example for a binary mixture, shown in Figure 1.3, is illustrative. In this example, known amounts of compounds 1 and 2 are mixed, and allowed to reach

equilibrium in an isolated system at a temperature, T, and pressure, P. The unknowns that need to be calculated are: the number of phases and the state of each phase (vapor, liquid) and the phase compositions. These computed outcomes must agree with data at the same set of conditions and are building blocks for the identification of the global phase behavior type, Figure 1.2, exhibited by all possible compositions of the two components over broad ranges of temperature and pressure. Equation of state models may provide accurate representations of phase equilibria locally, while misrepresenting the phase behavior type as a whole due to phase behavior mismatches with experimental data elsewhere in the phase diagram. As derivatives of EOS models are also used for computing thermodynamic properties such as compressibility [28] and heat capacity [29], incorrect values for these properties are also obtained.

Mispredictions by common thermodynamic models are rare but arise because of: inaccurate input data, such as the critical properties of large molecules; errors arising during numerical processing, local rather than global minima in Gibbs free energy are identified [30]; and inherent shortcomings in the models, noted above.

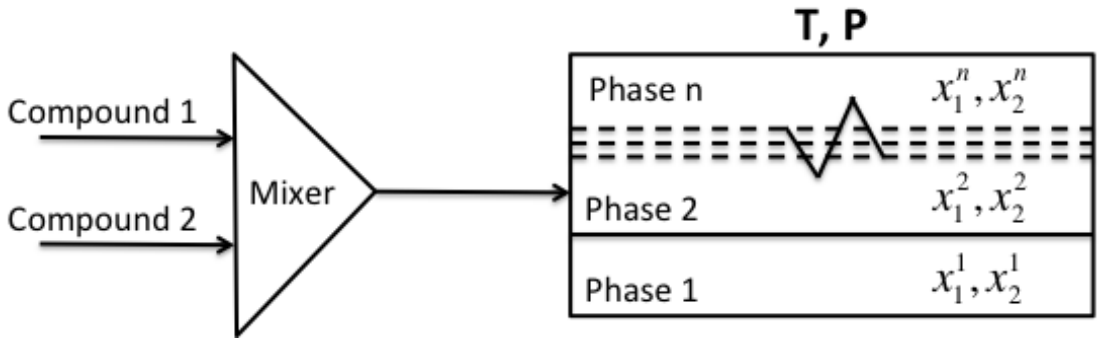

Figure 1.3 Schematic of a representative binary mixture at equilibrium.

1.3.1 Uncertainty in Thermophysical Data and Interaction Parameter

Input data required for selection and thermodynamic models include, but are not limited to the nature of mixture (polar/non-polar etc.), pure component

properties/parameters and interaction parameters. Although, experimental data (which have associated uncertainties) or parameters fitted to experimental data are available for a large number of compounds and mixtures, it is impractical to perform experiments with all possible mixtures. Often, there are no experimental data pertaining to mixtures and/or compounds of interest. In these cases, values for input parameters are interpolated or extrapolated using empirical or theoretical correlations. Extrapolation, in particular, adds significant uncertainty to computed outcomes [31]. Quantitative deviation from experiment is expected. Qualitative deviation, i.e., misprediction of phase behavior type, is less common.

1.3.2 Numerical Processing of Thermodynamic Models

At equilibrium, Gibbs free energy is minimized, and the chemical potential of individual species in each phase is the same. These calculations are complex and are solved numerically. In order to minimize computation time, the numeric solution techniques employ shortcuts that can yield, for example, local rather than global minima for Gibbs free energy. Wrong phase compositions and/or numbers of phases and phase compositions are then obtained. Rigorous global search techniques are not used in commercial and most academic codes, but improved local search techniques help avert these types of errors.

1.3.3 Shortcomings in Thermodynamic Models

Sometimes, incorrect phase behavior predictions are obtained in the absence of any numerical errors and in spite of using accurate thermophysical property values. Such mispredictions are caused due to inherent limitations of the thermodynamic models. For example, cubic EOS models, which are popular for their simplicity, do not account explicitly for intermolecular association, hydrogen bonding, molecular shape

and size etc. and therefore lack the ability to differentiate between isomers or compounds having similar critical properties but are qualitatively different.

1.4 Summary

Thermodynamic modeling of phase equilibrium is central to Chemical Engineering. Equations of state, especially PR, SRK and the more recent PC-SAFT EOS have proven to be excellent tools to model phase equilibrium of petroleum fluids comprising of n-alkanes, aromatics and naphthenes. However, models are not always perfect. These equations of state are also prone to pitfalls that can prove disastrous. Yet, the consequences can be circumvented if practitioners are aware of vulnerable areas. Moreover, knowledge of such shortcomings helps in developing better and more efficient models. Therefore, highlighting such inadequacies in commonly used equations of state, which is one of the objective of this work, is very important.

1.5 Nomenclature

a temperature dependent function of the equation of state

b covolume

EOS equation of state

ε/k segment energy parameter

k_{ij} binary interaction parameter

L liquid

LCEP Lower Critical End Point

LL liquid-liquid

LV liquid-vapor

LLV liquid-liquid-vapor

n-C_n n-alkane with n number of carbon atoms

ω	acentric factor
P	pressure
P_c	critical pressure
R	gas constant
T_c	critical temperature
UCEP	upper critical end point
V	vapor
v	molar volume
Z_C	critical compressibility

1.6 References

(1) Afidick, D.; Kaczorowski, N. J.; Bette, S. In Production performance of a retrograde gas reservoir: a case study of the Arun Field; SPE - Asia Pacific Oil & Gas Conference; Society of Petroleum Engineers: Melbourne, Australia, **1994**.

(2) Renon, H.; Prausnitz, J. M. Local compositions in thermodynamic excess functions for liquid mixtures. *AIChE J*. **1968**, 14, 135-144.

(3) Abrams, D. S.; Prausnitz, J. M. Statistical thermodynamics of liquid mixtures: a new expression for the excess Gibbs energy of partly or completely miscible systems. *AIChE J*. **1975**, 21, 116-128.

(4) Peng, D. -Y; Robinson, D. B. A new two-constant equation of state. *Ind. Eng. Chem. Fundament*. **1976**, 15, 59-64.

(5) Holderbaum, T.; Gmehling, J. PSRK: A group contribution equation of state based on UNIFAC. *Fluid Phase Equilib*. **1991**, 70, 251-265.

(6) J.D. van der Waals On the continuity of the gaseous and liquid State. Ph.D. Thesis, University of Leiden, The Netherlands, 1873.

(7) Redlich, O.; Kwong, J. N. S. On the thermodynamics of solutions. V: An equation of state. Fugacities of gaseous solutions. *Chem. Rev*. **1949**, 44, 233-244.

(8) Soave, G. Equilibrium constants from a modified Redlich-Kwong equation of state. *Chem. Eng. Sci*. **1972**, 27, 1197-1203.

(9) Huron, M.; Vidal, J. New mixing rules in simple equations of state for representing vapour-liquid equilibria of strongly non-ideal mixtures. *Fluid Phase Equilib*. **1979**, 3, 255-271.

(10) Boukouvalas, C.; Spiliotis, N.; Coutsikos, P.; Tzouvaras, N.; Tassios, D. Prediction of vapor-liquid equilibrium with the LCVM model: a linear combination of the Vidal and Michelsen mixing rules coupled with the original UNIFAC and the t-mPR equation of state. *Fluid Phase Equilib*. **1994**, 92, 75-106.

(11) Dahl, S.; Michelsen, M. L. High-pressure vapor-liquid equilibrium with a UNIFAC-based equation of state. *AIChE J*. **1990**, 36, 1829-1836.

(12) Wong, D. S. H.; Orbey, H.; Sandler, S. I. Equation of state mixing rule for nonideal mixtures using available activity coefficient model parameters and that allows extrapolation over large ranges of temperature and pressure. *Ind. Eng. Chem. Res*. **1992**, 31, 2033-2039.

(13) Gao, G.; Daridon, J.; Saint-Guirons, H.; Xans, P.; Montel, F. A simple correlation to evaluate binary interaction parameters of the Peng-Robinson equation of state: binary light hydrocarbon systems. *Fluid Phase Equilib.* **1992**, 74, 85-93.

(14) Chapman, W. G.; Gubbins, K. E.; Jackson, G.; Radosz, M. SAFT: Equation-of-state solution model for associating fluids. *Fluid Phase Equilib.* **1989**, 52, 31-38.

(15) Chapman, W. G.; Gubbins, K. E.; Jackson, G.; Radosz, M. New reference equation of state for associating liquids. *Ind. Eng. Chem. Res*. **1990**, 29, 1709-1721.

(16) Wertheim, M. S. Fluids with highly directional attractive forces. I. Statistical thermodynamics. *J. Stat. Phys*. **1984**, 35, 19-34.

(17) Wertheim, M. S. Fluids with highly directional attractive forces. II. Thermodynamic perturbation theory and integral equations. *J. Stat. Phys*. **1984**, 35, 35-47.

(18) Wertheim, M. S. Fluids with highly directional attractive forces. III. Multiple attraction sites. *J. Stat. Phys*. **1986**, 42, 459-476.

(19) Wertheim, M. S. Fluids with highly directional attractive forces. IV. Equilibrium polymerization. *J. Stat. Phys*. **1986**, 42, 477-492.

(20) Fu, Y. H.; Sandler, S. I. A simplified SAFT equation of state for associating compounds and mixtures. *Ind. Eng. Chem. Res*. **1995**, 34, 1897-1909.

(21) Kraska, T.; Gubbins, K. E. Phase equilibria calculations with a modified SAFT equation of state. 1. Pure alkanes, alkanols, and water. *Ind. Eng. Chem. Res*. **1996**, 35, 4727-4737.

(22) Gil-Villegas, A.; Galindo, A.; Whitehead, P. J.; Mills, S. J.; Jackson, G.; Burgess, A. N. Statistical associating fluid theory for chain molecules with attractive potentials of variable range. *J. Chem. Phys*. **1996**, 106, 4168-4186.

(23) Blas, F. J.; Vega, L. F. Thermodynamic behaviour of homonuclear and heteronuclear Lennard-Jones chains with association sites from simulation and theory. *Mol. Phys*. **1997**, 92, 135-150.

(24) Gross, J.; Sadowski, G. Perturbed-chain SAFT: An equation of state based on a perturbation theory for chain molecules. *Ind. Eng. Chem*. Res. **2001**, 40, 1244-1260.

(25) Von Solms, N.; Michelsen, M. L.; Kontogeorgis, G. M. Computational and physical performance of a modified PC-SAFT equation of state for highly asymmetric and associating mixtures. *Ind. Eng. Chem. Res*. **2003**, 42, 1098-1105.

(26) Konynenburg, v., P. H.; Scott, R. L. Critical lines and phase-equilibria in binary van der Waals mixtures. *Philos. Trans. R. Soc*. **1980**, 298, 495-540.

(27) Privat, R.; Conte, E.; Jaubert, J.; Gani, R. Are safe results obtained when SAFT equations are applied to ordinary chemicals? Part 2: Study of solid–liquid equilibria in binary systems. *Fluid Phase Equilib*. **2012**, 318, 61-76.

(28) Cañas-Marín, W. A.; Ortiz-Arango, J. D.; Guerrero-Aconcha, U. E.; Soto-Tavera, C. P. Thermodynamic derivative properties and densities for hyperbaric gas condensates: SRK equation of state predictions versus Monte Carlo data. *Fluid Phase Equilib*. **2007**, 253, 147-154.

(29) Dadgostar, N.; Shaw, J. M. On the use of departure function correlations for hydrocarbon isobaric liquid phase heat capacity calculation. *Fluid Phase Equilib*. **2015**, 385, 182-195.

(30) Saber, N.; Shaw, J. M. Rapid and robust phase behaviour stability analysis using global optimization. *Fluid Phase Equilib*. **2008**, 264, 137-146.

(31) Hajipour, S.; Satyro, M. A. Uncertainty analysis applied to thermodynamic models and process design – 1. Pure components. *Fluid Phase Equilib*. **2011**, 307, 78-94.

Chapter 2. Literature Review: Phase behavior of Binary Mixtures comprising Paraffins, Aromatics and Naphthenes

2.1 Introduction

Phase behavior predictions for a large number of binary and multicomponent mixtures comprising paraffins, aromatics and naphthenes have been studied and compared to their experimental analogues in the past due to their industrial and academic importance. Most of the studies compare the performance of equations of state, using different mixing rules, demonstrating the accuracy offered by specific thermodynamic models for specific families of mixtures. Examples where thermodynamic models fail to predict the phase behavior of simple and well-defined mixtures are also reported. Case studies, where phase behavior of the mixtures is inadequately or incorrectly represented by common equations of state, are important as they not only alert practitioners to categories of mixtures where extra care must be taken while modeling, but they also help researchers to develop and test models more rigorously.

2.2 The Importance of Aliphatic, Aromatic and Naphthenic Compounds in the Characterization of Crude Oil

Petroleum fluids are mainly composed of aliphatic, aromatic and naphthenic hydrocarbon compounds. Crude oils are immensely complex mixtures of molecules drawn primarily from these families of compounds[1-4]. Despite recent advances in analytical techniques such as FT-ICR MS that permit identification of literally millions of molecular species, quantitation has remained elusive[5-10]. Figure 2.1 from

Boduszynski and Altgelt[11] provides some idea about the diversity of molecules that are present in boiling cuts of crude oils. Reservoir fluid thermodynamic models are currently restricted to ten or fewer molecular constituents due to computational loads. Refinery fluid models may have up to only 100 or more molecular constituents[12] that link to oil valuation and separation/reaction leading to the preparation of specific products with defined characteristics. Consequently, lumping is used to characterize hydrocarbon mixtures. Pseudocomponents are based on boiling cuts (in conventional refinery models), but can also be chosen using individual compounds to represent specific regions in Figure 2.1, such that the mass balances, carbon types, density and other available properties of a fluid are respected. These artificial components represent the collective properties of groups of compounds with similar boiling points or having properties resembling those of molecules belonging to paraffin, aromatic or naphthenic hydrocarbon families. The information required to define pseudocomponents generally comes from oil assays, such as True Boiling Point (TBP) or Simulated Distillation (SIMDIST) curves. The number of pseudo components in thermodynamic models depends on the complexity of the application and the available data. For a more detailed discussion concerning this emerging topic, see Shaw et al. [13]

Proper selection of physical property values for pseudocomponents is crucial[14]. Otherwise the pseudocomponent approach generates unreliable results[15]. Characterization of mixtures using molecules is sometimes referred to as the Substitute Mixtures of Real Components (SMRCs) [16-18] approach. In this method, the "substitute mixture" comprises molecules drawn mainly from the aliphatic, aromatic and naphthenic families of compounds. The obvious advantage of this method is the

availability of physical properties of molecules in databases. This advantage, over the boiling cut approach, is limited to low boiling range components only because in high-boiling petroleum fractions the diversity of constituents is much greater and their properties are less well defined. For example, the critical properties of n-alkanes larger than n-C_{20} cannot be measured experimentally[19].

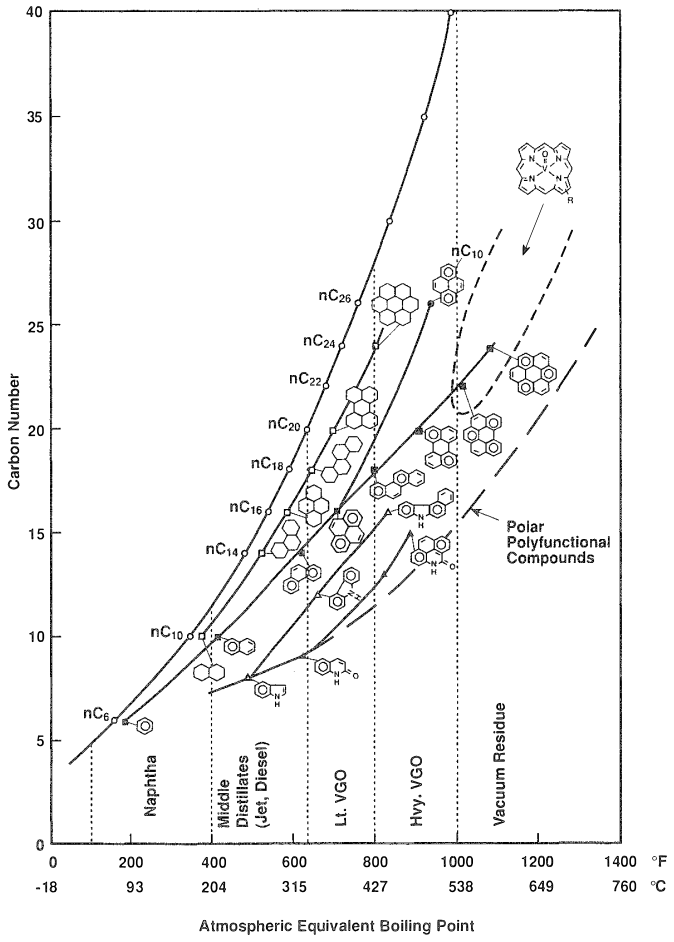

Figure 2.1 A graphic from Boduszynski and Altgelt [11] showing common hydrocarbon molecules of various families, present in different boiling cuts of crude oils.

Phase behavior knowledge of mixtures containing aliphatic, aromatic and naphthenic compounds is of great importance to industry, especially the petroleum and petrochemical industries. While common equations of state, such as the PR, SRK and PC-SAFT EOS typically provide excellent results, illustrations of phase behavior misprediction and insights into the root causes of phase behavior misprediction

comprise the balance of this chapter and set the stage for the specific experimental and computational foci of the thesis.

2.3 Phase behavior of Binary Mixtures of Paraffins, Aromatics and Naphthenes

2.3.1 n-Alkane + n-Alkane Mixtures

Compounds of same group have similar chemical nature. Their mixtures are generally not expected to show complex phase behavior. However, the size ratio of the two components in a binary mixture is a crucial deciding factor for fluid phase equilibria. For the n-alkane family, smaller members of the group, such as methane, ethane and propane are not fully miscible with larger members of the family, as shown in Figure 2.2 [20]. For example, Davenport and Rowlinson[21] first found hexane to be the lightest n-alkane that shows liquid-liquid partial miscibility with methane, exhibiting Type V phase behavior[22]. A number of cubic equations of state[23,24] are shown to successfully reproduce the experimental phase behavior of this mixture with zero values for interaction parameters. However, for the miscible methane + n-pentane mixture, PR and SRK incorrectly predict[25,26] the same Type V phase behavior for a range of binary interaction parameter. Moreover, most cubic EOS show Type V phase behaviour[23] for methane + heptane too, which exhibits Type III phase behavior experimentally[27]. The SAFT EOS correctly predicts phase behavior types for mixtures of methane with both pentane and hexane[28,29]. For mixtures of ethane + n-alkanes larger than n-C_{18}, Type V phase behavior is expected based on experimental results[30-36]. Cismondi et al. [37] showed that the PR EOS predicts Type III phase behavior for binary mixtures of n-alkanes with n-C_{28} and n-C_{36}. Saber and Shaw[38] showed, for mixtures of eicosane with ethane, how addition of a third component (methane) that is immiscible in both components can further complicate the phase behavior and lead to

incorrect phase behaviour type predictions. The asymmetry in size of components not only affects the topology of the predicted phase behavior, but may also impact quantitative phase behavior predictions. Extra attention is required while modeling such mixtures, as shown in recently published papers by Cismondi et al. [37,39] on phase behavior of various asymmetric n-alkane mixtures. Despite its importance, the complexity of the phase behavior of n-alkane mixtures is not broadly appreciated.

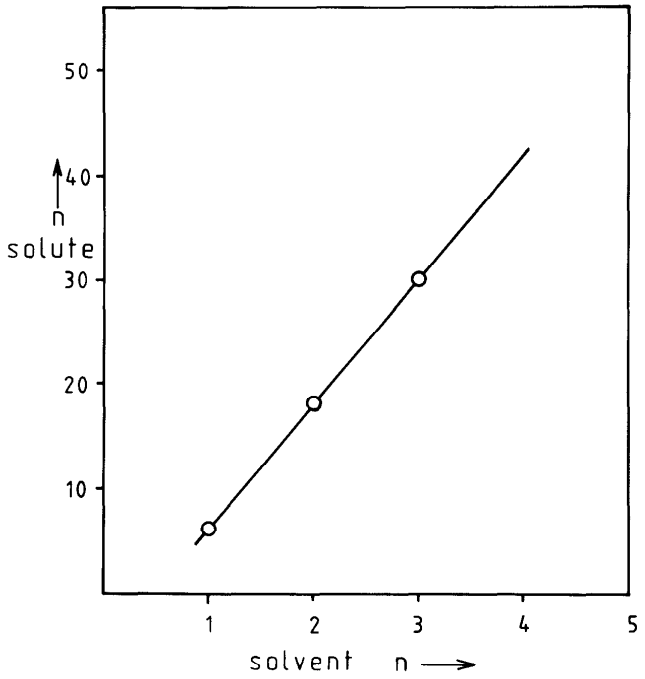

Figure 2.2 First occurrence of LL complex phase behavior in n-alkane + n-alkane binary mixtures, where n represents the carbon number. Graphic reproduced from Peters et al.[20]

2.3.2 n-Alkane-Alkanol mixtures

Ethane + ethanol exhibits Type V phase behavior[40,41] experimentally. The PR EOS fails to predict Type V phase behavior using a range of values of binary interaction parameter[26], and the nature of the predicted phase behavior is sensitive to the value of the binary interaction parameter in the model as shown in Figure 2.3[26]. A small increase in second decimal place of the binary interaction parameter value results in computed transitions from Type II (Figure 2.3a,b), to Type III (Figure 2.3c), to type III (Figure 2.3d). While, the PR EOS predicts incorrect global phase behavior of the

mixture, it successfully reproduces vapor liquid equilibrium experimental data[42] at low temperature. This example indicates that incorrect global phase behavior prediction does not preclude accurate vapor liquid equilibrium predictions over limited ranges of temperature, pressure and composition.

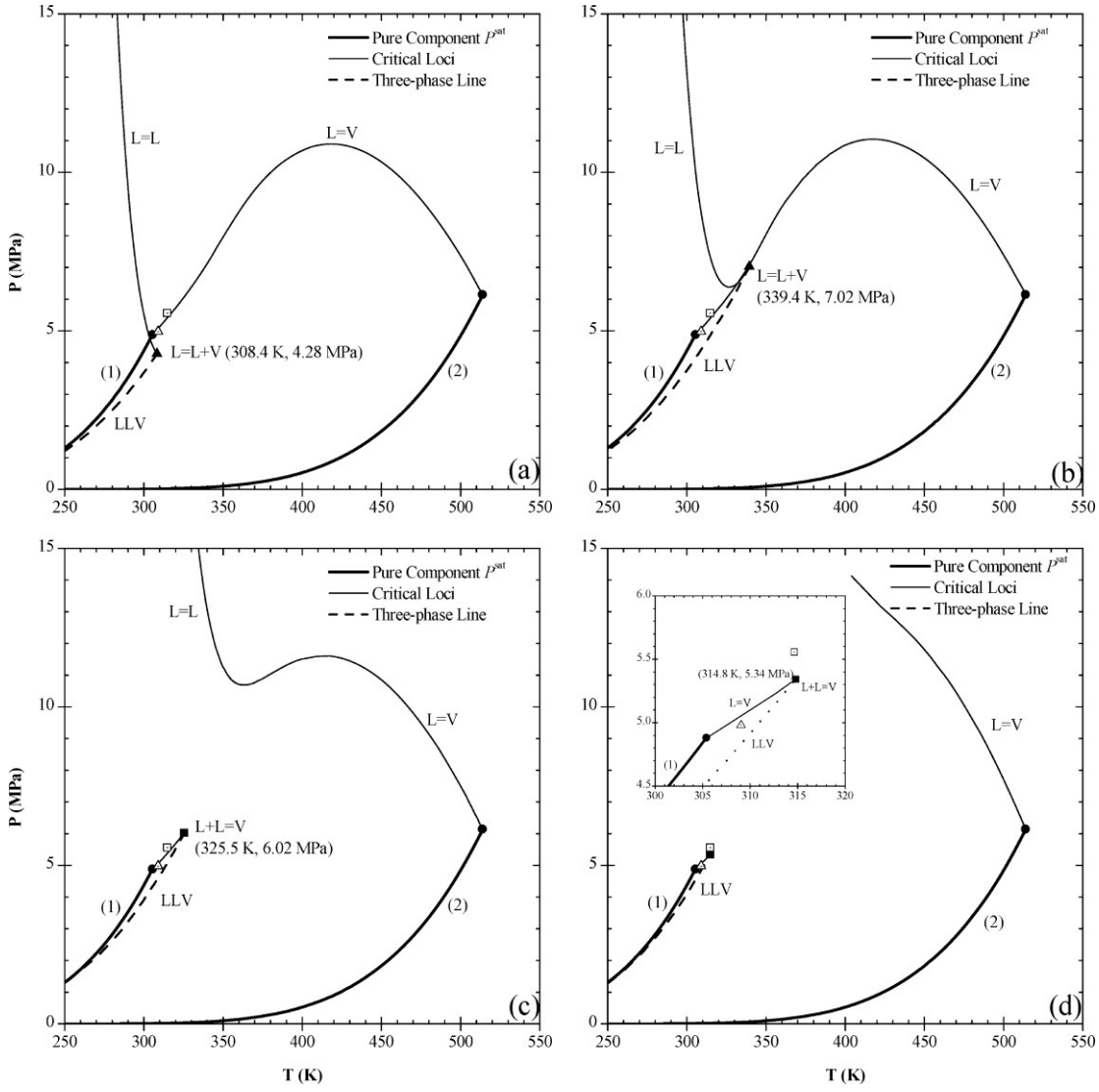

Figure 2.3 Predicted phase behavior type transitions introduced by systematically varying values of binary interaction parameter (k_{ij}) for ethane (1) + ethanol (2) mixtures using the PR EOS with (a) k_{ij} = 0.040, (b) k_{ij} = 0.048, (c) k_{ij} = 0.080, and (d) k_{ij} = 0.135. Figure is reproduced from Mushrif and Phoenix [26].

2.3.3 n-Alkane + Aromatic Mixtures

Phase equilibrium studies for aromatic-aliphatic hydrocarbon mixtures are of great industrial relevance, especially in separation processes. These mixtures are routinely

encountered in the petroleum industry. For example, the feed stream to a naphtha cracker generally contains around 20 per cent aromatics. Therefore, separation of aromatics from paraffins has attracted significant attention[43,44]. The phase behavior of these mixtures is also important in upstream operations. Phase equilibrium data for binary mixtures including benzene are available. Data for mixtures containing heavier n-alkanes and aromatics are scarce. The highest molar mass mixtures from this class, for which experimental phase equilibrium data are available are the anthracene and pyrene + hexadecane binaries, reported by Minicucci et al. [45] They also compared the experimental results with predicted phase behaviors using the PR EOS. Type II phase behavior is predicted by the equation of state for both the mixtures, whereas, solid-liquid-vapor and liquid-vapor phase behavior was observed experimentally.

Mixtures of benzene + n-alkanes exhibit Type I phase behavior both experimentally and computationally [up to n = 17]. Propane + phenanthrene, fluorene and triphenylmethane[20,47], exhibit Type III phase behavior experimentally. Jaubert et al. [48] showed that the PPR78 EOS plus temperature dependent k_{ij} values yields good predictions for the UCEP for propane + triphenylmethane but are silent on the type of phase behavior predicted. The original PR EOS predicts Type IV or V phase behavior using k_{ij} values equal to zero[26]. Mushrif et al. [26] predict Type IV or V phase behavior using the PR EOS for propane + fluorene and propane + phenanthrene, using kij equal to -0.05 and 0.01, respectively.

2.3.4 n-Alkane + Hydrogen Sulphide and Nitrogen Mixtures

Light paraffins in natural gas reservoirs are almost always found mixed with other gases such as carbon dioxide, nitrogen and hydrogen sulphide. These mixtures often exhibit very complex phase behaviors[49] and have implications for production and

processing. Reservoir models sometimes fail to predict correct phase behaviors. Saber and Shaw[50] showed that for a nitrogen-rich light hydrocarbon mixture, common models like the SRK EOS (which otherwise correctly obtains LL phase behavior) can converge to incorrect LV phase behavior due to inadequacies in the numerical solution algorithms. Similar mispredictions using the SRK EOS were also observed for binary mixtures of methane with hydrogen sulphide, where again LV phase behavior was obtained instead of LL[50]. Commercial simulators such as Aspen HYSYS and VMGSim were shown to be prone to such errors as well. The authors reported phase stability tests based on local search algorithms to be responsible for the erroneous phase behavior results because the models do predict correct phase behaviors if a robust phase stability tests based on global search techniques is used. The misprediction of phase behavior in these two examples arises due to inadequacies in numerical solution of models rather than shortcomings of the equation of state or inaccurate property inputs to the equations of state themselves.

2.4 Objectives and Thesis Outline

Phase behavior knowledge of mixtures containing aliphatic, aromatic and naphthenic hydrocarbon compounds is very important, from the perspectives of process design and process optimization, but cannot always be predicted/estimated reliably using common SAFT or cubic EOS thermodynamic models. The examples cited above point toward susceptibility of common equations of state to provide false phase behavior predictions for mixtures containing these three classes of compounds, and underscore the need for thorough testing of the models. Dissonance between predicted and experimental phase behaviour is common for mixtures where there is a considerable difference in molecular size of the constituent compounds. Asymmetric mixtures have attracted a lot of attention, and there are numerous reports concerning

mixtures of small n-alkanes with numerous larger sized compounds. Asymmetric mixtures containing long chain n-alkanes and comparatively smaller cyclic and aromatic compounds have received limited attention even though dissonance between experimental and predicted phase behaviors was demonstrated for two mixtures [45]. Knowledge gaps related to dissonance between experimental and predicted phase behaviors for binary n-alkane + aromatic and naphthenic mixtures are targeted in this work. While binary mixtures are rarely encountered in industrial applications, their study provides valuable information and foundational understanding of the phase behavior of related but more complex multicomponent mixtures.

The specific objectives of this work are to compare experimental and computed outcomes for the phase behavior types and the quality of bubble pressure predictions for binary mixtures of n-alkanes + aromatic and naphthenic compounds. To facilitate the workflow and the presentation of outcomes, Chapter 3 focuses on the global phase behavior, and Chapter 4 focuses on the vapor-liquid equilibria in the miscible region. General conclusions and future work are presented in Chapter 5.

Representative compounds, selected from the aromatic and naphthenic families, shown in Figure 2.4 and ten n-alkanes ranging from n-C_{10} to n-C_{50} selected from the aliphatic group comprise the computational matrix for the study of global phase behavior. Global phase equilibrium calculations are performed for all the possible combinations of n-alkane + aromatic and naphthenic binary mixtures containing these compounds. The Peng-Robinson, Soave-Redlich-Kwong and PC-SAFT EOS are used to predict phase behavior and the computed outcomes are compared with experimental data, where available. Care is taken to ensure that the calculations are

free of numerical artefacts. For example, a robust global phase stability test for cubic EOS is part of the workflow, and multiple calculation tools are employed that include diverse and proprietary numerical methods. Sensitivity analyses, showing the impact of selection of correlation for estimating pure component properties on phase behavior predictions are performed in order to assess the influence of the property values on the predicted phase behavior types. Causes for misprediction are investigated and addressed qualitatively.

To study vapor-liquid equilibria in the miscible region, bubble pressures and L=V critical loci of illustrative binary mixtures of benzene with thirteen aliphatic compounds ranging from n-C_6 to n-C_{36} are evaluated using the PR, SRK and PC-SAFT EOS and the predicted outcomes are compared with experimental values, where available. A limited number of experiments were carried out as a part of this work to measure bubble pressures for benzene + n-C_{20}, n-C_{24}, n-C_{28} and n-C_{36} binary mixtures in order to benchmark calculations. Binary interaction parameter values for PR and SRK EOS fitted to the new experimental VLE data are also reported for these mixtures. A comparison of PR and SRK outcomes obtained using multiple sets of k_{ij} values to experimental data and PC-SAFT, where experimental data is unavailable, is done in order to gauge the impact of non-zero binary interaction parameter values on the quality of predictions by these models. The role of uncertainty of pure component properties on deviations of model outcomes from experimental data is also evaluated.

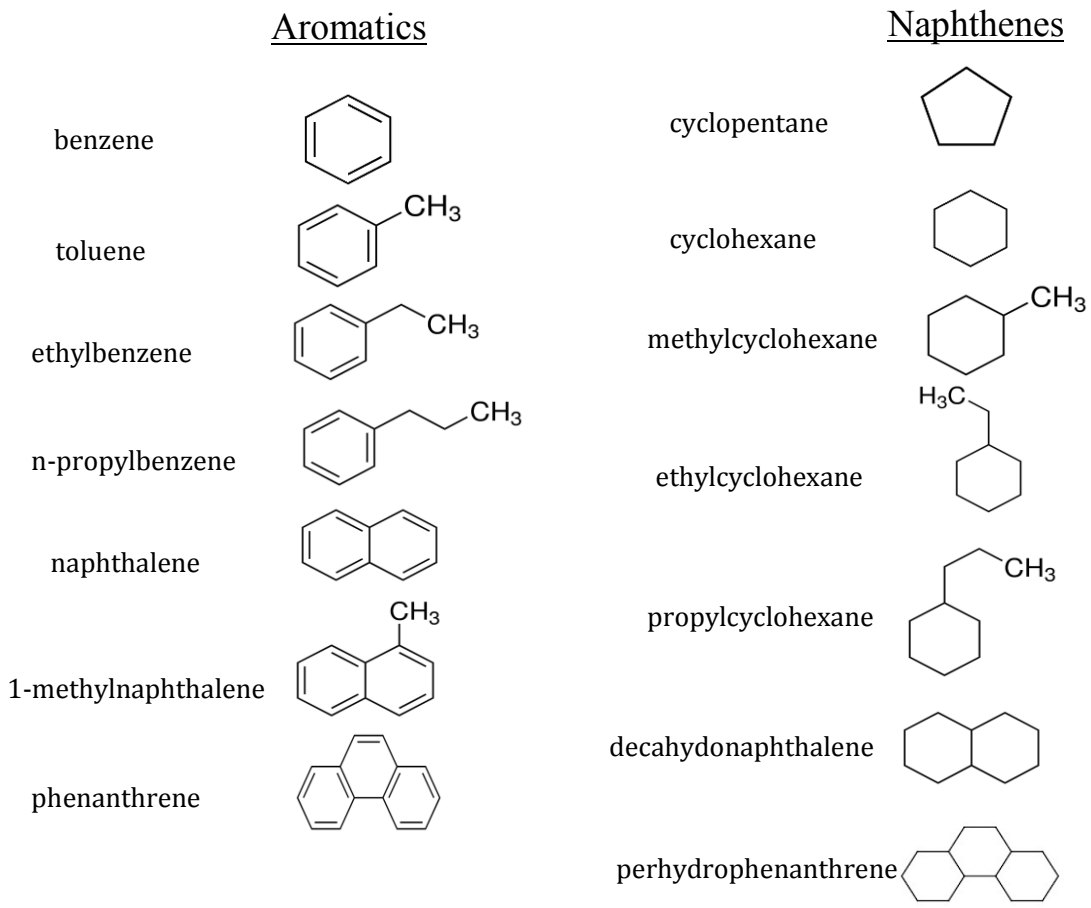

Figure 2.4 Examples of aromatic and naphthenic hydrocarbon compounds included in this study.

2.5 Nomenclature

EOS equation of state

k_{ij} binary interaction parameter

L liquid

LL liquid-liquid

LV liquid-vapor

n-C_n n-alkane with n number of carbon atoms

P pressure

T Temperature

V Vapor

2.6 References

(1) Boduszynski, M. M. Composition of heavy petroleums. 1. Molecular weight, hydrogen deficiency, and heteroatom concentration as a function of atmospheric equivalent boiling point up to 1400 °F (760 °C). *Energy Fuels* **1987**, 1, 2-11.

(2) Boduszynski, M. M. Composition of heavy petroleums. 2. Molecular characterization. *Energy Fuels* **1988**, 2, 597-613.

(3) Altgelt, K. H.; Boduszynski, M. M. Composition of heavy petroleums. 3. An improved boiling point-molecular weight relation. *Energy Fuels* **1992**, 6, 68-72.

(4) Boduszynski, M. M.; Altgelt, K. H. Composition of heavy petroleums. 4. Significance of the extended Atmospheric Equivalent Boiling Point (AEBP) scale. *Energy Fuels* **1992**, 6, 72-76.

(5) Fernandez-Lima, F.; Becker, C.; McKenna, A. M.; Rodgers, R. P.; Marshall, A. G.; Russell, D. H. Petroleum crude oil characterization by IMS-MS and FTICR MS. *Anal. Chem.* **2009**, 9941-9947.

(6) McKenna, A. M.; Purcell, J. M.; Rodgers, R. P.; Marshall, A. G. Heavy petroleum composition. 1. Exhaustive compositional analysis of Athabasca bitumen HVGO distillates by Fourier Transform Ion Cyclotron Resonance Mass Spectrometry: A definitive test of the Boduszynski model. *Energy Fuels* **2010**, 24, 2929-2938.

(7) McKenna, A. M.; Blakney, G. T.; Xian, F.; Glaser, P. B.; Rodgers, R. P.; Marshall, A. G. Heavy petroleum composition. 2. Progression of the Boduszynski model to the limit of distillation by ultrahigh-resolution FT-ICR mass spectrometry. *Energy Fuels* **2010**, 24, 2939-2946.

(8) McKenna, A. M.; Donald, L. J.; Fitzsimmons, J. E.; Juyal, P.; Spicer, V.; Standing, K. G.; Marshall, A. G.; Rodgers, R. P. Heavy petroleum composition. 3. Asphaltene aggregation. *Energy Fuels* **2013**, 27, 1246-1256.

(9) McKenna, A. M.; Marshall, A. G.; Rodgers, R. P. Heavy petroleum composition. 4. Asphaltene compositional space. *Energy Fuels* **2013**, 27, 1257-1267.

(10) Podgorski, D. C.; Corilo, Y. E.; Nyadong, L.; Lobodin, V. V.; Bythell, B. J.; Robbins, W. K.; McKenna, A. M.; Marshall, A. G.; Rodgers, R. P. Heavy

petroleum composition. 5. Compositional and structural continuum of petroleum revealed. *Energy Fuels* **2013**, 27, 1268-1276.

(11) Altgelt, K. H.; Boduszynski, M. M. *Composition and analysis of heavy petroleum fractions;* M. Dekker: New York, 1994.

(12) Quann, R. J.; Jaffe, S. B. Structure-oriented lumping: describing the chemistry of complex hydrocarbon mixtures. *Ind. Eng. Chem. Res.* **1993**, 32, 1800-1800.

(13) Shaw, J. M.; Satyro, M. A.; Yarranton, H. W. Chapter 7-The phase behaviour and properties of heavy oils. In *Practical Advances in Petroleum Production and Processing*; Hsu, C. S., Robinson, P. R., Eds.; Springer: New York, 2015.

(14) Aladwani, H. A.; Riazi, M. R. Some guidelines for choosing a characterization method for petroleum fractions in process simulators. *Chem. Eng. Res. Des.* **2005**, 83, 160-166.

(15) Eckert, E. Do we need pseudocomponents? *Chem. Listy* **2001**, 95, 368-373.

(16) Ba, A.; Eckert, E.; Vanek, T. Procedures for the selection of real components to characterize petroleum mixtures. *Chem. Pap.* **2003**, 57, 53-62.

(17) Eckert, E.; Vanek, T. New approach to the characterisation of petroleum mixtures used in the modelling of separation processes. *Comput. Chem. Eng.* **2005**, 30, 343-356.

(18) Eckert, E.; Vanek, T. Improvements in the selection of real components forming a substitute mixture for petroleum fractions. *Chem. Pap.* **2009**, 63, 399-405.

(19) Kontogeorgis, G. M.; Tassios, D. P. Critical constants and acentric factors for long-chain alkanes suitable for corresponding states applications. A critical review. *Chem. Eng. J.* **1997**, 66, 35-49.

(20) Peters, C. J.; Rijkers, M. P. W. M.; De Roo, J. L.; De Swaan Arons, J. Phase equilibria in binary mixtures of near-critical propane and poly-aromatic hydrocarbons. *Fluid Phase Equilib.* **1989**, 52, 373-387.

(21) Davenport, A. J.; Rowlinson, J. S. The solubility of hydrocarbons in liquid methane. *Trans. Faraday Soc.* **1963**, 59, 78-84.

(22) Lin, Y. N.; Chen, R. J. J.; Chappelear, P. S.; Kobayashi, R. Vapor-liquid equilibrium of the methane-n-hexane system at low temperature. *J. Chem. Eng. Data* **1977**, 22, 402-408.

(23) Polishuk, I.; Wisniak, J.; Segura, H. Prediction of the critical locus in binary mixtures using equation of state: I. Cubic equations of state, classical mixing rules, mixtures of methane–alkanes. *Fluid Phase Equilib.* **1999**, 164, 13-47.

(24) Castier, M.; Sandler, S. I. Critical points with the Wong-Sandler mixing rule - II. Calculations with a modified Peng-Robinson equation of state. *Chem. Eng. Sci.* **1997**, 52, 3579-3588.

(25) Polishuk, I.; Wisniak, J.; Segura, H. Prediction of the critical locus in binary mixtures using equation of state: I. Cubic equations of state, classical mixing rules, mixtures of methane–alkanes. *Fluid Phase Equilib.* **1999**, 164, 13-47.

(26) Mushrif, S. H.; Phoenix, A. V. Effect of Peng-Robinson binary interaction parameters on the predicted multiphase behavior of selected binary systems. *Ind. Eng. Chem. Res.* **2008**, 47, 6280-6288.

(27) Chang, H. L.; Hurt, L. J.; Kobayashi, R. Vapor-liquid equilibria of light hydrocarbons at low temperatures and high pressures: The methane-n-heptane system. *AIChE J.* **1966**, 12, 1212-1216.

(28) Blas, F. J.; Vega, L. F. Critical behavior and partial miscibility phenomena in binary mixtures of hydrocarbons by the statistical associating fluid theory. *J. Chem. Phys.* **1998**, 109, 7405-7413.

(29) McCabe, C.; Gil-Villegas, A.; Jackson, G. Predicting the high-pressure phase equilibria of methane + n-hexane using the SAFT-VR approach. *J. Phys. Chem. B* **1998**, 102, 4183-4188.

(30) Peters, C. J.; Van Der Kooi, H. J.; De Swaan Arons, J. Measurements and calculations of phase equilibria for (ethane + tetracosane) and (p, Vm′∗, T) of liquid tetracosane. *J. Chem. Thermodyn.* **1987**, 19, 395-405.

(31) Peters, C. J.; Spiegelaar, J.; De Swaan Arons, J. Phase equilibria in binary mixtures of ethane + docosane and molar volumes of liquid docosane. *Fluid Phase Equilib.* **1988**, 41, 245-256.

(32) Peters, C. J.; Lichtenthaler, R. N.; De Swaan Arons, J. Three phase equilibria in binary mixtures of ethane and higher n-alkanes. *Fluid Phase Equilib.* **1986**, 29, 495-504.

(33) Peters, C. J.; De Roo, J. L.; Lichtenthaler, R. N. Measurements and calculations of phase equilibria in binary mixtures of ethane + eicosane. *Fluid Phase Equilib.* **1991**, 69, 51-66.

(34) Peters, C. J.; De Roo, J. L.; Lichtenthaler, R. N. Measurements and calculations of phase equilibria of binary mixtures of ethane + eicosane. Part I: vapour + liquid equilibria. *Fluid Phase Equilib.* **1987**, 34, 287-308.

(35) Peters, C. J.; De Roo, J. L.; De Swaan Arons, J. Three-phase equilibria in (ethane + pentacosane). *J. Chem. Thermodyn.* **1987**, 19, 265-272.

(36) De Goede, R.; Peters, C. J.; Van Der Kooi, H. J.; Lichtenthaler, R. N. Phase equilibria in binary mixtures of ethane and hexadecane. *Fluid Phase Equilib.* **1989**, 50, 305-314.

(37) Cismondi Duarte, M.; Galdo, M. V.; Gomez, M. J.; Tassin, N. G.; Yanes, M. High pressure phase behavior modeling of asymmetric alkane + alkane binary systems with the RKPR EOS. *Fluid Phase Equilib.* **2014**, 362, 125-135.

(38) Saber, N.; Shaw, J. M. Toward multiphase equilibrium prediction for ill-defined asymmetric hydrocarbon mixtures. *Fluid Phase Equilib.* **2009**, 285, 73-82.

(39) Cismondi Duarte, M.; Cruz Doblas, J.; Gomez, M. J.; Montoya, G. F. Modelling the phase behavior of alkane mixtures in wide ranges of conditions: New parameterization and predictive correlations of binary interactions for the RKPR EOS. *Fluid Phase Equilib.* **2015**, 403, 49-59.

(40) Brunner, E. Fluid mixtures at high pressures II. Phase separation and critical phenomena of (ethane + an n-alkanol) and of (ethane + methanol) and (propane + methanol). *J. Chem. Thermodyn.* **1985**, 17, 871-885.

(41) Lam, D. H.; Jangkamolkulchai, A.; Luks, K. D. Liquid-liquid-vapor phase equilibrium behavior of certain binary ethane + n-alkanol mixtures. *Fluid Phase Equilib.* **1990**, 59, 263-277.

(42) Kariznovi, M.; Nourozieh, H.; Abedi, J. (Vapor + liquid) equilibrium properties of (ethane + ethanol) system at (295, 303, and 313) K. *J. Chem. Thermodyn.* **2011**, 43, 1719-1722.

(43) Meindersma, G. W.; de Haan, A. B. Conceptual process design for aromatic/aliphatic separation with ionic liquids. *Chem. Eng. Res. Design* **2008**, 86, 745-752.

(44) Meindersma, G. W.; Hansmeier, A. R.; De Haan, A. B. Ionic liquids for aromatics extraction. Present status and future outlook. *Ind. Eng. Chem. Res.* **2010**, 49, 7530-7540.

(45) Minicucci, D.; Zou, X.-Y.; Shaw, J. M. The impact of liquid–liquid–vapour phase behaviour on coke formation from model coke precursors. *Fluid Phase Equilib.* **2002**, 194–197, 353-360.

(46) Vostrikov, S. V.; Nesterova, T. N.; Nesterov, I. A.; Sosin, S. E.; Nazmutdinov, A. G. III. Study of critical and maximum temperatures of coexistence of liquid and gas phase in hydrocarbons binary mixtures of aromatic hydrocarbons with alkanes and cycloalkanes. *Fluid Phase Equilib.* **2014**, 377, 56-75.

(47) Peters, C. J.; De Roo, J. L.; De Swaan Arons, J. Phase equilibria in binary mixtures of propane and triphenylmethane. *Fluid Phase Equilib.* **1995**, 109, 99-111.

(48) Jaubert, J.; Vitu, S.; Mutelet, F.; Corriou, J. Extension of the PPR78 model (predictive 1978, Peng–Robinson EOS with temperature dependent kij calculated through a group contribution method) to systems containing aromatic compounds. *Fluid Phase Equilib.* **2005**, 237, 193-211.

(49) Michelsen, M. L. The isothermal flash problem. Part II. Phase-split calculation. *Fluid Phase Equilib.* **1982**, 9, 21-40.

(50) Saber, N.; Shaw, J. M. Rapid and robust phase behaviour stability analysis using global optimization. *Fluid Phase Equilib.* **2008**, 264, 137-146.

Chapter 3. Systematic misprediction of n-alkane + aromatic and naphthenic hydrocarbon phase behavior using common equations of state*†

3.1 Introduction

Accurate phase behavior measurements can be obtained by experiment, but generating experimental data for all mixtures of importance arising in diverse processes is a practical impossibility. Thermodynamic models are used to correlate, interpolate and predict phase behaviors and properties of mixtures in the wake of sparse experimental data. The Peng-Robinson (PR)[1] and Soave-Redlich-Kwong (SRK)[2] equations of state are commonly used thermodynamic models in the petroleum and petrochemical industries. The more recent Statistical Associating Fluid Theory (SAFT) equations of state and the Perturbed Chain (PC-SAFT) variants in particular[3,4] are beginning to find diverse applications in the petroleum industry, including the simulation of petroleum reservoir fluids[5] and highly asymmetric mixtures such as asphaltene-rich mixtures[6-8], despite known predictive pitfalls[9-11].

Incorrect prediction of phase behaviors and properties may arise as a consequence of the failure of stability analysis calculations[12] leading to the wrong number of phases being predicted at equilibrium, or due to poor selection of equation of state pure or

* This chapter was published as: Ahitan, S.; Satyro, M. A.; Shaw, J. M. Systematic Misprediction of n-Alkane + Aromatic and Naphthenic Hydrocarbon Phase Behavior Using Common Equations of State. *J. Chem. Eng. Data*, **2015,** *60* (11), pp 3300–3318, **DOI:** 10.1021/acs.jced.5b00539.

† Tables with serial number preceded with letter "S" (for e.g. Table S1) are located in APPENDIX 1.

mixture parameters, which also leads to the incorrect number of phases being predicted[13,14]. For example, if all compositions of a binary mixture only exhibit the fluid phase states L, LV, and V at equilibrium either experimentally or computationally, then according to the van Konynenburg and Scott naming scheme[15], the mixture is classified as a Type I binary possessing the pressure-temperature projection shown in Figure 1.2a. If in addition, LL and LLV phase behaviors are observed or predicted at equilibrium over specific ranges of temperature, pressure and composition, then one of the other five phase behavior types illustrated in Figure 1.2b-f is exhibited. Mismatches between Type I experimental phase behaviors, anticipated in the present work, and predicted Type II to Type VI phase behavior are readily detected due to the predicted presence of LL and LLV phase behaviors and their absence from experimental measurements.

In this screening study, phase behavior predictions for binary mixtures of n-alkanes with aromatics and cycloalkanes are evaluated based on the PR, SRK and PC-SAFT equations of state. The phase behavior predictions of 14 binary mixtures are compared with experimental analogues at atmospheric pressure. Divergence from observed single liquid phase behavior is tracked. A global search technique, DIviding RECTangles (DIRECT)[16] is used to eliminate computational errors in the stability analysis[12] for the PR and SRK equations of state in a custom code, and computed outcomes are also compared with values obtained from two popular commercial process simulators *VMGSim v8.0*[17] and *Aspen HYSYS v8.4*[18]. The PC-SAFT equation of state is evaluated using the software GPEC (Global Phase Equilibrium Calculations)[19]. As the aim of this work is to address phase behavior misprediction (LLV/LL instead of L/LV) rather than phase composition and bubble and dew point

accuracy, quantitative comparisons of predicted and measured phase compositions are not performed.

3.2 Phase Equilibrium Calculations

3.2.1 Equations of State

The PR and SRK EOS share a common framework:

$$P = \frac{RT}{v-b} - \frac{a}{v^2 + ubv + wb^2} \tag{3.1}$$

$$a = \sum_{i=1}^{N}\sum_{j=1}^{N} z_i z_j \sqrt{a_i a_j}\left(1 - k_{ij}\right) \qquad k_{ij} = k_{ji}\,; \quad k_{ii} = 0 \tag{3.2}$$

$$b = \sum_{i=1}^{N} z_i b_i \tag{3.3}$$

where

$$\begin{aligned} b_i &= \Omega_b \frac{RT_{c,i}}{P_{c,i}} \\ a_i(T) &= \Omega_a \frac{R^2 T_{c,i}^2}{P_{c,i}} \cdot \alpha_i\left(T, T_{c,i}, \omega_i\right) \\ \alpha_i\left(T, T_{c,i}, \omega_i\right) &= \left[1 + (r_1 + r_2\omega_i + r_3\omega_i^2 + r_4\omega_i^3)\left(1 - \sqrt{\frac{T}{T_{c,i}}}\right)\right]^2 \end{aligned} \tag{3.4}$$

P, T, v and *R* are pressure, temperature, molar volume of the fluid, and the universal gas constant respectively. $T_{c,i}$ is the critical temperature, $P_{c,i}$ is the critical pressure, ω_i is the acentric factor, and z_i is the mole fraction of i^{th} component in an *N* component mixture. For larger molecules, the critical properties cannot be measured[20] and estimated values possess significant uncertainty irrespective of method of estimation[21]. The binary interaction parameter k_{ij} between components *i* and *j* is based on the classical van der Waals mixing rules, equations 3.2 and 3.3. The k_{ij} value has a

significant impact on predicted phase behavior[13]. They are EOS specific and usually have a small positive value but can be negative. In the absence of experimental data, a value equal to zero or correlations[22-26] can be used to calculate k_{ij} values. Increasing the value of k_{ij} increases the size of immiscible zones in pressure-temperature projections and pressure-composition diagrams, if they are present, and can change the predicted phase behavior from Type I to Type II[27]. In this work, default interaction parameter values are used in the calculations with the cubic equations of state as estimated or regressed from experimental data in the commercial simulators without further adjustment. These values are listed in Table S1 and Table S2 for the PR equation of state for VMGSim and Aspen HYSYS, respectively. The binary interaction parameters for the SRK and PR equation of state are identical up to the 9th decimal place in Aspen HYSYS for most of the mixtures. In VMGSim, k_{ij} values are equal to zero for all the binary mixtures for the SRK equation of state. In the custom code, interaction parameters are assumed to be zero for the PR and SRK equations of state, and in addition a correlation developed by Gao et al.[22] is used to estimate k_{ij} values for the PR equation of state. Values for other coefficients in equations 3.1 through 3.4 are listed in Table 3.1.

Table 3.1 Constants used in PR and SRK EOS

Constants	**PR EOS**		**SRK EOS**
	If $\omega_i \leq 0.491$	If $\omega_i > 0.491$	
u	2	2	1
w	–1	–1	0
Ω_a	0.45724	0.45724	0.42747
Ω_b	0.0778	0.0778	0.08664
r_1	0.37464	0.379642	0.48

r_2	1.54226	1.48503	1.574
r_3	–0.26992	−0.164423	–0.176
r_4	0	0.016666	0

The PC SAFT equation of state[3,4] is one of the most popular versions of SAFT family of equations. PC SAFT employs a more elaborate molecular approach wherein molecular properties (characteristic energies and molecular sizes that are back calculated from liquid density and vapor pressure data) and not T_c, P_c and ω are used to represent a fluid. For non-associating components, like hydrocarbons, the Helmholtz free energy can be obtained using equation 3.5:

$$\frac{a^{\text{res}}}{RT} = \frac{a^{\text{hc}}}{RT} + \frac{a^{\text{disp}}}{RT} \tag{3.5}$$

where a^{res}, a^{hc}, and a^{disp} refer to residual Helmholtz energy, Helmholtz energy of a hard chain fluid and the contribution of dispersive attractions to the Helmholtz energy, respectively. Detailed PC-SAFT expressions can be found elsewhere[3,4]. PC SAFT requires three pure component parameters to characterize non-associating components: the segment number (m), the segment diameter (σ), and the segment energy parameter (ε/k). For mixtures, the Berthelot-Lorentz combining rules are used to calculate σ_{ij} and ε_{ij} as defined in equations 3.6 and 3.7:

$$\varepsilon_{\text{ij}} = \sqrt{\varepsilon_{\text{ii}}\varepsilon_{\text{jj}}}(1 - k_{\text{ij}}) \tag{3.6}$$

$$\sigma_{\text{ij}} = \frac{(\sigma_i + \sigma_j)}{2} \tag{3.7}$$

The binary interaction parameters (k_{ij}) are assumed to be zero for PC-SAFT based calculations in the GPEC software[19]. Other PC-SAFT parameters and their sources are provided in Table S3.

3.2.2 Phase Equilibrium Principles

Phase stability analysis is the key step in determining the correct number of phases at thermodynamic equilibrium. For a mixture to be at equilibrium, the overall material balance must be preserved, the chemical potential of a component must be equal in all of the phases present and the Gibbs free energy[28] must be at a global minimum. The last restriction can be difficult to determine in a completely reliable manner. Mathematically the minimization of Gibbs free energy is done using the tangent plane criterion[29] at the system pressure and temperature. If the tangent plane distance is negative at any composition, it implies that the mixture is unstable and flash calculations using a greater number of phases must be performed to find a globally stable equilibrium solution. For mixtures showing multiphase behavior, the Gibbs energy surface can have multiple or shallow local minima and identification of a global minimum can become mathematically difficult. Detection of global minima is imperative because local minima can cause false convergence yielding the prediction of the wrong number of co-existing phases. Several phase stability tests based on global minimization techniques have been developed[30-35]. A global phase stability test[12] based on the DIRECT optimization algorithm[16] is used in the custom coded phase stability analysis calculations performed in this work for the PR and SRK equations of state. The commercial software packages include proprietary stability analysis algorithms.

3.2.3 Phase Behavior Prediction Calculation Procedure

3.2.3.1 Phase Stability Analysis Calculations with the PR and SRK Equations of State

Phase stability analysis calculations were performed with the n-alkane + aromatic and n-alkane + naphthenic binary mixtures shown in Table 3.2. Each of the aromatic and naphthenic compounds listed forms 10 binary mixtures with the aliphatic compounds

listed. Phase stability analysis was performed for all 150 binary mixtures with both the SRK and PR equations of state using a custom phase stability test and flash calculation algorithm[36]. A tangent plane distance function value greater than zero was considered as the condition for stability of a mixture. The input variables required for the stability analysis calculations can be divided into three categories: (i) pure component properties, (ii) system conditions and (iii) binary interaction parameters (k_{ij}). Pure component properties: critical temperature, critical pressure and acentric factor values were obtained from NIST/TDE[37] and are listed in Table S4. These values are referred to as the standard pure component properties in this work. A systematic approach was implemented to avoid conditions where solid or vapor phases would arise experimentally. Calculations were performed at temperatures greater than or equal to the melting point temperature of the higher melting component in each binary mixture. Pressure was set at 1 bar except for cases where the vapor pressure of the lower boiling component exceeded this value. Examples include binary mixtures of benzene + n-C_{40}, cyclopentane + n-C_{24} and cyclohexane + n-C_{40}. For such cases the pressure was set at 10 bar. Phase stability analyses were performed at mole fractions from 0.025 to 0.975 using 0.025 mole fraction increments. For the PR equation of state, sets of survey calculations were performed using interaction parameter values set to zero and set using the Gao et al. correlation[22]. For calculations based on the SRK equation of state, all k_{ij} values were set to zero. Complementary calculations were performed using the commercial codes.

Table 3.2 List of pure components selected in this work.

n-alkanes	Aromatics	Naphthenes
n-C_{10}	Benzene	Cyclopentane
n-C_{15}	Toluene	Cyclohexane

n-C_{17}	Ethylbenzene	Methylcyclohexane
n-C_{20}	n-Propylbenzene	Ethylcyclohexane
n-C_{24}	Naphthalene	n-Propylcyclohexane
n-C_{28}	1-Methylnaphthalene	Bicyclohexyl
n-C_{30}	Phenanthrene	cis-Decahydronaphthalene
n-C_{36}		Perhydrophenanthrene
n-C_{40}		
n-C_{50}		

3.2.3.2 Identification of Maximum k_{ij} Values for Generating Type I Phase Behavior Using SRK and PR Equations of State

For binary mixtures where one liquid phase was found to be unstable, phase stability analysis calculations were repeated at the same temperatures, pressures and compositions, with the k_{ij} values as adjustable parameters. The values were reduced until one phase was found to be stable. As different values were obtained for each binary mixture at different compositions, the smallest k_{ij} value identified is reported. This k_{ij} value does not necessarily correspond to an accurate thermodynamic model for the binary mixture (for example bubble pressures or temperatures may be inaccurate) but it corresponds to a value that allows the model to predict the correct phase behavior as defined by experiment.

3.2.3.3 Phase Behavior Calculations Using the PC SAFT Equation of State

Pressure-Temperature projections for the n-C_{50} subset of binary n-alkane + aromatic and n-alkane + naphthenic mixtures were generated using the PC-SAFT equation of state and GPEC. Some of these calculations were repeated using *Aspen Plus v8.4*[38]. The pure component parameters, obtained from[3,39,40], are listed in Table S3, and all of the binary interaction parameter values were set to zero for the survey. This subset

was chosen because it comprises the most asymmetric mixtures. As none of the mixtures exhibited liquid-liquid phase behavior at temperatures exceeding the melting point of both components no additional survey calculations were performed. The robustness of the phase stability analyses in these software packages was not verified. However, they reproduce the known Type V phase behavior for the methane + n-hexane binary, if computed phase behaviors more than 50 °C below the freezing point of hexane are ignored, while non-zero k_{ij} values are needed to reproduce the known Type III phase behavior of the methane n-heptane binary.

3.2.3.4 Sensitivity Analysis

Experimental critical properties and acentric factors for the naphthenic and aromatic compounds are available except for perhydrophenanthrene. This compound was not included in the sensitivity analysis. For n-alkanes larger than n-C_{20} critical point data is scant and uncertain. So, to test the sensitivity of phase behavior predictions to the uncertainties in experimental or estimated pure component properties of n-alkanes, phase stability analysis calculations were repeated for all the binary mixtures including n-alkanes larger than n-C_{20}. Values for critical temperature, critical pressure and acentric factor for n-alkanes were varied independently from the standard values listed in Table S4 until Type I phase behavior was predicted. An additional set of phase stability calculations was performed where the critical temperature, critical pressure and acentric factor for n-alkanes were set jointly at the maxima and minima suggested by Stamataki and Tassios[21] as their study includes a broad range of correlations for extrapolating n-alkane critical properties. These ranges reflect common practice, and as shown in Figure 3.1, they follow the trends of means and ranges suggested by NIST/TDE[37] for critical pressure, Figure 3.1a, and critical temperature, Figure 3.1b. Acentric factor uncertainty is not available from NIST/TDE,

but can be substantial[41]. Figure 3.1 underscores the uncertainty of critical property values for large n-alkanes that range up to multiple bar for critical pressure and to more than 100 K for critical temperature. The ranges of property values evaluated are listed in Table S5. Binary interaction parameter values were recalculated for the PR equation of state based on Gao's correlation[22] and for SRK equation of state, they were again assumed to be zero.

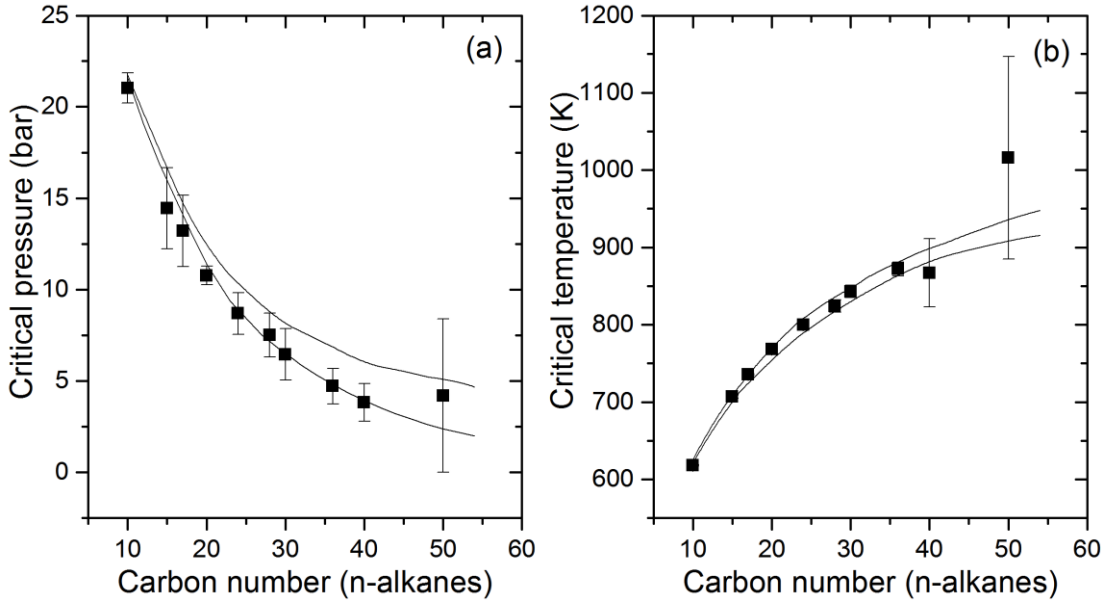

Figure 3.1 Critical pressure (a) and critical temperature (b) ranges for n-alkanes. The points (■) with error bars comprise values and uncertainties from NIST/TDE[37]; the curves are the limits from Stamataki and Tassios[21].

3.3 Experimental

Compounds used in the experiments were procured from Aldrich, Acros and Fisher Scientific with the following purities: bicyclohexyl (99% w/w), hexatriacontane (98% w/w), n-propylbenzene (98% w/w), tetracosane (99% w/w), 1-methylnaphthalene (97% w/w), octacosane (99% w/w) and cyclohexane (99.98% w/w). These compounds were used as received. Binary mixture subsamples possessing a mass of approximately 2 grams and a composition uncertainty of less than +/- 0.001 wt. fraction were prepared in clear glass vials using a Mettler-Toledo MS603S balance with an uncertainty of +/-1 mg. The vials were then sealed and placed in a

temperature controlled water bath. The temperature of the water bath was increased in increments of 5 °C up to the temperature just above which the solids melted. Visual observations were made to detect whether two liquid phases were present. By performing experiments over a range of compositions with each binary mixture close to but above the solidification temperature, Type II, III and IV phase behavior is readily detected and distinguished from Type I phase behavior.

3.4 Results and Discussion

3.4.1 Phase Stability Analysis Results

Phase stability analysis results for binary mixtures of n-alkane + aromatic and n-alkane + naphthenic compounds, obtained for the cubic equations of state are summarized in Figures 3.2a and 3.2b respectively. For both equations of state and for both types of mixtures the outcomes and trends are similar. One liquid phase is predicted to be stable for binaries with short n-alkanes, and two liquid phases are predicted for binaries with long n-alkane chains. There is significant variation in the computed carbon number values for the n-alkane where the transition between one and two phases is predicted, but all of the calculations are qualitatively similar, including results from the commercial process simulators. For example, the predicted transition for n-alkanes + toluene ranges from n-C_{17} to n-$C_{24,}$ and for mixtures with cyclohexane, the corresponding range is n-C_{24} to n-C_{30}. For aromatic compound + n-alkane binaries, the maximum deviation for the prediction of the transition from one to two phase stability is a carbon number difference of 7, as shown in Figure 3.2a. For naphthenic compound + n-alkane binaries, the difference can be as large as 16 as shown in Figure 3.2b. Setting k_{ij} values appearing in the PR equation of state to zero has a minimal impact on predicted stability transitions. Outcomes for the PC-SAFT

equation of state are not included in this summary graphic because, at the test conditions, one liquid phase was found to be stable for all mixtures surveyed.

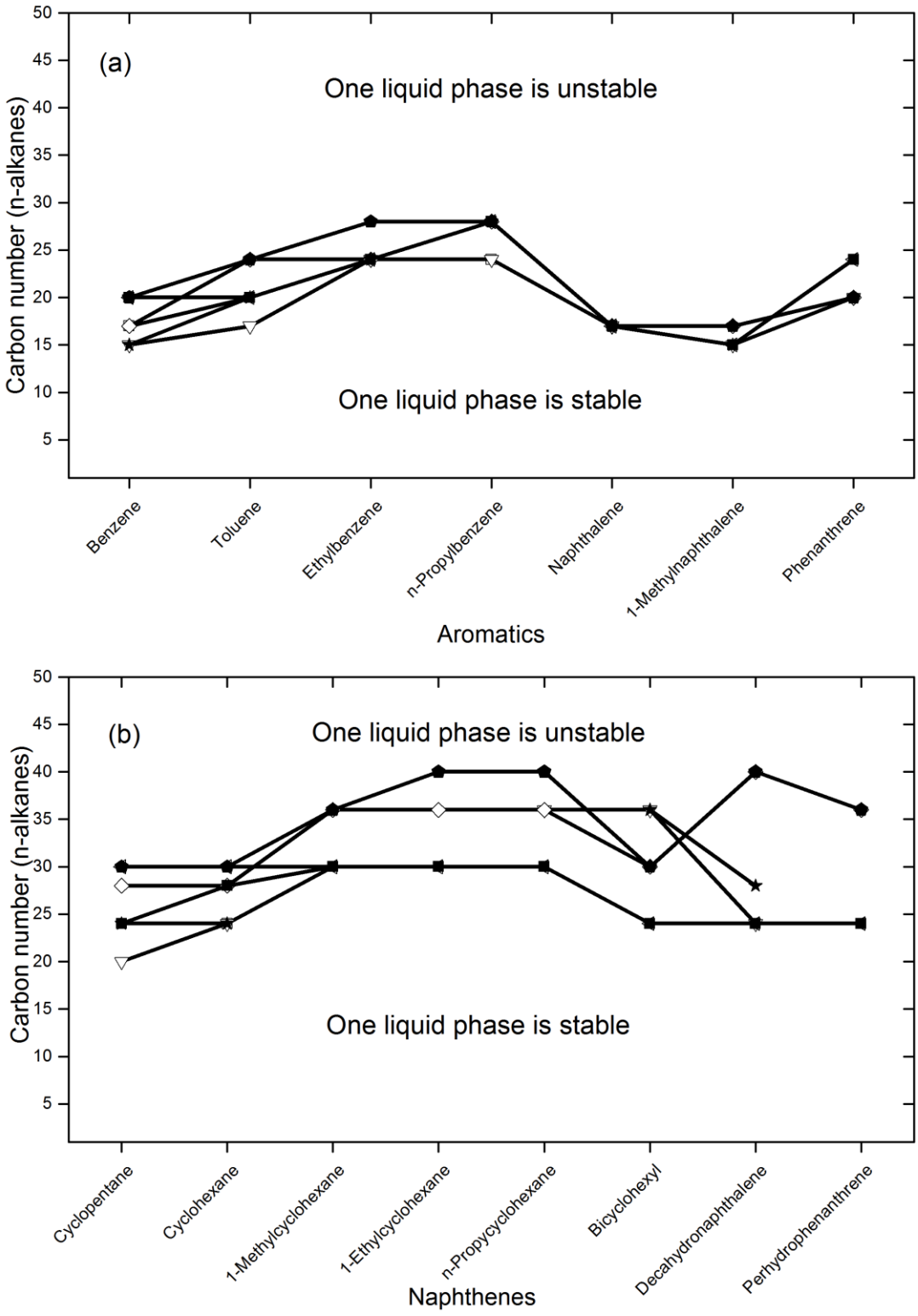

Figure 3.2 Phase stability analysis result summary showing the first unstable binary mixture in: (a) binary mixtures of n-alkanes + aromatics, (b) binary mixtures of n-alkanes + naphthenes. Symbols: (—□—) PR equation of state with correlated k_{ij} values and (—■—) with k_{ij}=0, and (—◁—) SRK equation

of state all from this work; PR equation of state in (—▽—) Aspen HYSYS and in (—◇—) VMGSim; SRK equation of state in (—★—) Aspen HYSYS and in (—⬟—) VMGSim.

3.4.2 Phase Behavior Type Prediction

An illustrative series of pressure-temperature projections for toluene and cyclohexane + n-alkane binary mixtures is provided in Figures 3.3 and 3.4 for predictions based on the PR and SRK equations of state respectively. In all cases Type II phase behavior is predicted. However, for short n-alkanes, the predicted LL behavior arises at temperatures well below the freezing points of both constituents and is of minor interest from a phase behavior prediction perspective, because the conditions are well outside the range of validity of the fluid models. Incorrect phase behavior prediction is only relevant if the predicted upper critical end point (UCEP) at the intersection of the liquid-liquid critical locus with the liquid-liquid-vapor curve arises under conditions where solids do not occur. In this work, the temperature selected is the higher of the two melting point temperatures of the binary constituents. This designation provides a conservative lower bound on the application of the PR and SRK equations of state and avoids the ambiguity inherent in composition dependent lower temperature limits and in eutectic calculations, both with respect to temperature and composition. On this basis, the effective phase behavior type for toluene + n-C_{15} is Type I, whereas for toluene + n-C_{20} the designation is Type II, whether the PR or SRK equation of state is used to calculate the projection. The computed projections for cyclohexane + n-alkanes, also shown in Figures 3.3 and 3.4 are qualitatively similar. Again as the n-alkane chain length grows, the predicted UCEP shifts to higher temperatures, and exceeds the melting point of n-triacontane for cyclohexane + n-triacontane mixtures, triggering an effective phase behavior designation change from Type I to Type II.

Pressure-temperature projections obtained using the PC SAFT equation of state for binary mixtures of n-C_{50} + aromatic and naphthenic compounds are shown in Figures 3.5 and 3.6 respectively. For all of the n-alkane + aromatic and some of the n-alkane + naphthenic binaries these pressure-temperature projections are nominally Type II but the calculated upper critical end points (UCEPs) are at temperatures much lower than those obtained using the cubic equations of state. All are below the relevant melting points and the effective phase behavior for all these cases is Type I. However there are a few cases, e.g.: 1-methynaphthalene + n-C_{50} (Figure 3.5f), where the UCEP approaches the melting point of lower melting component and Type II phase behavior may be predicted at temperatures approaching the eutectic temperature for these mixtures. Thus incorrect phase behavior prediction is possible at low temperatures, and in multicomponent mixtures where freezing points are depressed. However, these two topics are beyond the scope of the current work.

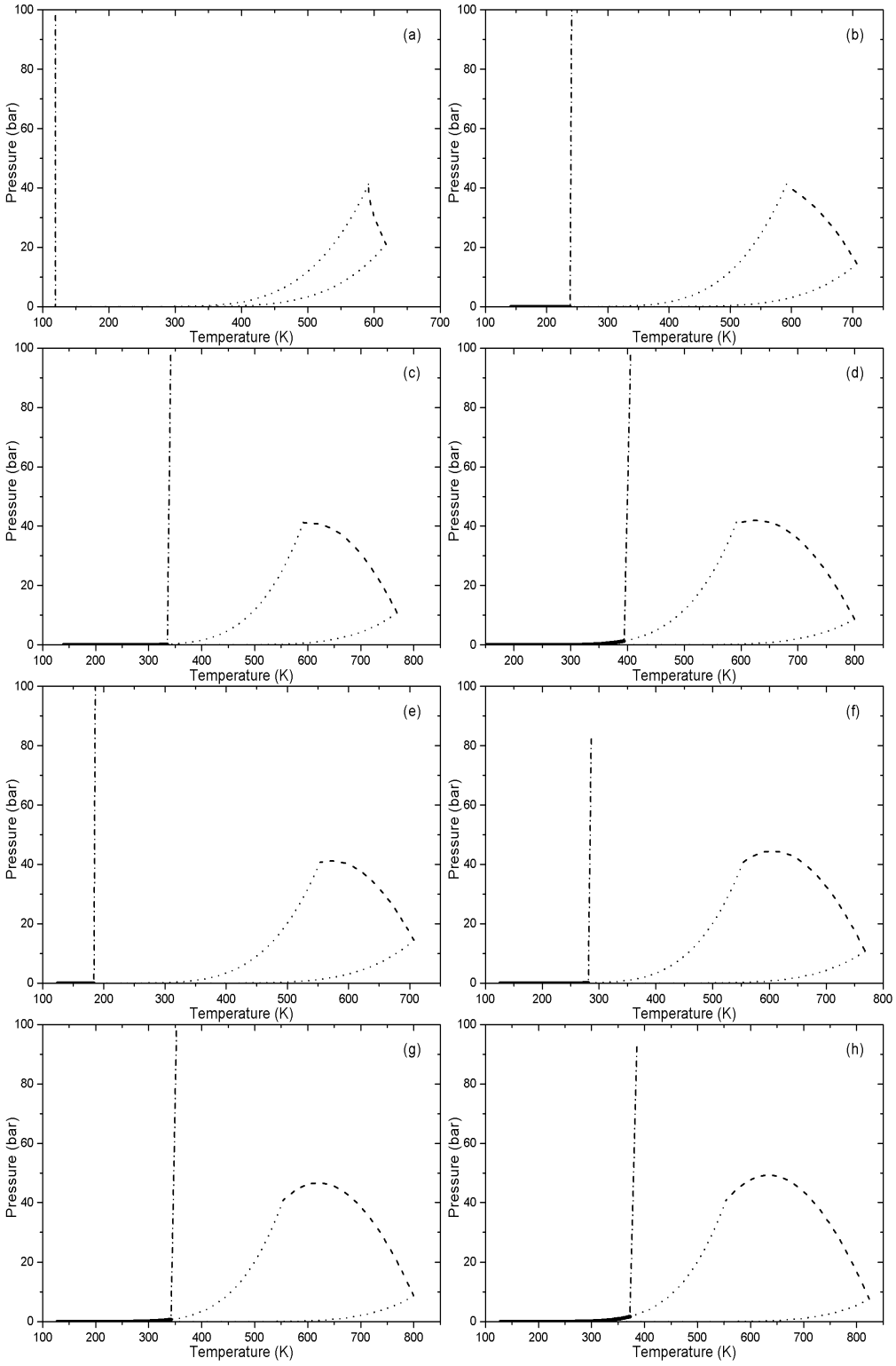

Figure 3.3 Example binary Pressure-Temperature projections calculated using the PR EOS: (a) toluene + n-C_{10}, (b) toluene + n-C_{15}, (c) toluene + n-C_{20}, (d) toluene + n-C_{24}, (e) cyclohexane + n-C_{15}, (f) cyclohexane + n-C_{20}, (g) cyclohexane + n-C_{24}, (h) cyclohexane + n-C_{28}. (····) pure component vapor pressure curve, (– –) liquid-vapor critical locus, (–·–) liquid-liquid critical locus, (——) liquid-liquid-vapor co-existence curve.

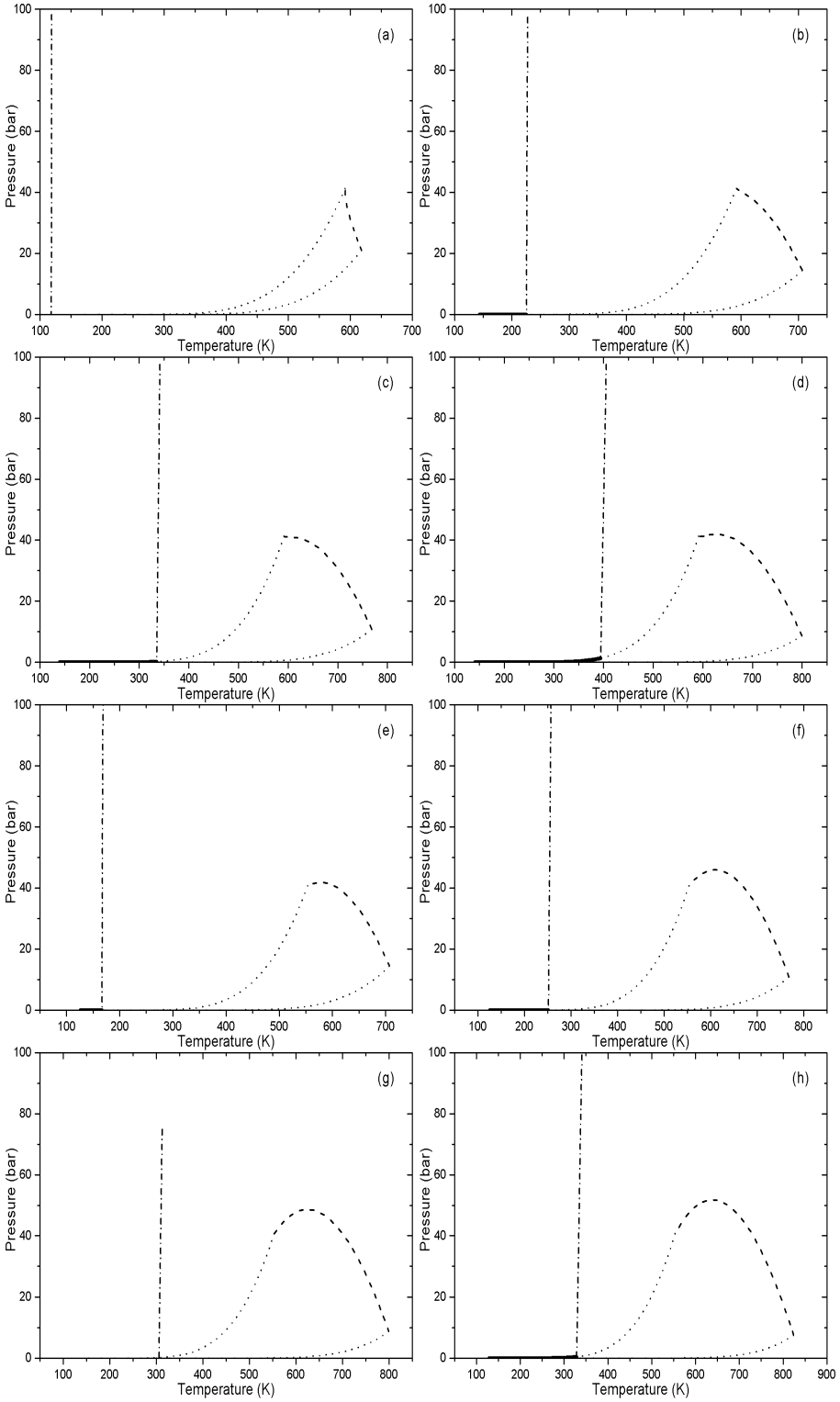

Figure 3.4 Example binary Pressure-Temperature projections calculated using the SRK equation of state: (a) toluene + n-C_{10}, (b) toluene + n-C_{15}, (c) toluene + n-C_{20}, (d) toluene + n-C_{24}, (e) cyclohexane + n-C_{15}, (f) cyclohexane + n-C_{20}, (g) cyclohexane + n-C_{24}, (h) cyclohexane + n-C_{28}. (····) pure component vapor pressure curve, (– –) liquid-vapor critical locus, (– . –) liquid-liquid critical locus, (——) liquid-liquid-vapor co-existence curve.

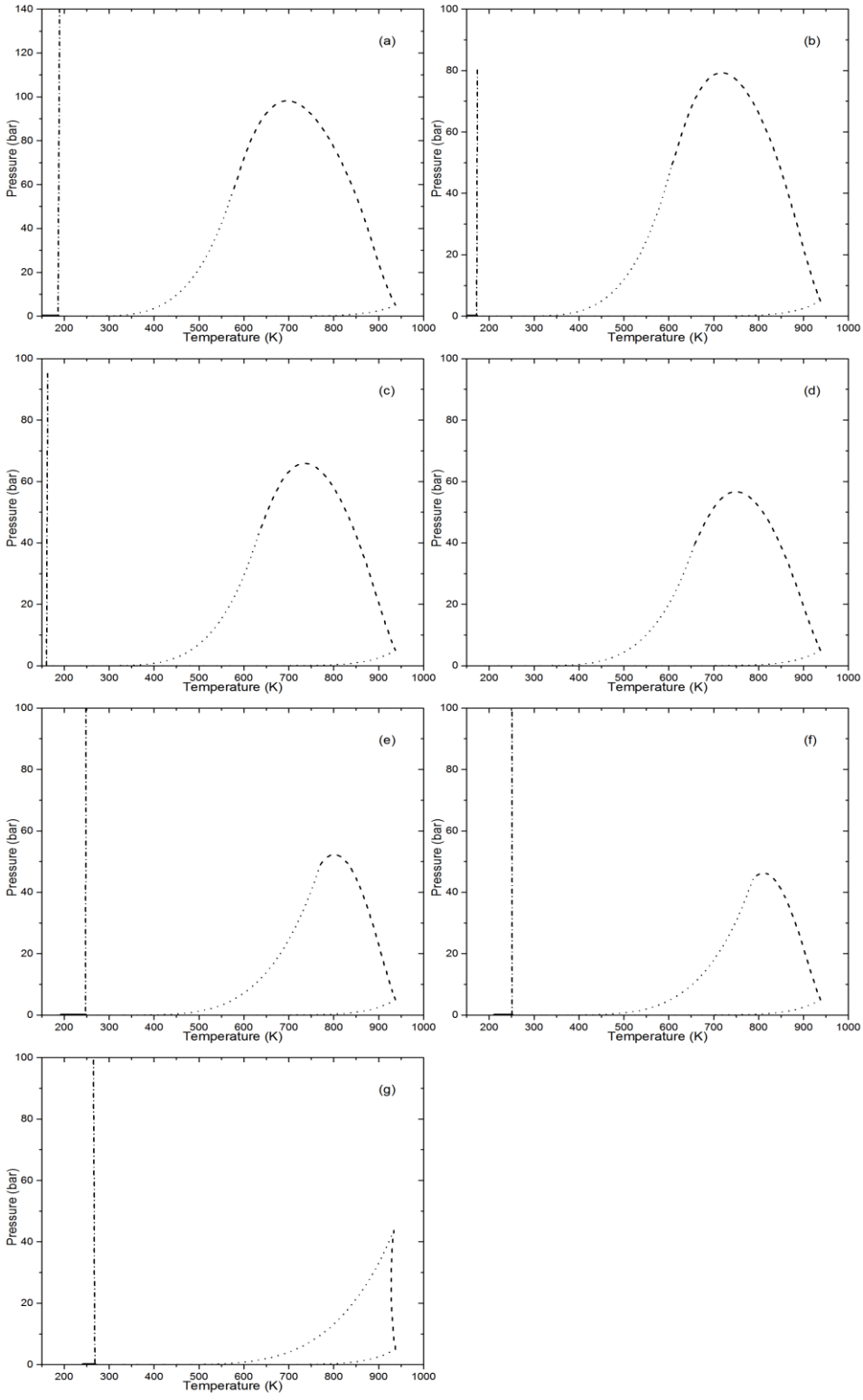

Figure 3.5 Example Pressure-Temperature projections for binary mixtures of n-C_{50} + aromatic compounds computed using the PC SAFT equation of state: (a) benzene + n-C_{50}; (b) toluene + n-C_{50}; (c) ethylbenzene + n-C_{50}; (d) n-propylbenzene + n-C_{50}; (e) naphthalene + n-C_{50}; (f) 1-methylnaphthalene + n-C_{50}; (g) phenanthrene + n-C_{50}. Curves: (····) pure component vapor pressure curve, (– –) liquid-vapor critical locus, (– . –) liquid-liquid critical locus, (——) liquid-liquid-vapor co-existence curve.

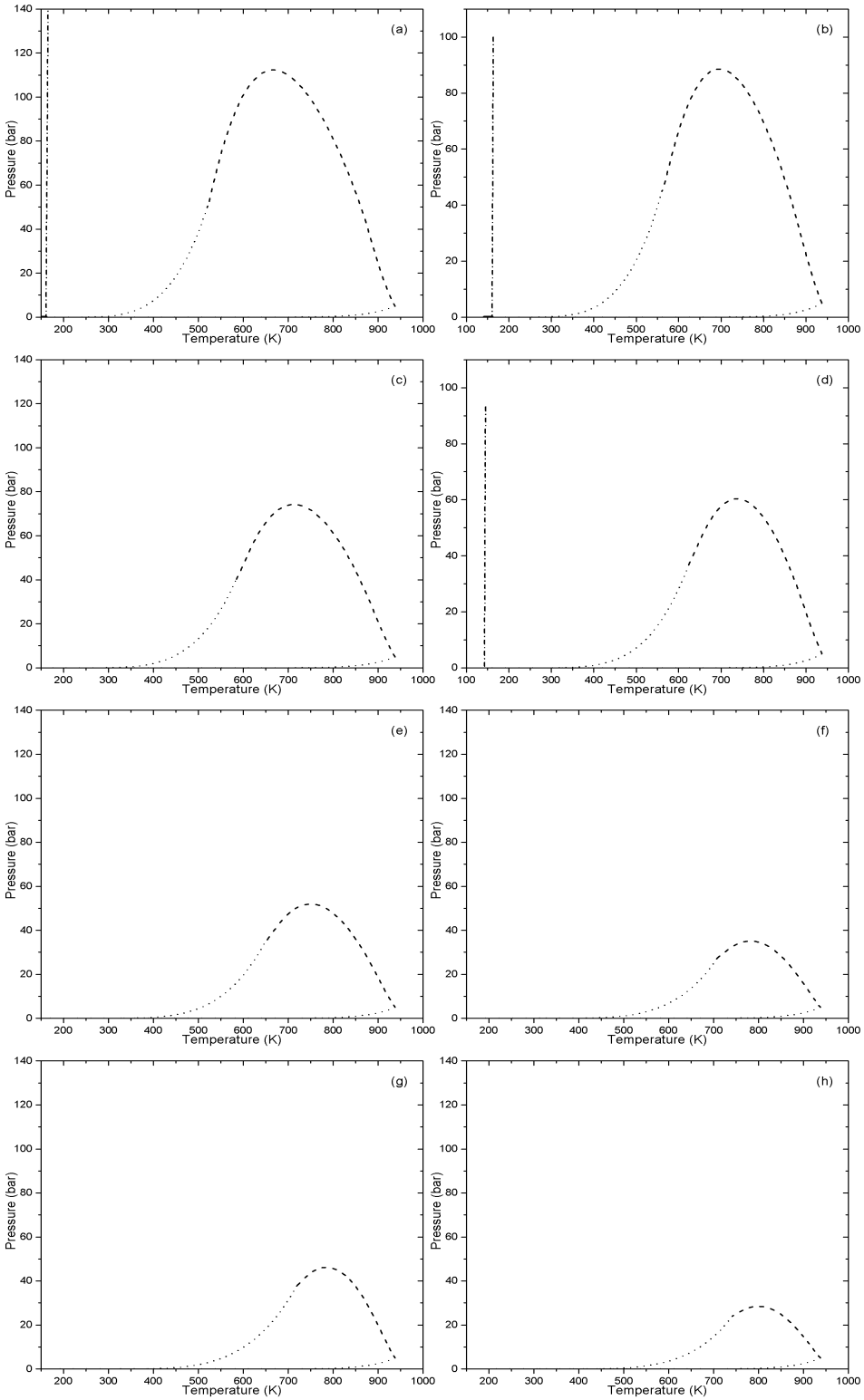

Figure 3.6 Example Pressure-Temperature projections for binary mixtures of n-C_{50} + naphthenic compounds computed using the PC SAFT equation of state: (a) cyclopentane + n-C_{50}; (b) cyclohexane + n-C_{50}; (c) methylcyclohexane + n-C_{50}; (d) ethylcyclohexane + n-C_{50}; (e) n-propylcyclohexane + n-C_{50}; (f) bicyclohexyl + n-C_{50}; (g) cis-decahydronaphthalene + n-C_{50}; (h) perhydrophenanthrene + n-C_{50}. Curves: (····) pure component vapor pressure curve, (– –) liquid-vapor critical locus, (– . –) liquid-liquid critical locus, (——) liquid-liquid-vapor co-existence curve.

3.4.3 Predicted vs Measured Phase Behaviors

Computed temperature-composition phase diagrams showing liquid-liquid phase behavior for illustrative binary mixtures at 1 bar, based on both the PR and SRK equations of state are compared with measured single phase behaviors in Figure 3.7. Most of the experiments were performed under conditions where these equations of state incorrectly predict the presence of two liquid phases. Liquid-liquid phase behavior was not observed in any of the experiments. Moreover, there is no evidence in the literature of LLE data for any of the binary mixtures studied in this paper. Available liquid to solid-liquid phase boundary data for binary n-alkane + aromatic and n-alkane + naphthenic mixtures, shown in Table 3.3, are also consistent with a Type I phase behavior designation while for most saturated liquid compositions along the L-SL boundaries, the PR and SRK equations of state incorrectly predict liquid-liquid phase behavior. By contrast, the PC-SAFT equation of state in both the GPEC and Aspen Plus software predicts one liquid phase to be stable.

These outcomes underscore the disagreement between the measured and predicted phase behaviors obtained using the PR and SRK equations of state. While it can be argued that these experimental measurements do not preclude the possible presence of a lower critical end point at higher temperatures and pressures and hence possible Type V or Type VI phase behavior as shown in Figure 1.2, extant examples of these other phase behavior types are unrelated to mixtures in the present study, and binary mixtures of n-alkanes + aromatic and naphthenic compounds can be assumed to exhibit Type I phase behavior. As global searches were performed during the stability analysis with the PR and SRK equations of state, the source of the disagreement rests with inappropriate selection of pure component properties and/or binary interaction parameters that define the phase equilibrium calculations.

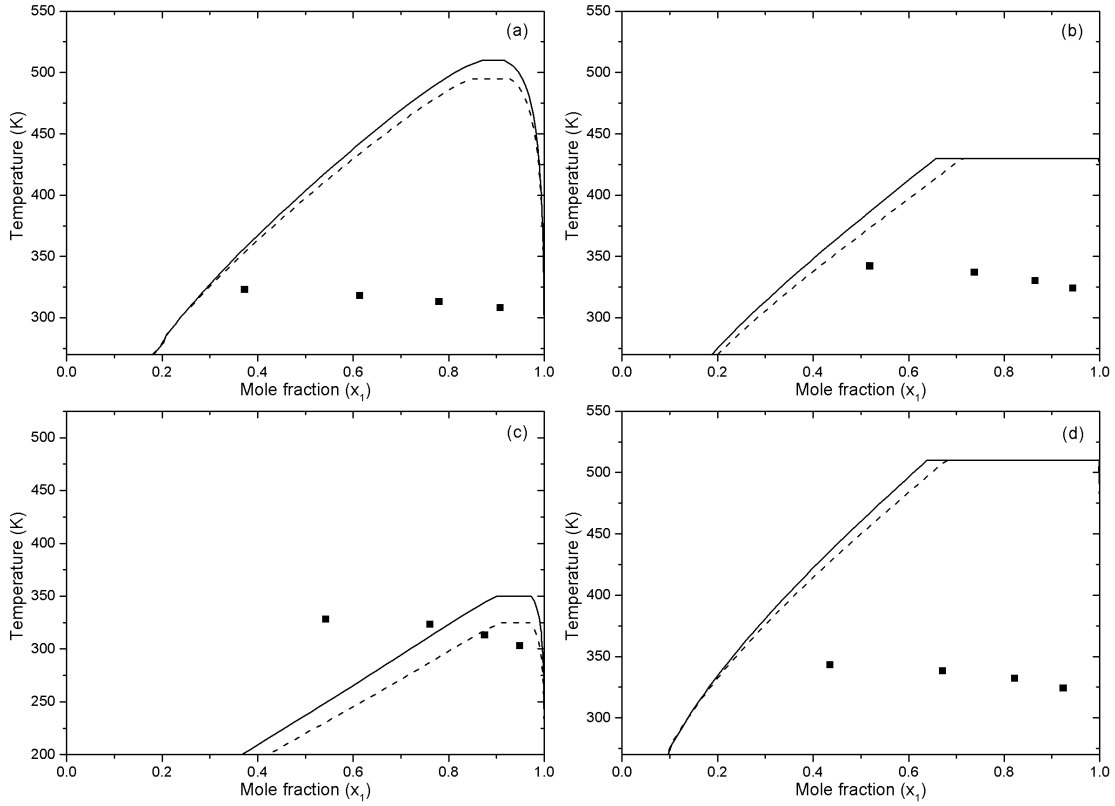

Figure 3.7 Temperature-composition phase diagrams at 1 bar for the binary mixtures: a) 1-methylnaphthalene(1) + n-C_{24}(2), (b) n-propylbenzene(1) + n-C_{36}(2), (c) cyclohexane(1) + n-C_{28}(2). (d) bicyclohexyl(1)+ n-C_{36}(2). Curves: LL boundary according to the PR (—) and SRK (– –) equations of state, (▪) experimental observation of one liquid phase.

Table 3.3 Liquid phase stability at the liquid to solid-liquid phase boundary composition data for binary n-alkane + aromatic and naphthenic mixtures.

Component 1	Component 2	T (K)	wt % (1)	Experiments	PR	SRK	Ref.
$C_{20}H_{42}$	Benzene	282	13.66	Stable	Unstable	Unstable	42
		284	19.51	Stable	Unstable	Unstable	
		289	33.39	Stable	Unstable	Unstable	
		292	44.31	Stable	Unstable	Unstable	
		294	53.20	Stable	Unstable	Unstable	
		299	70.39	Stable	Stable	Stable	
		299	71.54	Stable	Stable	Stable	
$C_{24}H_{50}$	Toluene	277	1.45	Stable	Unstable	Unstable	43
		279	2.02	Stable	Unstable	Unstable	
		282	3.02	Stable	Unstable	Unstable	
		284	4.01	Stable	Unstable	Unstable	

		289	7.78	Stable	Unstable	Unstable	
$C_{28}H_{58}$	Cyclopentane	283	4.03	Stable	Unstable	Stable	44
		286	5.28	Stable	Unstable	Stable	
		292	9.83	Stable	Unstable	Unstable	
		300	23.70	Stable	Unstable	Unstable	
		305	32.14	Stable	Unstable	Unstable	
		310.2	45.71	Stable	Unstable	Unstable	
		313.95	56.00	Stable	Unstable	Unstable	
$C_{28}H_{58}$	Cyclohexane	280.65	1.39	Stable	Stable	Stable	45
		289.45	4.74	Stable	Stable	Stable	
		296	10.97	Stable	Unstable	Stable	
		300	17.69	Stable	Unstable	Unstable	
		307	31.69	Stable	Unstable	Unstable	
		309	36.03	Stable	Unstable	Unstable	
		316	53.30	Stable	Unstable	Unstable	
		319	61.63	Stable	Unstable	Unstable	
		322	69.36	Stable	Unstable	Unstable	
$C_{28}H_{58}$	Toluene	280	0.40	Stable	Unstable	Unstable	43
		283	0.67	Stable	Unstable	Unstable	
		286	1.03	Stable	Unstable	Unstable	
		290	2.02	Stable	Unstable	Unstable	
		293	3.01	Stable	Unstable	Unstable	
		297	5.80	Stable	Unstable	Unstable	
		301	9.66	Stable	Unstable	Unstable	
$C_{36}H_{74}$	1-Methylnaphthalene	308	0.28	Stable	Unstable	Unstable	43
		312	0.66	Stable	Unstable	Unstable	
		314	0.99	Stable	Unstable	Unstable	
		318	2.05	Stable	Unstable	Unstable	
		320	3.07	Stable	Unstable	Unstable	
		321	4.06	Stable	Unstable	Unstable	
		325	8.00	Stable	Unstable	Unstable	
		327	12.00	Stable	Unstable	Unstable	
$C_{36}H_{74}$	Toluene	298	0.31	Stable	Unstable	Unstable	

		302	0.66	Stable	Unstable	Unstable	[43]
		303	1.00	Stable	Unstable	Unstable	
		307	2.00	Stable	Unstable	Unstable	
		309	3.02	Stable	Unstable	Unstable	
		311	4.01	Stable	Unstable	Unstable	
		314	7.97	Stable	Unstable	Unstable	
		317	12.03	Stable	Unstable	Unstable	
$C_{36}H_{74}$	Cyclohexane	295	0.6	Stable	Unstable	Unstable	[43]
		297	0.99	Stable	Unstable	Unstable	
		301	2.04	Stable	Unstable	Unstable	
		303	3.25	Stable	Unstable	Unstable	
		305	4.06	Stable	Unstable	Unstable	
		309	8.02	Stable	Unstable	Unstable	
		312	11.98	Stable	Unstable	Unstable	
$C_{36}H_{74}$	Cyclopentane	290	0.5	Stable	Unstable	Unstable	[43]
		294	0.99	Stable	Unstable	Unstable	
		298	2.11	Stable	Unstable	Unstable	
		301	3	Stable	Unstable	Unstable	
		302	4	Stable	Unstable	Unstable	
		306	8	Stable	Unstable	Unstable	
$C_{36}H_{74}$	Decahydronaphthalene	296	0.33	Stable	Unstable	Unstable	[43]
		299	0.67	Stable	Unstable	Unstable	
		301	1	Stable	Unstable	Unstable	
		305	2.01	Stable	Unstable	Unstable	
		307	3.04	Stable	Unstable	Unstable	
		308	4.01	Stable	Unstable	Unstable	
		313	7.97	Stable	Unstable	Unstable	
		316	12.1	Stable	Unstable	Unstable	
$C_{40}H_{82}$	Toluene	304	0.32	Stable	Unstable	Unstable	[43]
		307	0.60	Stable	Unstable	Unstable	
		309	1.00	Stable	Unstable	Unstable	
		313	2.00	Stable	Unstable	Unstable	
		315	3.02	Stable	Unstable	Unstable	

		317	4.00	Stable	Unstable	Unstable	

3.4.4 Sensitivity of PR and SRK Phase Behavior Type Predictions to Input Parameters T_c, P_c , and ω for n-alkanes

The critical temperature, critical pressure and acentric factor of a compound are used to calculate generalized parameters in the PR and SRK equations of state. One tends to think of these as measured properties but for large and thermally unstable compounds this is not the case. For n-alkanes, these input parameters are generally estimated using correlations for compounds larger than n-eicosane[46-49] and they possess significant uncertainty as noted in Figure 3.1. Depending on the correlations or combinations of correlations that are selected, predicted phase behavior types may differ. To examine the impact of individual properties on phase behavior Type calculations, critical temperature, critical pressure and acentric pressure were varied individually while the other properties were kept constant at their respective standard values shown in Table S4. Measured critical properties are available for the aromatic and naphthenic compounds used in this parametric investigation. The outcomes from the independent variation of n-alkane critical pressure, critical temperature and acentric pressure from their respective standard values are summarized in Figure 3.8, for n-alkane + aromatic binaries, and in Figure 3.9, for n-alkane + naphthenic compounds. Increasing n-alkane critical pressures from standard values leads to Type I phase behavior prediction. The required critical pressure values lie inside the ranges indicated by Stamataki and Tassios[21] and NIST/TDE[37] for some of the binary n-alkane + naphthene and n-alkane + aromatics mixtures while required acentric factors and critical temperatures fall outside the ranges indicated by Stamataki and Tassios[21]. Outcomes for the joint variation of pure n-alkane component properties within the

ranges suggested by Stamataki and Tassios[21] are shown in Figures 3.10a and 3.10b. While there are some examples where Type I phase behavior is predicted rather than Type II phase behavior, for specific n-alkane + naphthenic and n-alkane + aromatic binaries, there are no systematic impacts affecting the trends observed with standard values, for n-alkane + aromatic and n-alkane + naphthenic binary mixtures. Uncertainty of n-alkane pure component properties contributes to the misprediction of the phase behavior type but correct phase behavior type predictions are not guaranteed systemically if these input parameters are adjusted within their uncertainty limits. Hence, incorrect phase behavior type prediction cannot be attributed to the uncertainty of n-alkane pure component properties.

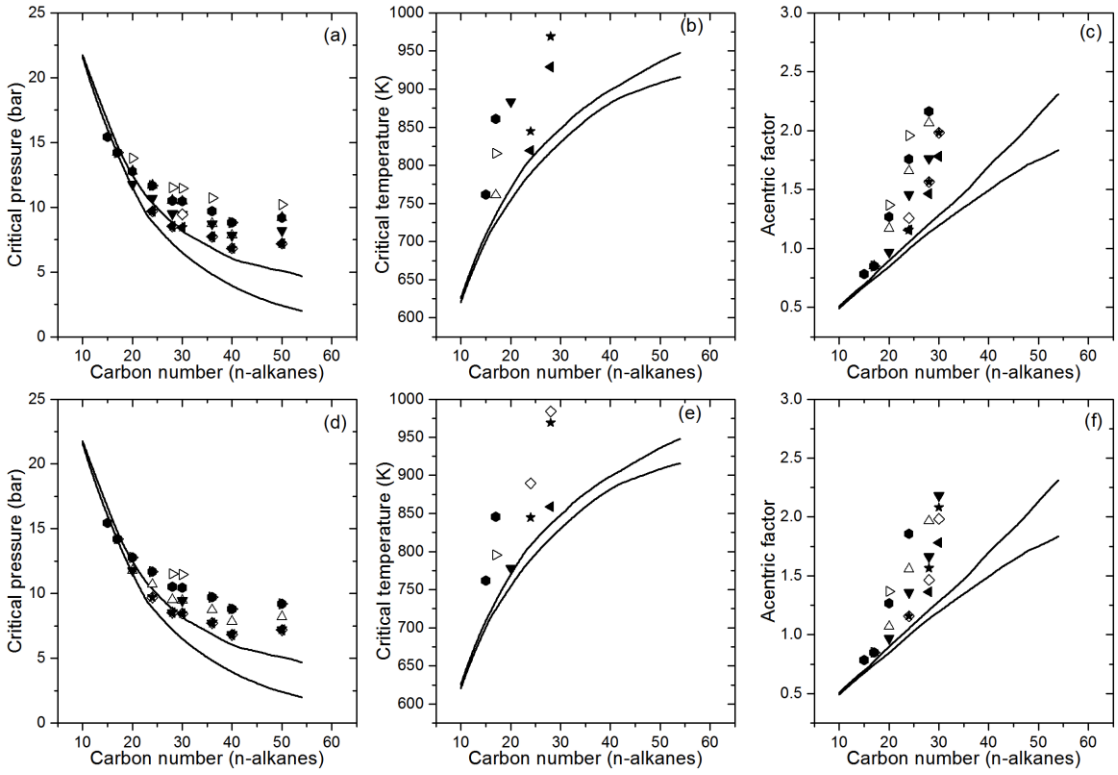

Figure 3.8 Required pure component properties for n-alkanes to obtain Type I phase behavior prediction for binary mixtures of n-alkanes + aromatics using the PR (a-c) and SRK (d-f) equations of state. Symbols: (△) benzene, (▼) toluene, (◇) ethylbenzene, (◀) n-propylbenzene, (▷) naphthalene, (⬢) 1-methylnaphthalene, (★) phenanthrene. Curves (—) bounds suggested by Stamataki and Tassios[21].

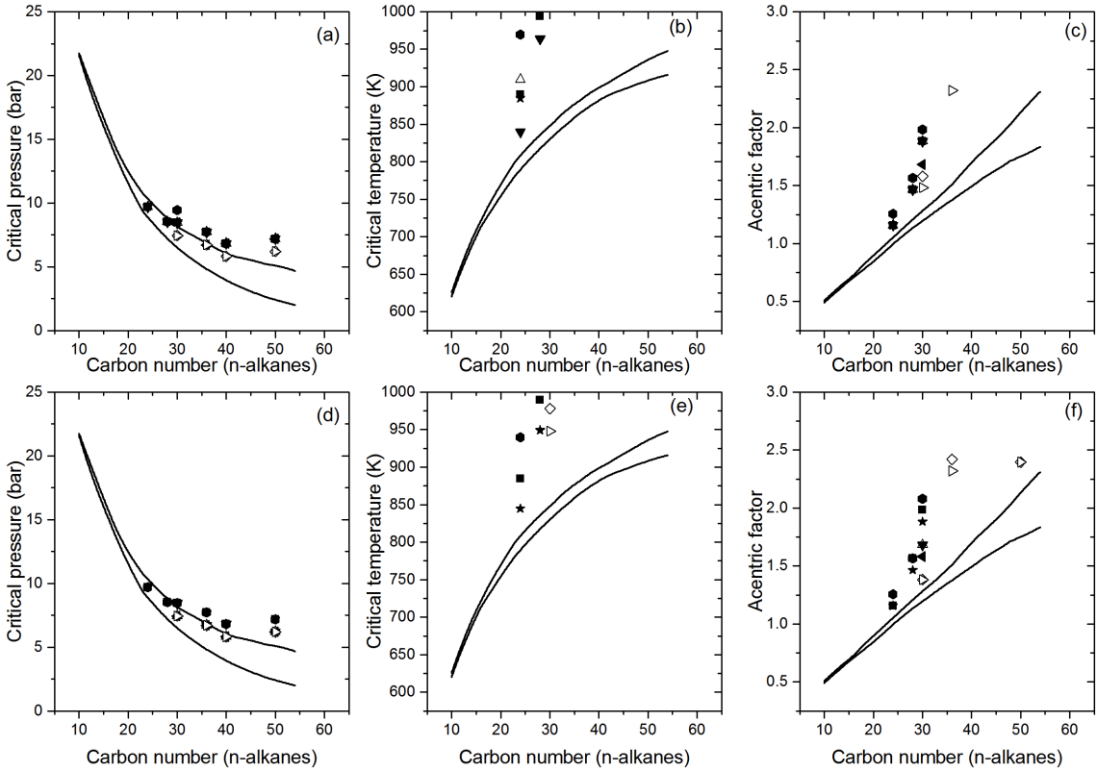

Figure 3.9 Required pure component properties for n-alkanes to obtain Type I phase behavior prediction for binary mixtures of n-alkanes + naphthenic compounds using the PR (a-c) and SRK (d-f) equations of state. Symbols: (△) cyclopentane, (▼) cyclohexane, (◇) methylcyclohexane, (◀) ethylcyclohexane, (▷) n-propylcyclohexane, (⬢) bicyclohexyl, (★) decahydronaphthalene, (■) perhydrophenanthrene. Curves: (—) bounds suggested by Stamataki and Tassios[21].

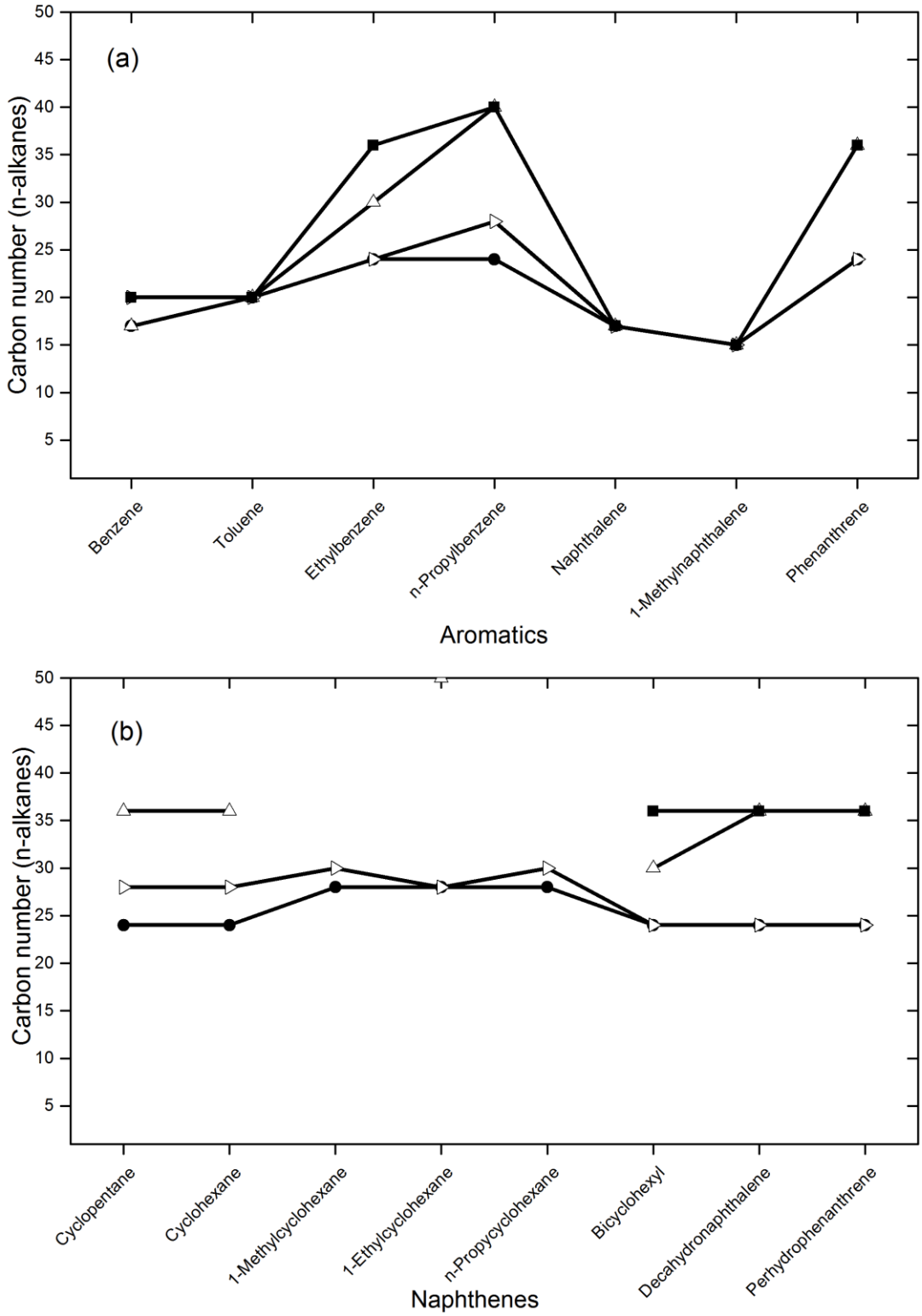

Figure 3.10 Phase stability analysis result summary showing the first unstable binary mixture in a series: (a) binary mixtures of n-alkanes + aromatics, (b) binary mixtures of n-alkanes + naphthenes. Symbols: PR equation of state with pure component properties at the lower (—●—) and (—△—) upper bounds and the SRK equation of state with pure component properties at lower (—▷—) and upper (—■—) bounds listed in Table S5.

3.4.5 Sensitivity of PR and SRK Phase Behavior Type Predictions to k_{ij} Values

Sensitivity analyses paralleling the calculations performed for pure component properties were performed for k_{ij} values. The maximum k_{ij} values that lead to the prediction of Type I phase behavior are presented in Figures 3.11 (a-f) and 3.12 (a-f). Irrespective of the assumptions made regarding the pure component property values of n-alkanes, the trends are qualitatively similar. The k_{ij} values trend to negative values with increasing chain length. From a quantitative perspective, the magnitudes of the k_{ij} values required for the SRK equation of state are smaller than the corresponding values required for the PR equation of state, c.f.: Figures 3.11a vs 3.11d, and Figure 3.12a vs 3.12d. This outcome shows that both of these equations of state provide skewed fits for these classes of mixtures, relative to expectation, and that the skew is worse for the PR than for the SRK equation of state. More typically, interaction parameter values are expected to be positive and are expected to increase, not decrease with compound molar mass[22] if the properties of the second component are fixed. This point is illustrated in Figure 3.13 for n-alkane + benzene mixtures. Binary interaction parameter values calculated using a correlation by Gao et al.[22], are contrasted with maximum values yielding Type I phase behavior calculated in this work, and interaction parameter values fit[50] to experimental vapor-liquid equilibrium data[37], also part of this work, for binary mixtures of benzene with n-C_5, n-C_6, n-C_7, n-C_8, n-C_9, n-C_{10}, n-C_{14}, n-C_{16}, and n-C_{17}. Fitted k_{ij} values for benzene + n-alkane binary mixtures larger than n-nonane are negative, for both the PR and SRK equations of state and the trend of the fit k_{ij} values is consistent with the corresponding maximum k_{ij} values that yield Type I phase behavior for both cubic equations of state. All of the fit values, and their extrapolation to larger n-alkanes, fall at or below the maximum values. By contrast the predicted k_{ij} values, based on the correlation by Gao

et al.[22] are all positive and increase with n-alkane molar mass. While this correlation, based on benzene and toluene, performs quite well when calculating bubble and dew pressures of light paraffins and benzene or cyclohexane, it is clearly inadequate for heavier paraffin/aromatic mixtures.

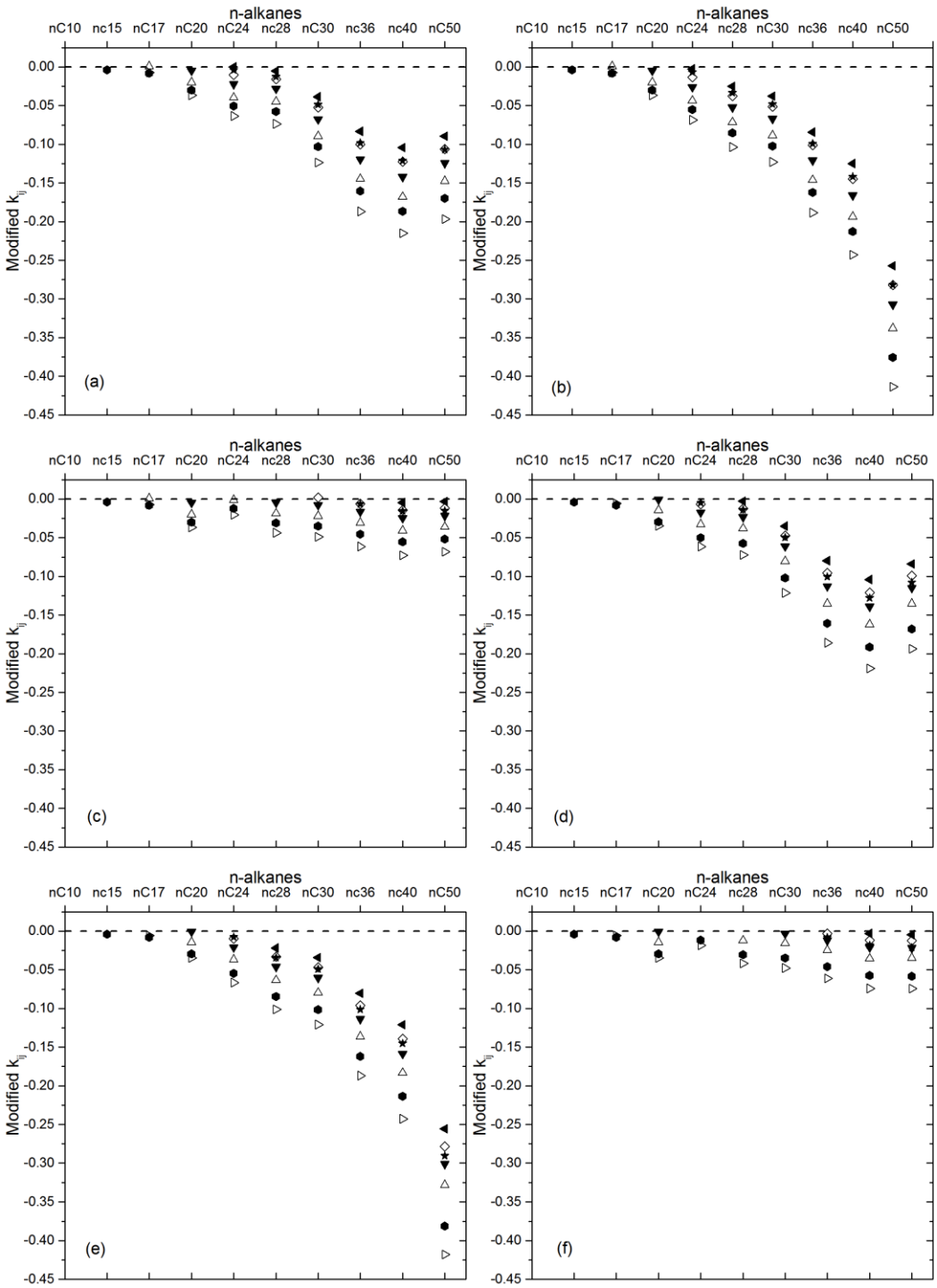

Figure 3.11 Maximum k_{ij} values for n-alkane + aromatic binary mixtures yielding Type I phase behavior for the PR (a-c) and SRK (d-f) equations of state: (a) standard pure component property

values; (b) pure component property values at lower bound; (c) pure component property values at upper bound; (d) standard pure component property values; (e) pure component property values at lower bound; (f) pure component property values at upper bound. Symbols: (△) benzene, (▼) toluene, (◇) ethylbenzene, (◀) n-propylbenzene, (▷) naphthalene, (⬢) 1-methylnaphthalene, (★) phenanthrene.

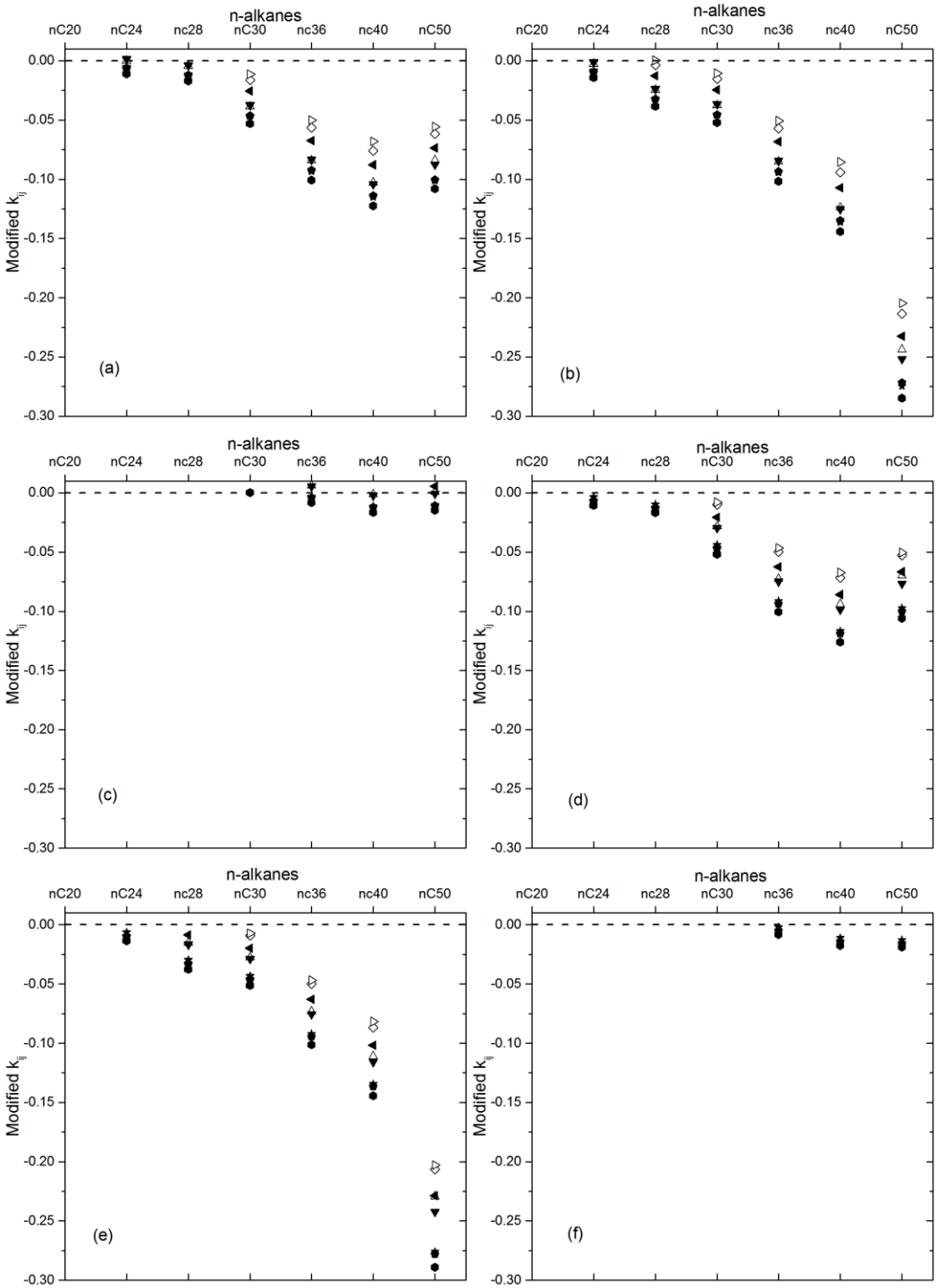

Figure 3.12 Maximum k_{ij} values for n-alkane + naphthenic binary mixtures yielding Type I phase behavior for the PR (a-c) and SRK (d-f) equations of state: (a) standard pure component property values; (b) pure component property values at lower bound; (c) pure component property values at upper bound; (d) standard pure component property values; (e) pure component property values at lower bound; (f) pure component property values at upper bound. Symbols: (△) cyclopentane, (▼)

cyclohexane, (◇) methylcyclohexane, (◀) ethylcyclohexane, (▷) n-propylcyclohexane, (⬢) bicyclohexyl, (★) cis-decahydronaphthalene, (⬟) perhydrophenanthrene

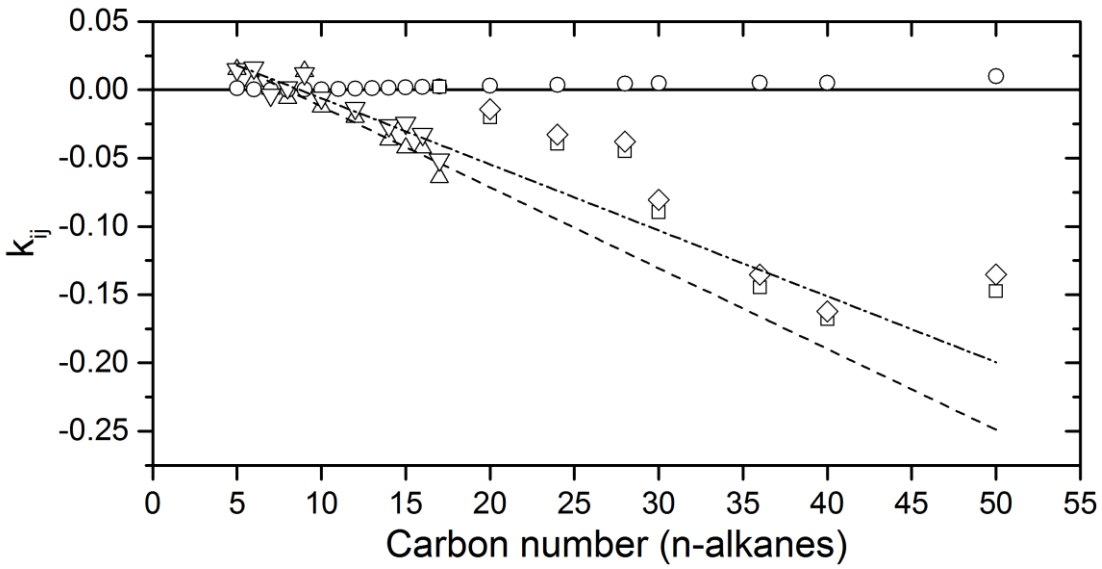

Figure 3.13 k_{ij} values for the PR and SRK EOS for binary benzene + n-alkanes mixtures: (△) regressed from experimental data for PR EOS (this work); (▽) regressed from experimental data for SRK EOS (this work); (○) estimated using a correlation by Gao et al.[22] for PR EOS; (□) upper limit calculated in this work based on standard values for pure component properties for PR EOS; (◇) upper limit calculated in this work based on standard values for pure component properties for SRK EOS. Curve: (– –) linear extrapolation of fit k_{ij} values for benzene + n-alkane mixtures for PR EOS; (–·–) linear extrapolation of fit k_{ij} values for benzene + n-alkane mixtures for SRK EOS.

3.5 Conclusions and Future Work

The Peng-Robinson and Soave-Redlich-Kwong cubic equations of state overestimate the non-ideality of binary mixtures of long chain n-alkane + aromatic and long chain n-alkane + naphthenic compounds and systematically predict non-physical phase behaviors. Type II phase behavior is predicted while Type I phase behavior is observed experimentally. Phase behavior misprediction is insensitive to the values of critical temperature, critical pressure and acentric factor of long chain n-alkanes which must be obtained from correlations, and the details of phase stability analysis procedures. To obtain qualitatively correct phase behavior predictions, negative binary interaction parameter values must be used for these two classes of mixture and the value must trend to larger negative values with increasing n-alkane chain length. This trend is shown to be at odds with widely used correlations for interaction

parameter estimation, which yield positive values and which trend to larger positive values with chain length or equivalently with increasing differences in molecular size. These results underscore the need for revised interaction parameters and generalized correlations so that predicted phase behaviors are consistent with available measurements. They also highlight the need for additional experimental data so that quantitative phase composition comparisions can be made between predicted and measured phase behaviors. The PC-SAFT equation of state with standard pure component parameters and zero binary interaction parameters is shown to predict the correct phase behavior of long chain n-alkane + aromatic and long chain n-alkane + naphthenic binary mixtures. However, the possibility of incorrect phase behavior prediction cannot be precluded in multicomponent mixtures near eutectic points. This work points to the need for a comprehensive comparison between cubic equations of state and SAFT from a global phase behaviour prediction perspective – phase envelope topology, VLE, VLLE and critical point prediction accuracy – in order to define models that provide comprehensive pictures of the correct thermodynamic landscape with reasonable accuracy. Development of better methods for binary interaction parameter estimation comprise a key part of this future work.

3.6 Nomenclature

a temperature dependent function of the equation of state

b covolume

EOS equation of state

ε/k segment energy parameter

k_{ij} binary interaction parameter

L liquid

LL liquid-liquid

LV	liquid-vapor
LLV	liquid-liquid-vapor
LLE	liquid-liquid equilibrium
m	shape parameter
n-C_n	n-alkane with n number of carbon atoms
ω	acentric factor
P	pressure
P_c	critical pressure
R	gas constant
σ	segment diameter
SL	solid-liquid
T_B	normal boiling temperature
T_c	critical temperature
T_F	freezing temperature
UCEP	upper critical end point
V	vapor
v	molar volume
Z_C	critical compressibility

3.7 References

(1) Peng, D. -Y; Robinson, D. B. New two-constant equation of state. *Ind. Eng. Chem. Fundam.* **1976**, 15, 59-64.

(2) Soave, G. Equilibrium constants from a modified Redlich-Kwong equation of state. *Chem. Eng. Sci.* **1972**, 27, 1197-1203.

(3) Gross, J.; Sadowski, G. Perturbed-chain SAFT: An equation of state based on a perturbation theory for chain molecules. *Ind. Eng. Chem. Res.* **2001**, 40, 1244-1260.

(4) Gross, J.; Sadowski, G. Modeling polymer systems using the perturbed-chain statistical associating fluid theory equation of state. *Ind. Eng. Chem. Res.* **2002**, 41, 1084-1093.

(5) Leekumjorn, S.; Krejbjerg, K. Phase behavior of reservoir fluids: Comparisons of PC-SAFT and cubic EOS simulations. *Fluid Phase Equilib.* **2013**, 359, 17-23.

(6) Gonzalez, D. L.; Hirasaki, G. J.; Creek, J.; Chapman, W. G. Modeling of asphaltene precipitation due to changes in composition using the perturbed chain statistical associating fluid theory equation of state. *Energy Fuels* **2007**, 213, 1231-1242.

(7) Gonzalez, D. L.; Vargas, F. M.; Hirasaki, G. J.; Chapman, W. G. Modeling study of CO2-induced asphaltene precipitation. *Energy Fuels* **2008**, 22, 757-762.

(8) Vargas, F. M.; Gonzalez, D. L.; Hirasaki, G. J.; Chapman, W. G. Modeling asphaltene phase behavior in crude oil systems using the perturbed chain form of the statistical associating fluid theory (PC-SAFT) equation of state. *Energy Fuels* **2009**, 23, 1140-1146.

(9) Yelash, L.; Müller, M.; Paul, W.; Binder, K. Artificial multiple criticality and phase equilibria: An investigation of the PC-SAFT approach. *Phys. Chem. Chem. Phys.* **2005**, 7, 3728-3732.

(10) Privat, R.; Gani, R; Jaubert, J. Are safe results obtained when the PC-SAFT equation of state is applied to ordinary pure chemicals? *Fluid Phase Equilib.* **2010**, 295, 76-92.

(11) Yelash, L.; Müller, M.; Paul, W.; Binder, K. A global investigation of phase equilibria using the perturbed-chain statistical-associating-fluid-theory approach. *J. Chem. Phys.* **2005**, 123, 014908.

(12) Saber, N.; Shaw, J. M. Rapid and robust phase behaviour stability analysis using global optimization. *Fluid Phase Equilib.* **2008**, 264, 137-146.

(13) Mushrif, S. H.; Phoenix, A. V. Effect of Peng-Robinson binary interaction parameters on the predicted multiphase behavior of selected binary systems. *Ind. Eng. Chem. Res.* **2008**, 47, 6280-6288.

(14) Saber, N.; Shaw, J. M. Toward multiphase equilibrium prediction for ill-defined asymmetric hydrocarbon mixtures. *Fluid Phase Equilib.* **2009**, 285, 73-82.

(15) Konynenburg, van, P. H.; Scott, R. L. Critical lines and phase-equilibria in binary van der Waals mixtures. *Philos. Trans. R. Soc., A* **1980**, 298, 495-540.

(16) Jones, D. R.; Perttunen, C. D.; Stuckman, B. E. Lipschitzian optimization without the Lipschitz constant. *J. Optimiz. Theory Appl.* **1993**, 79, 157-181.

(17) *VMGSim Process Simulator*, Version 8.0; Virtual Materials Group Inc.: Calgary, AB 2013.

(18) *Aspen HYSYS,* Version 8.4; Aspen Technology, Inc.: Burlington, MA 2013.

(19) Cismondi, M.; Nuñez, D. N.; Zabaloy, M. S.; Brignole, E. A.; Michelsen, M. L.; Mollerup, J. M. In *GPEC: A Program for Global Phase Equilibrium Calculations in Binary Systems*, Proceedings of Equifase 2006: VII Iberoamerican Conference on Phase Equilibria and Fluid Properties for Process Design, Morelia, Michoacán, México, 2006.

(20) Elhassan, A. E.; Barrufet, M. A.; Eubank, P. T. Correlation of the critical properties of normal alkanes and alkanols. *Fluid Phase Equilib.* **1992**, 78, 139-155.

(21) Stamataki, S.; Tassios, D. Performance of cubic eos at high pressures. *Rev. Inst. Fr. Pet.* **1998**, 53, 367–378.

(22) Gao, G.; Daridon, J. L.; Saint-Guirons, H.; Xans, P.; Montel, F. A simple correlation to evaluate binary interaction parameters of the Peng-Robinson

equation of state : Binary light hydrocarbon systems. *Fluid Phase Equilib.* **1992**, 74, 85–93.

(23) Nishiumi, H.; Arai, T.; Takeuchi, K. Generalization of the binary interaction parameter of the Peng-Robinson equation of state by component family. *Fluid Phase Equilib.* **1988**, 42, 43-62.

(24) Kordas, A.; Magoulas, K.; Stamataki, S.; Tassios, D. Methane-hydrocarbon interaction parameters correlation for the Peng-Robinson and the t-mPR equation of state. *Fluid Phase Equilib.* **1995**, 112, 33-44.

(25) Jaubert, J.; Mutelet, F. VLE predictions with the Peng–Robinson equation of state and temperature dependent kij calculated through a group contribution method. *Fluid Phase Equilib.* **2004**, 224, 285-304.

(26) Jaubert, S.; Mutelet, F.; Corriou, J. Extension of the PPR78 model (predictive 1978, Peng–Robinson EOS with temperature dependent kij calculated through a group contribution method) to systems containing aromatic compounds. *Fluid Phase Equilib.* **2005**, 237, 193-211.

(27) Polishuk, I.; Wisniak, J.; Segura, H. Prediction of the critical locus in binary mixtures using equation of state: I. cubic equations of state, classical mixing rules, mixtures of methane–alkanes. *Fluid Phase Equilib.* **1999**, 164, 13-47.

(28) Baker, L. E.; Pierce, A. C.; Luks, K. D. Gibbs energy analysis of phase equilibria. *Soc. Pet. Eng. J.* **1982**, 22, 731-742.

(29) McDonald, C. M.; Floudas, C. A. Global optimization for the phase stability problem. *AIChE J.* **1995**, 41, 1798-1814.

(30) Sun, A. C.; Seider, W. D. Homotopy-continuation method for stability analysis in the global minimization of the Gibbs Free energy. *Fluid Phase Equilib.* **1995**, 103, 213-249.

(31) Hua, J. Z.; Maier, R. W.; Tessier, S. R.; Brennecke, J. F.; Stadtherr, M. A. Interval analysis for thermodynamic calculations in process design: A novel and completely reliable approach. *Fluid Phase Equilib.* **1999**, 158, 607-615.

(32) Balogh, J.; Csendes, T.; Stateva, R. P. Application of a stochastic method to the solution of the phase stability problem: Cubic equations of state. *Fluid Phase Equilib.* **2003**, 212, 257-267.

(33) Nichita, D. V.; Gomez, S.; Luna E. Phase stability analysis with cubic equations of state by using a global optimization method. *Fluid Phase Equilib.* **2002**, 194, 411-437.

(34) Nichita, D. V.; Gomez, S.; Luna, E. Multiphase equilibria calculation by direct minimization of Gibbs free energy with a global optimization method. *Comput. Chem. Eng.* **2002**, 26, 1703-1724.

(35) Yushan, Z.; Zhihong, X. Lipschitz optimization for phase stability analysis: Application to Soave-Redlich-Kwong equation of state. *Fluid Phase Equilib.* **1999**, 162, 19-29.

(36) Saber, N. Phase Behaviour Prediction for Ill-Defined Hydrocarbon Mixtures. Ph.D. Thesis, University of Alberta, AB, 2011.

(37) *NIST Standard Reference Database 103b: NIST ThermoData Engine*, Version 7.1, accessed from Aspen Plus.

(38) *Aspen Plus*, Version 8.4; Aspen Technology, Inc.: Burlington, MA, 2013.

(39) Tihic, A.; Kontogeorgis, G. M.; Solms, von, N.; Michelsen, M. L. Applications of the simplified perturbed-chain SAFT equation of state using an extended parameter table. *Fluid Phase Equilib.* **2006**, 248, 29-43.

(40) Ting, P. D.; Gonzalez, D. L.; Hirasaki, G. J.; Chapman, W. G. Application of the PC-SAFT equation of state to asphaltene phase behavior. In *Asphaltenes, Heavy Oils, and Petroleomics*; Mullins, O.C., Sheu, E.Y., Hammami, A., Marshall, A.G., Eds.; Springer: New York, **2007**; 301-327.

(41) Hajipour, S.; Satyro, M.A. Uncertainty analysis applied to thermodynamic models and process design - 1. Pure components. *Fluid Phase Equilib.* **2011**, 307, 78-94.

(42) Domanska, U.; Hofman, T.; Rolinska, J. Solubility and vapour pressures in saturated solutions of high-molecular-weight hydrocarbons. *Fluid Phase Equilib.* **1987**, 32, 273-293.

(43) Jennings, D. W.; Weispfennig, K. Experimental solubility data of various n-alkane waxes: Effects of alkane chain length, alkane odd versus even carbon number structures, and solvent chemistry on solubility. *Fluid Phase Equilib.* **2005**, 227, 27-35.

(44) Domanska, U.; Kniaz, K. Solid-liquid equilibrium. cyclopentane-octacosane system. *Int. DATA Ser., Sel. Data Mixtures, Ser. A* **1990**, 206.

(45) Domanska, U.; Rolinska, J.; Szafranski, A. M. Solid-liquid equilibrium. cyclohexane-octacosane system. *Int. DATA Ser., Sel. Data Mixtures, Ser. A* **1987***,* 276.

(46) Joback, K. G.; Reid, R. C. Estimation of pure-component properties from group-contributions. *Chem. Eng. Commun.* **1987**, 57, 233-243.

(47) Constantinou, L.; Gani, R. New group contribution method for estimating properties of pure compounds. *AIChE J.* **1994**, 40, 1697-1709.

(48) Marrero-Morejón, J.; Pardillo-Fontdevila, E. Estimation of pure compound properties using group-interaction contributions. *AIChE J.* **1999**, 45, 615-621.

(49) Marrero, J.; Gani, R. Group-contribution based estimation of pure component properties. *Fluid Phase Equilib.* **2001**, 183, 183-208.

(50) *Thermo Explorer User's Manual*, version 1.0; Virtual Materials Group Inc.: Calgary, AB 2009.

Chapter 4. Quantitative Comparison Between Predicted and Experimental Binary n-Alkane + Benzene Phase Behaviors Using Cubic and PC-SAFT EOS*

4.1 Introduction

Global phase behavior knowledge of hydrocarbon mixtures is important for process design, process optimization, and the safe operation of industrial processes. The Perturbed-Chain Statistical Associating Fluid Theory (PC-SAFT) [1] equation of state correctly predicts Type I phase behavior for binary n-alkane + aromatic and naphthenic mixtures, according to the van Konynenburg and Scott classification scheme [2], while cubic equations of state (Peng-Robinson (PR) [3] and Soave-Redlich-Kwong (SRK) [4]) predict a transition from Type I to Type II phase behavior (Figure 4.1) within these families of mixtures, unless unconventional large and negative interaction parameters (k_{ij}) [5] are used. Pure component critical property uncertainty also plays an important role in phase behavior predictions of these mixtures because the distinction between Type I (miscible components) and Type II phase behaviour (immiscible liquid behaviour at low temperatures) is subtle. Typically the immiscibility is not observed because it arises under conditions where solid-liquid phase behaviour is observed experimentally. Cubic EOS are not typically used for phase equilibrium calculations under such conditions. At higher temperatures (above the L_1=L_2 critical locus) qualitatively correct phase behaviors (L, LV, V, L=V) are

* This chapter has been submitted to Fluid Phase Equilibria journal as "Ahitan, S.; Shaw, J. M. Quantitative Comparison Between Predicted and Experimental Binary n-Alkane + Benzene Phase Behaviors Using Cubic and PC-SAFT EOS."

predicted. However, for process design and process operation optimization, quantitative agreement between predicted and measured phase behaviors and phase compositions is essential. Uncertainty analysis is also a crucial aspect of phase equilibrium calculations even though it is often neglected [6-9]. Over time, calculation uncertainties (phase compositions, phase boundaries, critical points, etc.) are expected to be included as a standard feature in chemical engineering process simulators [10,11].

In this work, agreement between calculated and measured phase behavior of binary n-alkane + benzene mixtures is probed, for carbon number (n) ≤ 36. New bubble pressure data and fitted k_{ij} values are provided for the benzene + n-C_{20}, n-C_{24}, n-C_{28} and n-C_{36} binary mixtures. The focus is on the correctness of predicted vapor-liquid equilibria and, where possible, vapor-liquid (L=V) critical loci. For the PR and SRK cubic EOS, the impact of the selection of k_{ij} values is assessed at three levels (k_{ij} = 0, k_{ij} values fit to experimental bubble pressure data, and maximum k_{ij} values yielding Type I phase behaviour) and the sensitivity of k_{ij} values to selection of critical pressure and temperature is discussed. For the PC-SAFT EOS k_{ij} values are assumed to be zero. These mixtures are illustrative and the calculations provide clear indications of the inherent uncertainty of the shapes of bubble pressure curves, and vapor-liquid critical loci that arise when EOS models are used and common assumptions are applied.

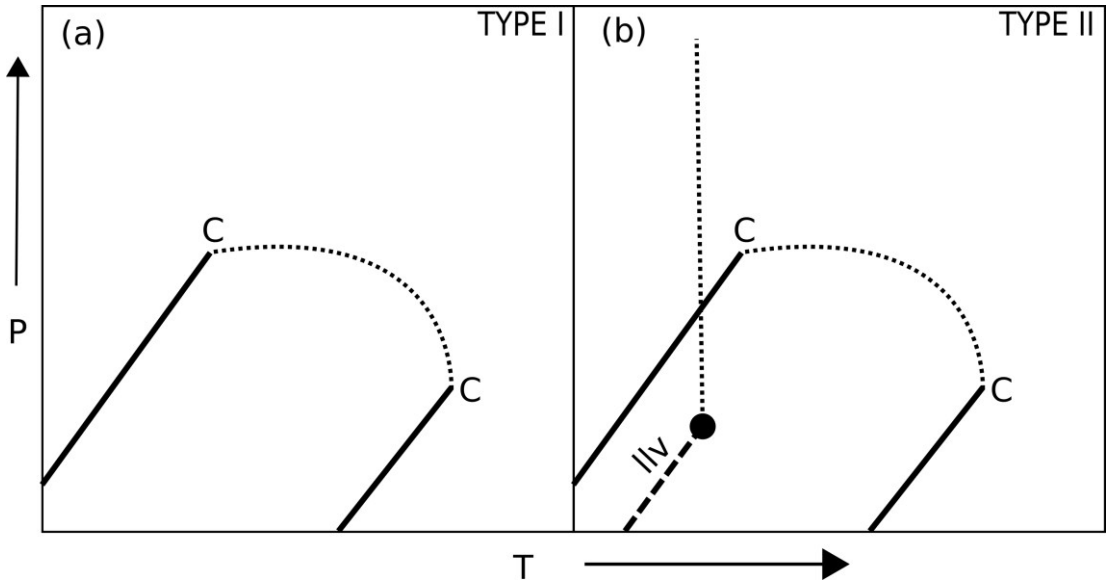

Figure 4.1 Type I (a) and Type II (b) binary phase behavior based on the van Konynenburg and Scott classification scheme: (—) pure component vapor pressure curve, (·····) L=V critical locus, (–––) liquid-liquid-vapor curve, (●) upper critical end point.

4.2 Experimental

4.2.1 Materials

Tetracosane (99%), octacosane (99%) and hexatriacontane (98%) were procured from Aldrich. Benzene (99.9%) was supplied by Sigma-Aldrich, heptane (99%) and eicosane (99%) was supplied by Sigma. These chemicals were used without further purification.

4.2.2 X-ray View Cell Apparatus.

The phase behavior of benzene + n-C_{20}, n-C_{24}, n-C_{28} and n-C_{36} binary mixtures was studied using a custom View Cell [12-14]. The view cell consists of a hollow open-ended beryllium cylinder that has an internal volume of approximately 200 ml and a variable volume bellows that is attached to the upper end cap. The internal volume of the cell is adjusted by expanding or contracting the bellows using high-pressure nitrogen. Feed lines are attached to the view cell and they are used to remove air once the cell is assembled and to inject gases or liquids to adjust composition. These tubes possess a volume of 10 ml and are heated to 573.15 K to prevent condensation. The cell is

placed in a lead-lined cabinet between a polychromatic X-ray source and an X-ray sensitive camera. The camera captures transmitted X-rays and reports intensity as a digital image using a 256 point grey scale. These images are monitored during an experiment and are recorded digitally. The temperature inside the cell is monitored and controlled using a RTD (resistance temperature detector) over the temperature range: 290 - 700 K. Pressure is monitored and controlled using transducers with an operating range: 0 - 276 bar. The apparatus and procedures were validated in this work using deviations from high precision vapor pressure measurements [15] for pure benzene and a benzene + n-C_7 mixture.

4.3 Modeling

4.3.1 Bubble Pressure and Critical Loci Calculations Using the PR, SRK and PC-SAFT Equations of State

Equation of state models, PR and SRK (as implemented in VMGSim [16]) and PC-SAFT (as implemented in Aspen Plus [17] and GPEC [18]) are used for vapor-liquid equilibrium and critical loci calculations. Here, computed bubble pressures for binary mixtures of benzene + n-C_6, n-C_{10}, n-C_{12}, n-C_{14}, n-C_{16}, and n-C_{17}, and critical points for binary mixtures of benzene + n-C_6, n-C_7, n-C_8, n-C_9, n-C_{10}, and n-C_{16} are compared with available experimental data [15]. Bubble pressures and critical loci were also calculated for binary mixtures of benzene + n-C_{20}, n-C_{24}, n-C_{28}, and n-C_{36}, and compared with a limited experimental data set presented below. These selections were motivated by the dissonance between cubic EOS predicted (Type II) and observed (Type I) phase behavior for these binaries [5].

Pure compound properties (T_c, P_c, ω) obtained from NIST/TDE [15], are used in VMGSim [16] for both the PR and SRK EOS. These property values, shown in Figure

4.2, differ somewhat from default values in the simulators, particularly for the larger n-alkanes. Three sets of binary interaction parameter values are used for calculations with the cubic equations of state: (i) Set I - $k_{ij} = 0$, (ii) Set II - k_{ij} values calculated using linear trends for fit k_{ij} values for binary mixtures of benzene with n-C_5, n-C_6, n-C_7, n-C_8, n-C_9, n-C_{10}, n-C_{12}, n-C_{14}, n-C_{15}, n-C_{16}, and n-C_{17} [5], (iii) Set III - maximum k_{ij} values that predict Type I phase behaviour based on standard pure component property values [5]. These k_{ij} values, calculated on the basis of NIST recommended pure component properties, are shown in Table 4.1. Individual fitted k_{ij} values are also shown.

The pure component parameters for the PC-SAFT EOS were rescaled [19] to the pure component property values that were used with the PR and SRK EOS in order to match the end points of the vapor-liquid critical loci obtained with the cubic EOS. The rescaled parameter values are listed in Table 4.2. If this is not done, the phase envelopes remain qualitatively but not quantitatively similar. Rescaling the parameters to the critical properties of pure component also improves the predictions in the near critical region for these mixtures. Alfradique and Castier [20] showed with calculations for more than 29 hydrocarbon mixtures, using both standard [1] and rescaled PC-SAFT pure component parameters [19], that the latter approach results in lower deviations from experimental critical pressure and temperature data. Volumetric and VLE data for hydrocarbon mixtures are also represented without major deviations using the rescaled parameters [21-23]. The interaction parameters for the PC-SAFT EOS are assumed to be zero.

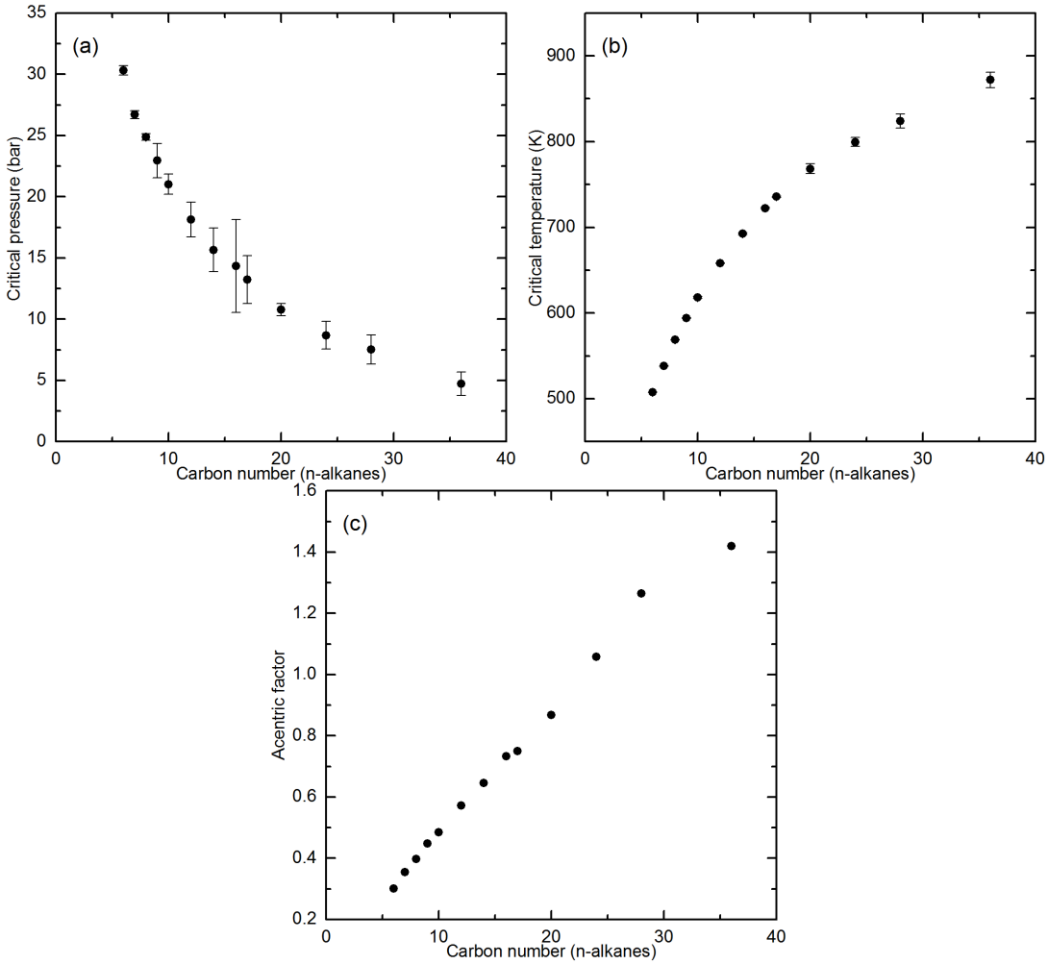

Figure 4.2 (a) Critical pressure, (b) critical temperature and (c) acentric factor values for n-alkanes. Symbols: ●, values and uncertainties from NIST/TDE [15].

Table 4.1 Binary interaction parameter values for the PR and SRK EOS based on NIST property data.

Component		Fitted k_{ij} values		k_{ij} (set II) [5]		k_{ij} (set III) [5]	
1	2	PR	SRK	PR	SRK	PR	SRK
n-C_6	benzene	0.01 [a]	0.02 [a]	0.0114	0.0130	>0	>0
n-C_7	benzene	0.00 [a]	0.00 [a]	0.0055	0.0082	>0	>0
n-C_8	benzene	-0.01 [a]	0.00 [a]	-0.0004	0.0034	>0	>0
n-C_9	benzene	0.01 [a]	0.01 [a]	-0.0064	-0.0015	>0	>0
n-C_{10}	benzene	-0.01 [a]	-0.01 [a]	-0.0123	-0.0063	>0	>0
n-C_{12}	benzene	-0.02 [a]	-0.01 [a]	-0.0241	-0.0160	>0	>0
n-C_{14}	benzene	-0.04 [a]	-0.03 [a]	-0.0359	-0.0256	>0	>0
n-C_{16}	benzene	-0.04 [a]	-0.03 [a]	-0.0478	-0.0353	>0	>0
n-C_{17}	benzene	-0.06 [a]	-0.05 [a]	-0.0537	-0.0401	>0	>0
n-C_{20}	benzene	-0.06 [b]	-0.06 [b]	-0.0714	-0.0546	-0.0201	-0.0144
n-C_{24}	benzene	-0.1 [b]	-0.09 [b]	-0.0951	-0.0739	-0.0394	-0.0327
n-C_{28}	benzene	-0.12 [b]	-0.11 [b]	-0.1188	-0.0933	-0.0448	-0.0379
n-C_{36}	benzene	-0.13 [b]	-0.12 [b]	-0.1661	-0.1319	-0.1447	-0.1352

[a] k_{ij} values fitted to experimental data from literature [15] (prior work [5])
[b] k_{ij} values fitted to the new experimental data (this work)

Table 4.2 Pure component parameters for the PC-SAFT equation of state rescaled based on the pure component properties used with PR and SRK EOS.

Compound	m	σ [Å]	ε/k (K)
benzene	2.5911	3.7122	275.7399
n-C_6	3.2976	3.8624	224.1272
n-C_7	3.7136	3.9325	226.6047
n-C_8	4.0615	3.9649	231.2929
n-C_9	4.4684	3.9826	233.2685
n-C_{10}	4.7638	4.0518	237.2445
n-C_{12}	5.4660	4.1143	241.3234
n-C_{14}	6.0792	4.2048	245.5468
n-C_{16}	6.8037	4.1876	247.7351
n-C_{17}	6.9561	4.2883	250.7709
n-C_{20}	7.9635	4.3921	252.4083
n-C_{24}	9.6121	4.3930	250.7388
n-C_{28}	11.4663	4.2885	248.4358
n-C_{36}	12.8911	4.8242	256.6683

4.3.2 Sensitivity Analysis

Uncertainties in pure component property values are not normally taken into account for process equilibrium calculations with equations of state in process simulators.

Critical properties and acentric factor values for pure compounds have uncertainties associated to them due to the errors linked with experiments or correlations used to measure or estimate these values, respectively. For example, critical point data is scant and uncertain for n-alkanes larger than n-C_{20}. These uncertainties in turn have implications for thermo-physical properties estimated using equations of state. With recent advances in chemical engineering data collection, NIST Thermo Data Engine [15] estimates uncertainties at approximately the 95% confidence level [24]. To test the sensitivity of predicted vapor-liquid equilibria and L=V critical loci to the uncertainties in the pure component properties in this work, calculations were repeated for binary mixtures of benzene with n-C_{16} and n-C_{28}, using three sets of property values: the mean values and the upper and lower extrema of the ranges recommended by NIST/TDE (Figures 4.2a and b) for each compound. Uncertainty in acentric factor value is not available from NIST/TDE and therefore it is treated as a constant. The three sets of pure component properties used for calculations with the PR and SRK EOS and corresponding rescaled parameters used for calculations with PC-SAFT EOS are shown in Table 4.3. The impact of binary interaction parameter was also studied for each set of pure component properties for the cubic EOS.

Table 4.3 Pure component parameter ranges used for sensitivity analysis calculations with the PR, SRK and PC-SAFT EOS.

Compounds	Property set	Tc (K)	Pc (bar)	ω	m	σ [Å]	ε/k (K)
n-C_{16}	Upper bound	723.07	18.12	0.7324	6.8037	3.8747	248.0188
n-C_{28}		832.00	8.71	1.2640	11.4663	4.0958	250.8478
benzene		562.16	49.14	0.2099	2.5911	3.7074	275.8061
n-C_{16}	Mean values	722.25	14.34	0.7324	6.8037	4.1876	247.7351
n-C_{28}		824.00	7.51	1.2640	11.4663	4.2885	248.4358
benzene		562.02	48.94	0.2099	2.5911	3.7122	275.7399
n-C_{16}	Lower bound	721.42	10.56	0.7324	6.8037	4.6360	247.4514
n-C_{28}		816.00	6.32	1.2640	11.4663	4.5286	246.0238
benzene		561.89	48.74	0.2099	2.5911	3.7171	275.6736

4.4 Results and discussion

4.4.1 Binary Mixtures of Benzene + Short Chain n-Alkanes

For these binary mixtures, bubble pressure and critical loci data are available in the literature, and all three equations of state correctly predict Type I phase behaviour with standard interaction parameter values. Bubble pressure calculation results for binary mixtures of benzene + n-C_6, n-C_{10}, n-C_{12}, n-C_{14}, n-C_{16}, and n-C_{17} using all three equations of state along with their experimental analogues are presented for $k_{ij} = 0$ and k_{ij} set II in Figure 4.3. For $k_{ij} = 0$, the cubic equations of state tend to overestimate bubble pressures, and the deviation from experimental data increases with temperature and with molecular size of the n-alkane at fixed temperature. For example, the difference between predictions and experimental values is greater for benzene + n-C_{17} (Figure 4.3f) than for benzene + n-C_{14} (Figure 4.3d) at similar temperatures and compositions. By using non-standard and increasingly negative k_{ij} values (set II) for octane-benzene binaries and above, close agreement between the cubic EOS models and the data is achieved, Figure 4.3 a-f. By contrast, there are no systematic impacts of temperature or n-alkane molecule size on

predictions obtained using the PC-SAFT EOS with k_{ij} = 0. The PC-SAFT EOS consistently underestimates vapor pressure values, but follows the trends of the experimental data closely.

Experimental and computed pressure-temperature, pressure-composition, and temperature-composition L=V critical loci are shown in Figures 4.4-4.6 respectively for benzene + n-C_6, n-C_7, n-C_8, n-C_9, n-C_{10}, and n-C_{16} binary mixtures. By plotting the data in these three ways, relative skews in fits with respect to pressure, temperature and composition become evident. The qualitative behavior of all three EOS is similar to the measured critical behaviors and the deviations in most cases are modest. The PC-SAFT EOS clearly provides better quantitative critical point estimates. k_{ij} value variation has only a marginal effect on cubic EOS performance vis-à-vis critical point estimation. Directionally, use of larger negative k_{ij} values, than required to fit low temperature bubble pressure data, improves the quality of predictions of both PR and SRK EOS, and suggests that the best fit k_{ij} values for cubic EOS for these mixtures are temperature dependent.

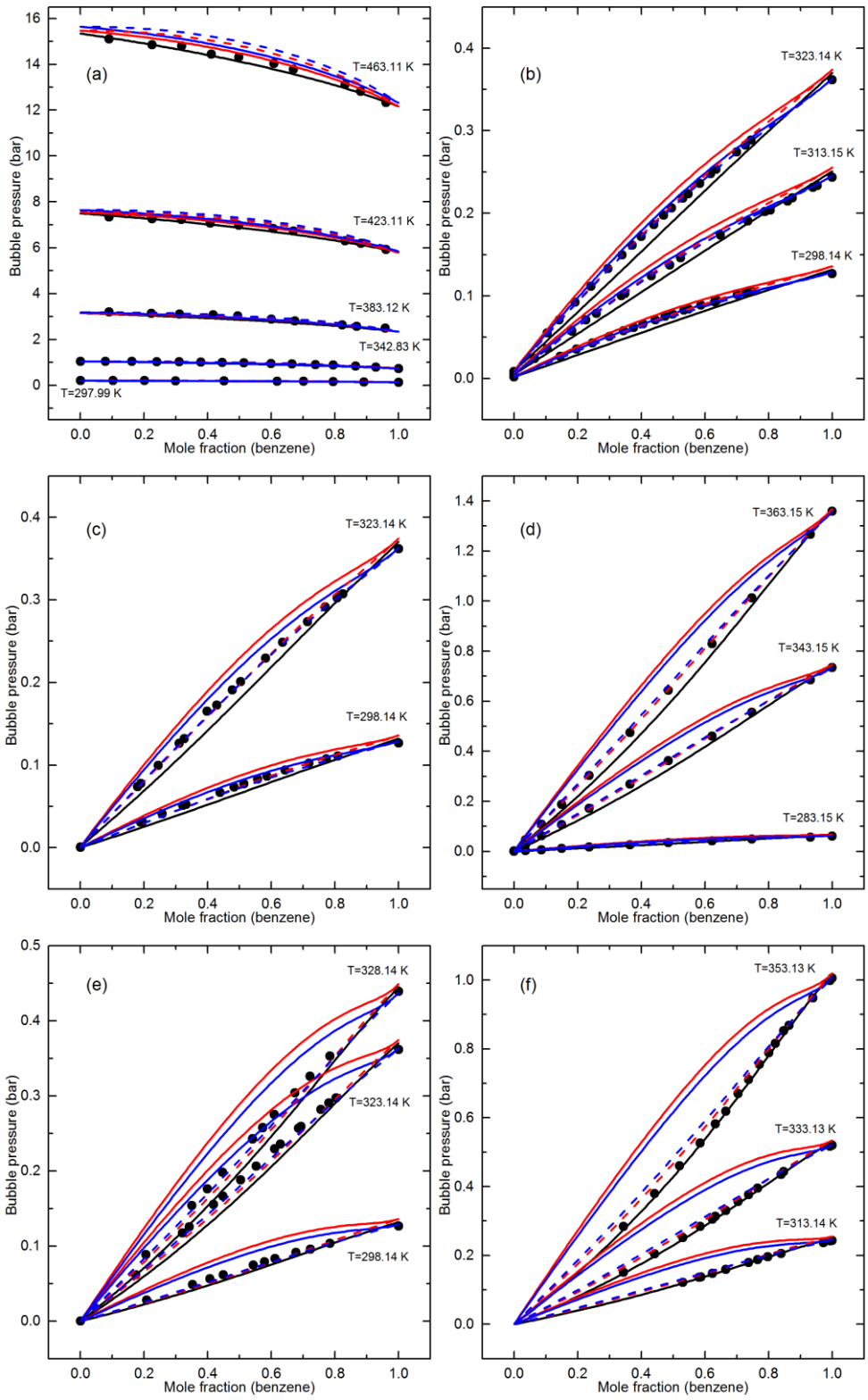

Figure 4.3 Bubble pressure-mole fraction diagrams: (a) benzene + n-C_6, (b) benzene + n-C_{10}, (c) benzene + n-C_{12}, (d) benzene + n-C_{14}, (e) benzene + n-C_{16}, (f) benzene + n-C_{17}. Black dots (●) represent experimental values [15], continuous (—) and dashed (– – –) curves represent the calculated values for $k_{ij} = 0$ and set II, respectively. PR, SRK and PC-SAFT results are shown using red, blue and black curves, respectively. Temperature is a parameter.

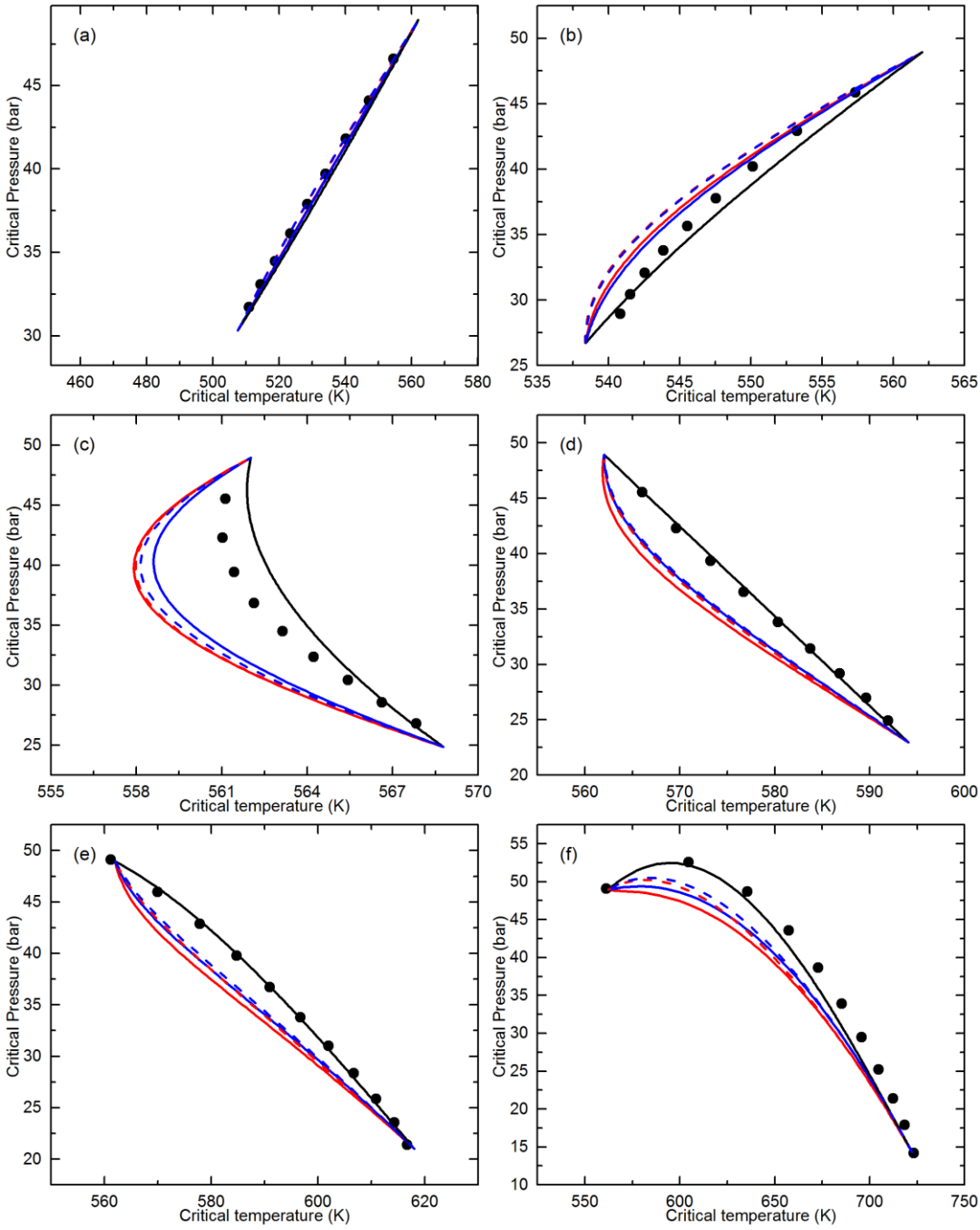

Figure 4.4 Pressure-temperature projections: (a) benzene + n-C_6, (b) benzene + n-C_7, (c) benzene + n-C_8, (d) benzene + n-C_9, (e) benzene + n-C_{10}, (f) benzene + n-C_{16}. Black dots (●) represent experimental values [15]. PR, SRK and PC-SAFT results are shown using red, blue and black curves, respectively. k_{ij} values used in the calculations: (—) $k_{ij} = 0$; (– – –) k_{ij} = Set II (Table 4.1).

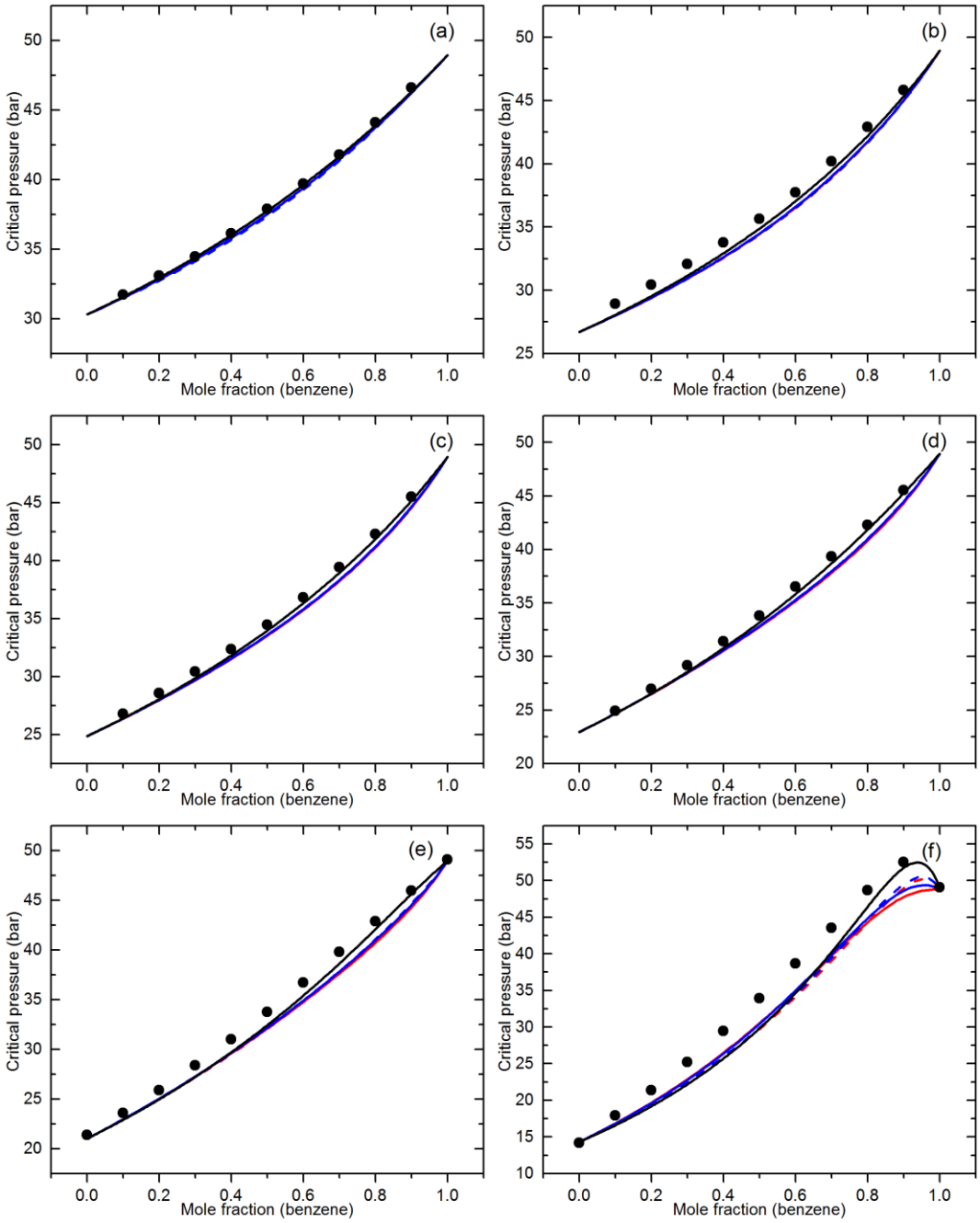

Figure 4.5 Pressure-composition projections for benzene + n-alkane binary mixtures. See caption on Figure 4.4 for details.

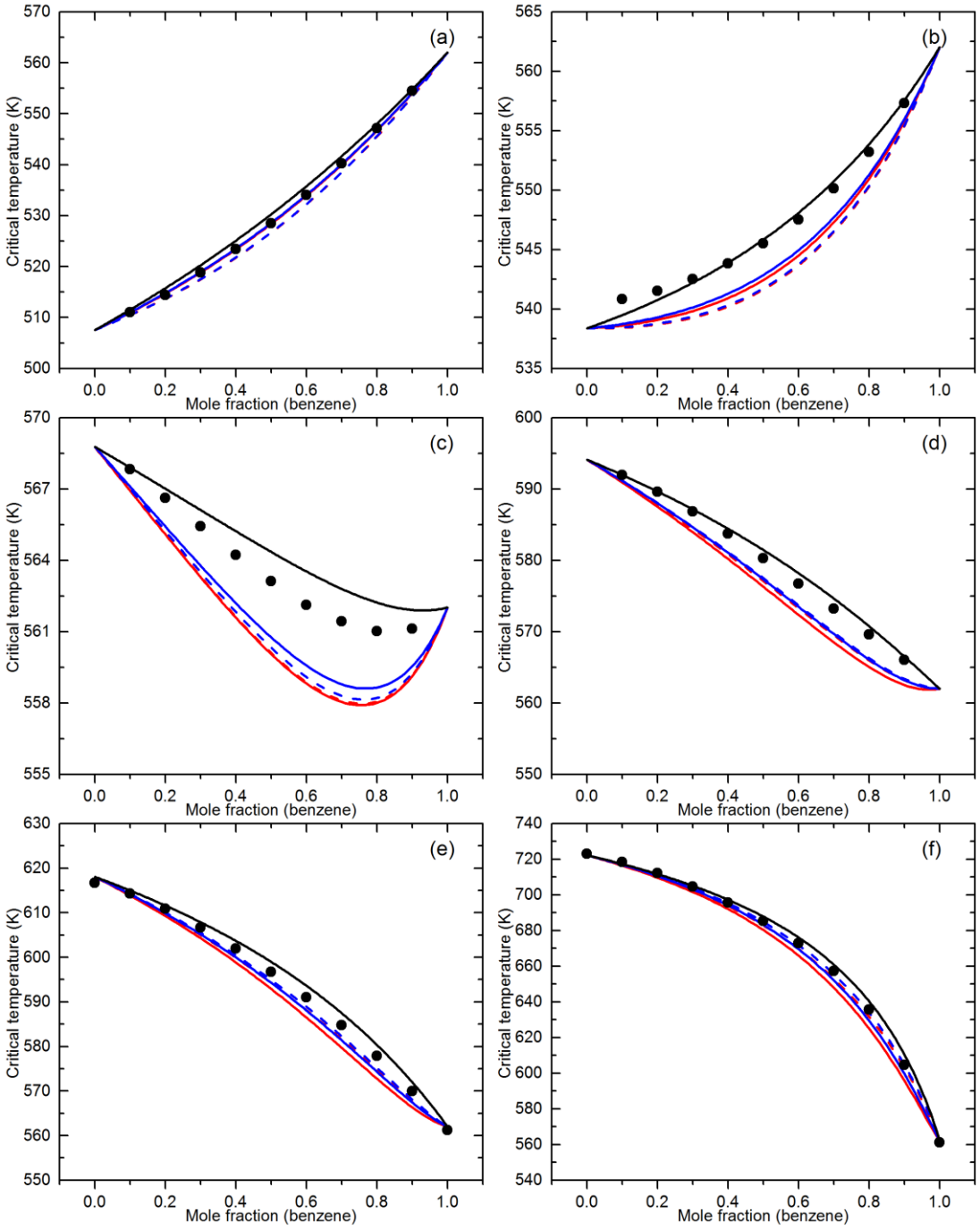

Figure 4.6 Temperature-composition projections for benzene + n-alkane mixtures. See caption on Figure 4.4 for details.

4.4.2 Binary Mixtures of Benzene + Long Chain n-Alkanes

There are no bubble pressure data for benzene + n-alkanes larger than n-heptadecane in the open literature. Benzene + long chain n-alkane phase equilibrium experiments were performed in this work. The quality of the data is demonstrated with calibration trials. Vapor pressures of benzene and the bubble pressures of benzene (0.7 mole

fraction) + n-C_7 were measured and compared with data from the literature[15]. The results are reported in Table 4.4. The calibrations have random error of 1.2 % and there is a systematic positive bias of approximately 1.4 % relative to the literature data. The source of the bias is unclear, but a bias correction was applied to all of the bubble pressure data obtained in this work. Measurements for the benzene + n-C_{36} binary mixture are not reported above 452 K due to the onset of thermal cracking. Cracking was observed at 483 K, in this work, and has also been reported elsewhere [25].

Computed bubble pressure values for binary mixtures of benzene with long chain n-alkanes: n-C_{20}, n-C_{24}, n-C_{28}, and n-C_{36}, computed using the PR and SRK EOS (k_{ij} value sets I, II, III) and the PC-SAFT EOS (k_{ij} = 0), are compared with the experimental measurements in Figure 4.7. Cubic equations of state with standard interaction parameter values (k_{ij} > or = 0) over predict bubble pressures significantly. The large quantitative deviations increase with mixture asymmetry and with temperature. A qualitative deviation is also evident in Figure 4.7j, where a LLV to LL transition and not a LV to L transition (bubble point) is predicted for benzene + n-C_{36} up to more than 450 K. By contrast, the PC-SAFT EOS consistently under predicts bubble pressures but follows the trend of the data closely. Negative interaction parameter values significantly reduce the over prediction of bubble pressures computed using cubic EOS.

One of the goals of this research is to identify strategies for estimating interaction parameters for aromatic and naphthenic mixtures with n-alkanes that not only yield correct phase behaviours but also provide quantitative bubble pressure estimates

particularly for mixtures where data are not available. k_{ij} values from set II test the concept that k_{ij} values for mixtures of a single small molecule (benzene) with increasingly large molecules in a family (n-alkanes) for which there are no data, can be obtained by extrapolation based on the behaviors of mixtures in the same series for which data are available. This data intensive approach, where feasible, appears preferred over choosing set III k_{ij} values, which only guarantee that the correct phase diagram is computed, but it is not preferred over the rescaled PC-SAFT EOS with k_{ij} =0. For this example, the cubic EOS provide an upper bound (either k_{ij} sets II or III) and the PC-SAFT EOS provides a lower bound for bubble pressure. It is not clear whether this is a generalizable result even for a closely related ethylbenzene + n-alkane binary series. Residual uncertainty is unavoidable.

A further source of uncertainty related to the cubic equations of state concerns the temperature sensitivity of interaction parameters. Best-fit temperature-independent k_{ij} values are reported in Table 4.1 based on minimizing the square of error for bubble pressure data (least-squares objective function [26]). Local best-fit values fit at each temperature, Table 4.5, show clear trends toward larger negative numbers as temperature is increased. This suggests that the cubic EOS models have a skewed fit to the bubble pressure data, if constant k_{ij} values are used and that distortions in the critical region, where experiments are not readily performed, also arise. Computed pressure-temperature, pressure-composition, and temperature-composition L=V critical loci shown in Figures 4.8, for the benzene + n-C_{28} binary, are illustrative. The greatest divergence among the models arises in benzene-rich mixtures, where critical pressures differ by up to ~ 10 bar.

Table 4.4 Experimental bubble pressure data (this work).

Sample	Benzene (mol fraction) ± 0.0001	Temperature (K) ± 0.1	Bubble Pressure (bar)		
			Measured	Bias corrected ± 1.2 %	Reference data[15]
Benzene	1.0000	378.35	2.05	2.03	2.07
		401.25	3.66	3.61	3.63
		421.85	5.72	5.64	5.67
		437.45	7.78	7.67	7.71
		460.35	11.73	11.57	11.63
		480.45	16.22	16.00	16.14
		500.15	21.83	21.53	21.70
		520.05	28.77	28.37	28.65
Benzene + n-C_7	0.6986	412.97	4.61	4.55	4.47
		427.96	6.22	6.14	6.00
		442.96	8.24	8.12	7.96
		457.96	10.72	10.57	10.32
		472.96	13.72	13.53	13.36
		487.96	17.32	17.08	17.09
Benzene + n-C_{20}	0.6033	422.65		3.54	
		453.15		5.59	
		483.35		8.23	
		513.85		11.52	
		544.05		15.42	
		574.35		19.94	
Benzene + n-C_{24}	0.5988	424.05		3.06	
		453.05		4.89	
		482.95		7.31	
		513.55		10.31	
		543.75		13.75	
		573.75		17.57	
Benzene + n-C_{28}	0.6743	422.55		3.32	
		453.25		5.55	
		483.55		8.38	
		513.55		11.72	
		543.95		15.54	
		574.65		19.72	
Benzene + n-C_{36}	0.6986	392.95		1.97	
		422.65		3.41	
		452.65		5.49	

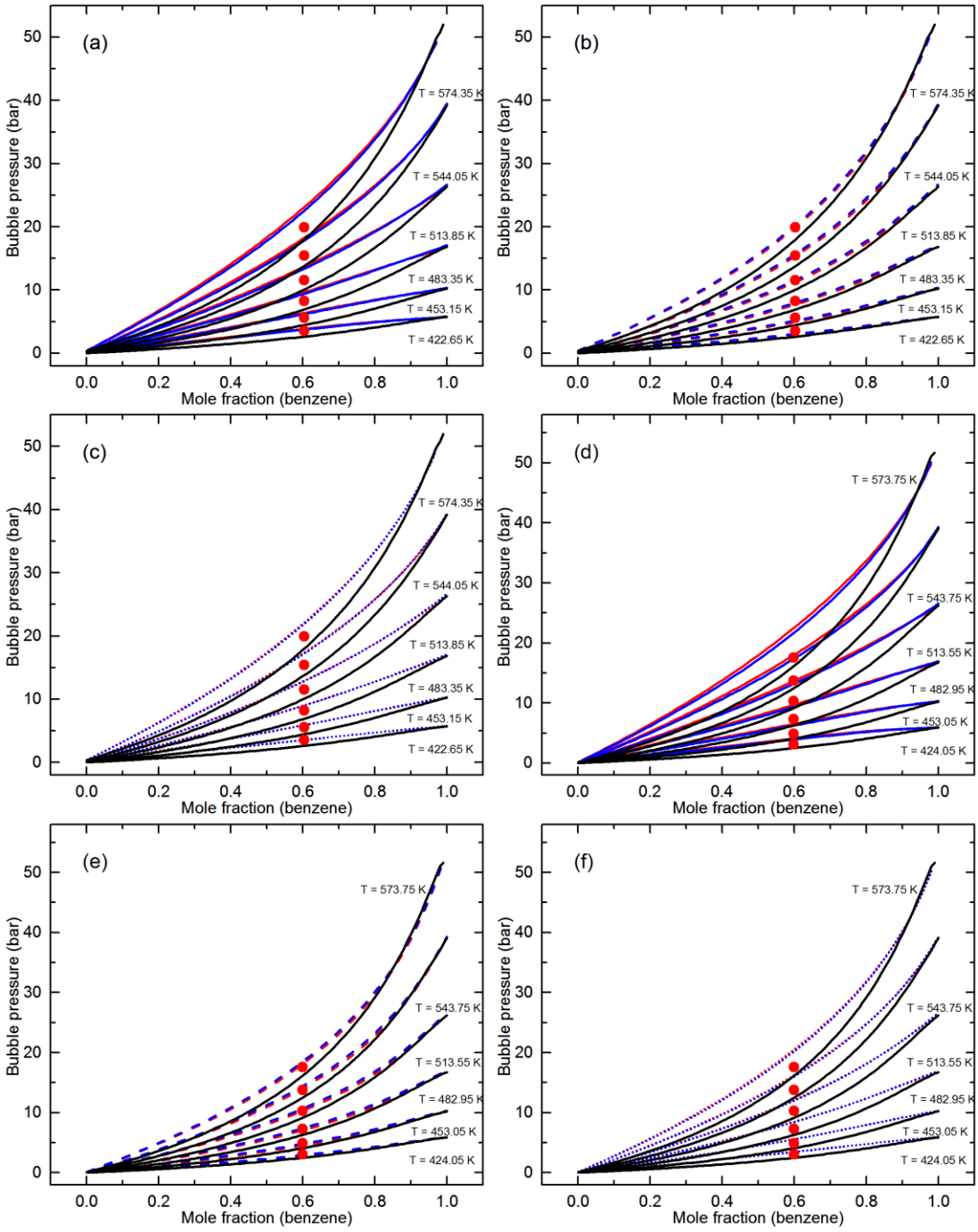
(a)
T = 574.35 K
T = 544.05 K
T = 513.85 K
T = 483.35 K
T = 453.15 K
T = 422.65 K
(b)
T = 574.35 K
T = 544.05 K
T = 513.85 K
T = 483.35 K
T = 453.15 K
T = 422.65 K
(c)
T = 574.35 K
T = 544.05 K
T = 513.85 K
T = 483.35 K
T = 453.15 K
T = 422.65 K
(d)
T = 573.75 K
T = 543.75 K
T = 513.55 K
T = 482.95 K
T = 453.05 K
T = 424.05 K
(e)
T = 573.75 K
T = 543.75 K
T = 513.55 K
T = 482.95 K
T = 453.05 K
T = 424.05 K
(f)
T = 573.75 K
T = 543.75 K
T = 513.55 K
T = 482.95 K
T = 453.05 K
T = 424.05 K
Bubble pressure (bar)
Mole fraction (benzene)
0
10
20
30
40
50
0.0
0.2
0.4
0.6
0.8
1.0

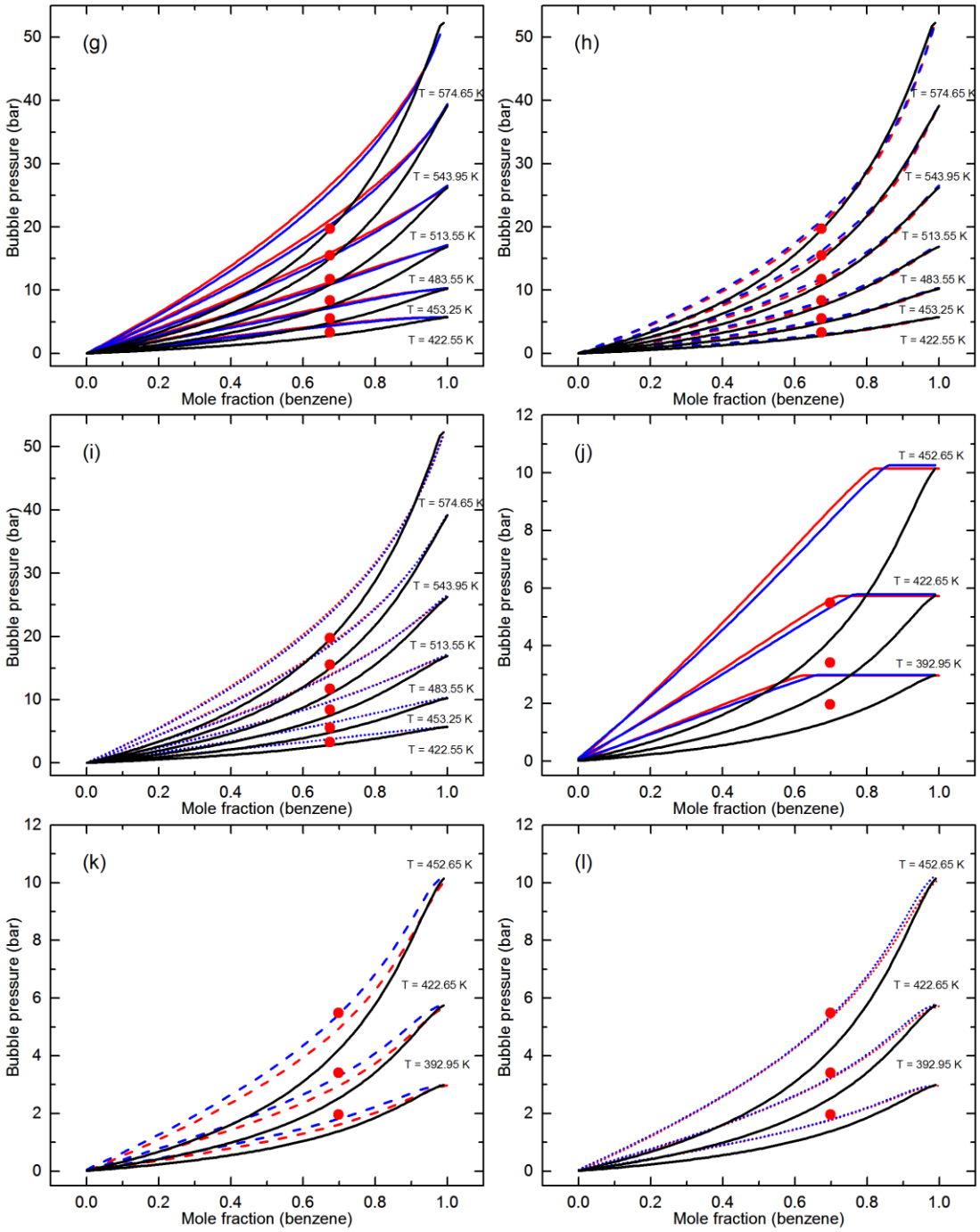

Figure 4.7 Bubble pressure-mole fraction diagrams for: benzene + n-C_{20} (a-c), benzene + n-C_{24} (d-f), benzene + n-C_{28} (g-i) and benzene + n-C_{36} (j-l). Red dots (●) represent experimental values from this work. PR, SRK and PC-SAFT results are shown using red, blue and black curves, respectively. k_{ij} values used in calculations are: (——) $k_{ij} = 0$; (– – –) k_{ij} = Set II; (. . . .) k_{ij} = Set III.

Table 4.5 k_{ij} values fit to measured bubble pressure data.

Temperature (K)	k_{ij} PR	k_{ij} SRK	Temperature (K)	k_{ij} PR	k_{ij} SRK
	Benzene + n-C_{20}			Benzene + n-C_{24}	
422.65	-0.02	-0.01	424.05	-0.07	-0.06
453.15	-0.04	-0.03	453.05	-0.08	-0.07
483.35	-0.05	-0.04	482.95	-0.08	-0.08
513.85	-0.06	-0.06	513.55	-0.09	-0.09
544.05	-0.06	-0.06	543.75	-0.10	-0.09
574.35	-0.07	-0.06	573.75	-0.11	-0.10
	Benzene + n-C_{28}			Benzene + n-C_{36}	
422.55	-0.08	-0.07	392.95	-0.12	-0.11
453.25	-0.08	-0.08	422.65	-0.13	-0.12
483.55	-0.09	-0.09	452.65	-0.14	-0.12
513.55	-0.11	-0.10			
543.95	-0.12	-0.11			
574.65	-0.14	-0.13			

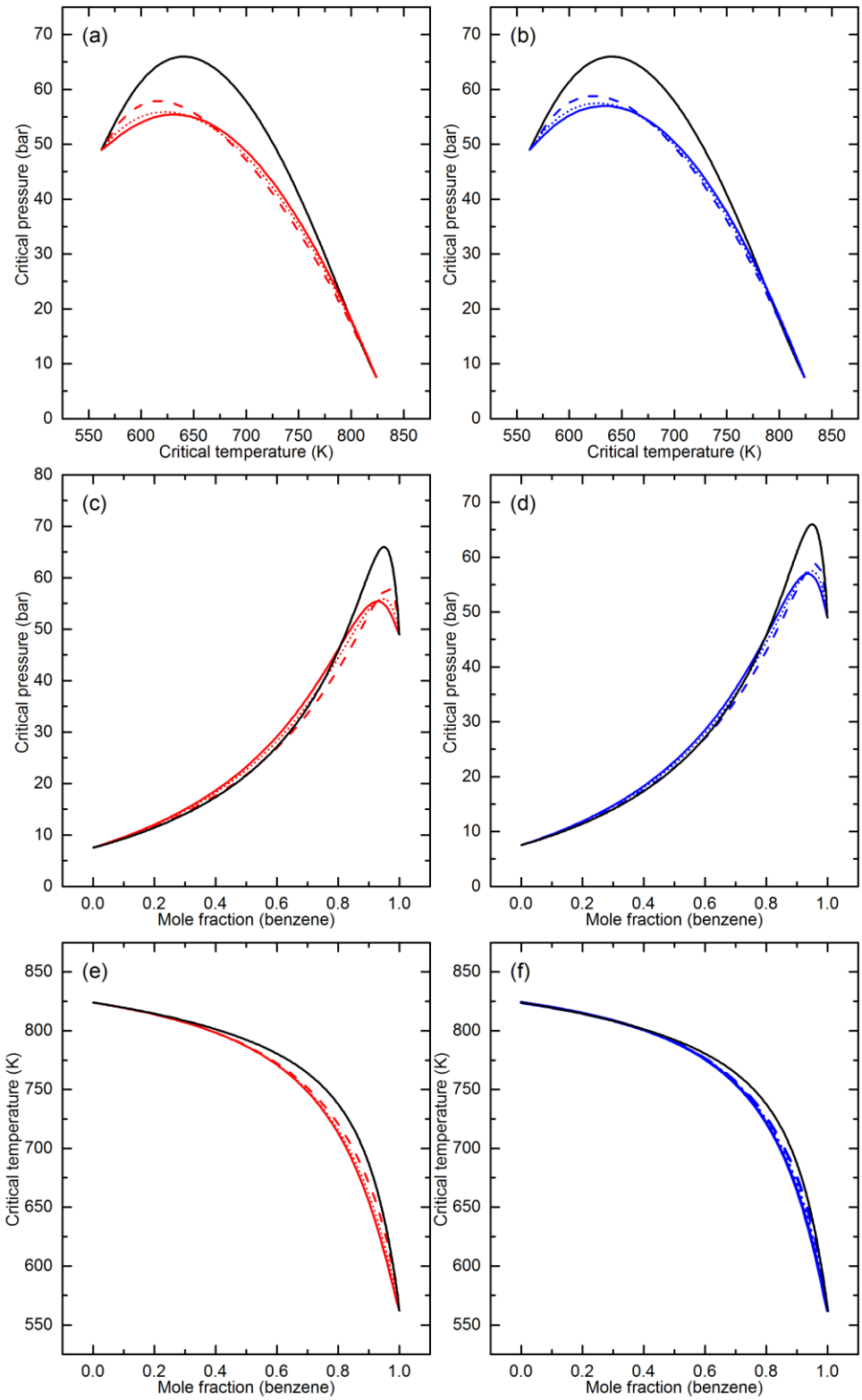

Figure 4.8 Predicted critical loci for benzene + n-C_{28} mixture. (a, b) P-T projections, (c, d) P-x projections and (e, f) T-x Projections for the PR, SRK and PC-SAFT EOS shown using red, blue and black curves respectively. k_{ij} values used in calculations: (—) k_{ij} = 0; (– – –) k_{ij} = Set II; (. . . .) k_{ij} = Set III.

4.4.3 Sensitivity of PR, SRK and PC-SAFT Vapor-Liquid Equilibria and Critical Loci Predictions to T_c and P_c Uncertainty

Illustrative sensitivity calculations of vapor-liquid equilibria and critical loci were performed for binary mixtures of benzene with n-C_{16} and n-C_{28} using the upper bound, mean and lower bound values of pure component T_c and P_c properties based on uncertainties obtained from NIST/TDE. For calculations with PC SAFT, the segment number (m), the segment diameter (σ), and the segment energy parameter (ε/k) were rescaled for each case. Computed bubble pressure outcomes for benzene + n-C_{16} and n-C_{28} are compared with measurements in Figures 4.9 a-e and 4.10 a-g, respectively. For the cubic equations, incorrect prediction of liquid-liquid phase separation can also occur at low temperatures as shown in Figure 4.9a and 4.9c for benzene + n-C_{16}. For the PC SAFT EOS, larger pure component T_c and P_c values improve the quality of predictions – Figure 4.9 and 4.10. The variation in computed outcomes for all three equations of state is significant in the critical region - Figure 4.11a-f. In the critical region, the outcomes are very sensitive to the pure component parameters selected for calculations. Upper and lower bound critical properties uniformly shift the critical loci to higher and lower pressures, respectively. Using upper bound critical properties improves the quality of prediction for all three equations of state (Figure 4.11a). For the cubic EOS, negative k_{ij} values (Set II and Set III) used with upper bound critical properties yield a close fit to the experimental critical loci of benzene + n-C_{16}, a quality of fit not obtained by varying the k_{ij} value alone (Figure 4.4).

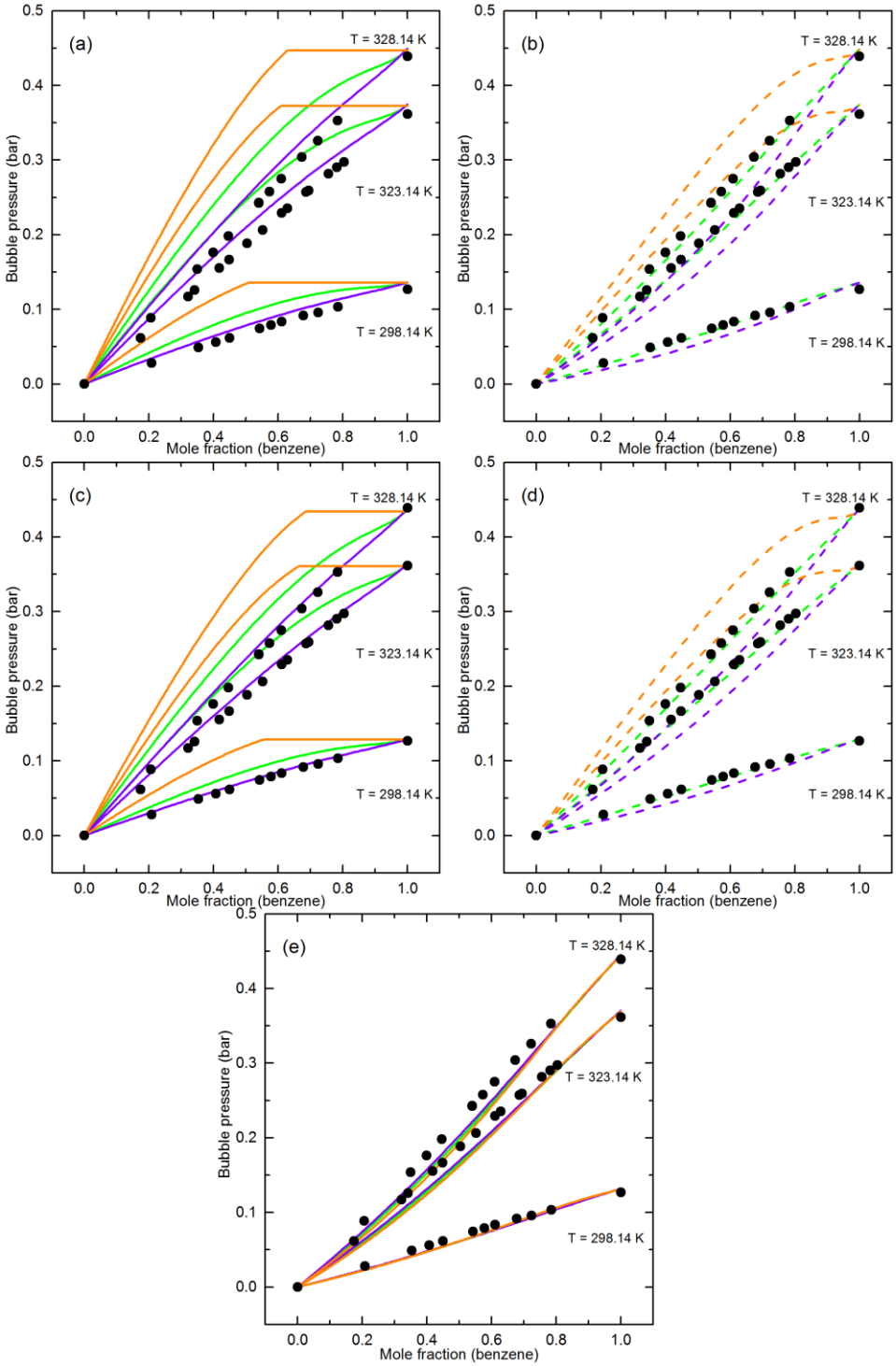

Figure 4.9 Sensitivity analysis of bubble pressure predictions for benzene + n-C_{16} using the PR (a,b), the SRK (c,d) and PC SAFT (e) equations of state. Black dots (●) represent experimental values [15]. Calculation outcomes using upper, mean and lower bound pure compound critical properties are shown using violet, green and orange curves, respectively. k_{ij} values used in calculations: (—) k_{ij} = 0; (– – –) k_{ij} = Set II (Table 4.1).

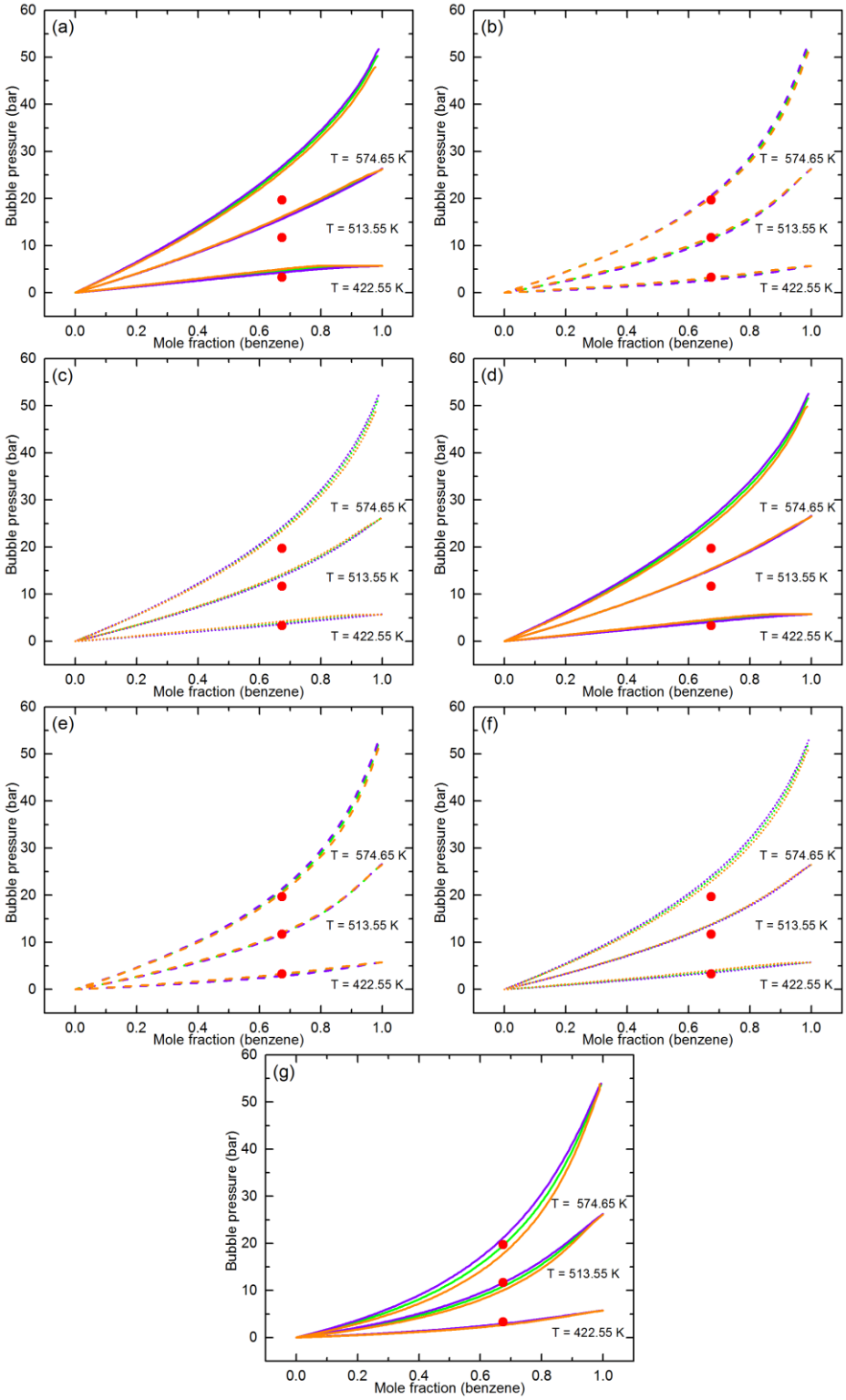

Figure 4.10 Sensitivity analysis of bubble pressure predictions for benzene + n-C_{28} using the (a-c) PR, (d-f) the SRK and (g) the PC-SAFT. Calculation outcomes using upper, mean and lower bound pure compound critical properties are shown using violet, green and orange curves respectively. Red dots (●) represent experimental values from this work. k_{ij} values used in calculations: (—) k_{ij} = 0; (– – –) k_{ij} = Set II; (. . . .) k_{ij} = Set III (Table 4.1).

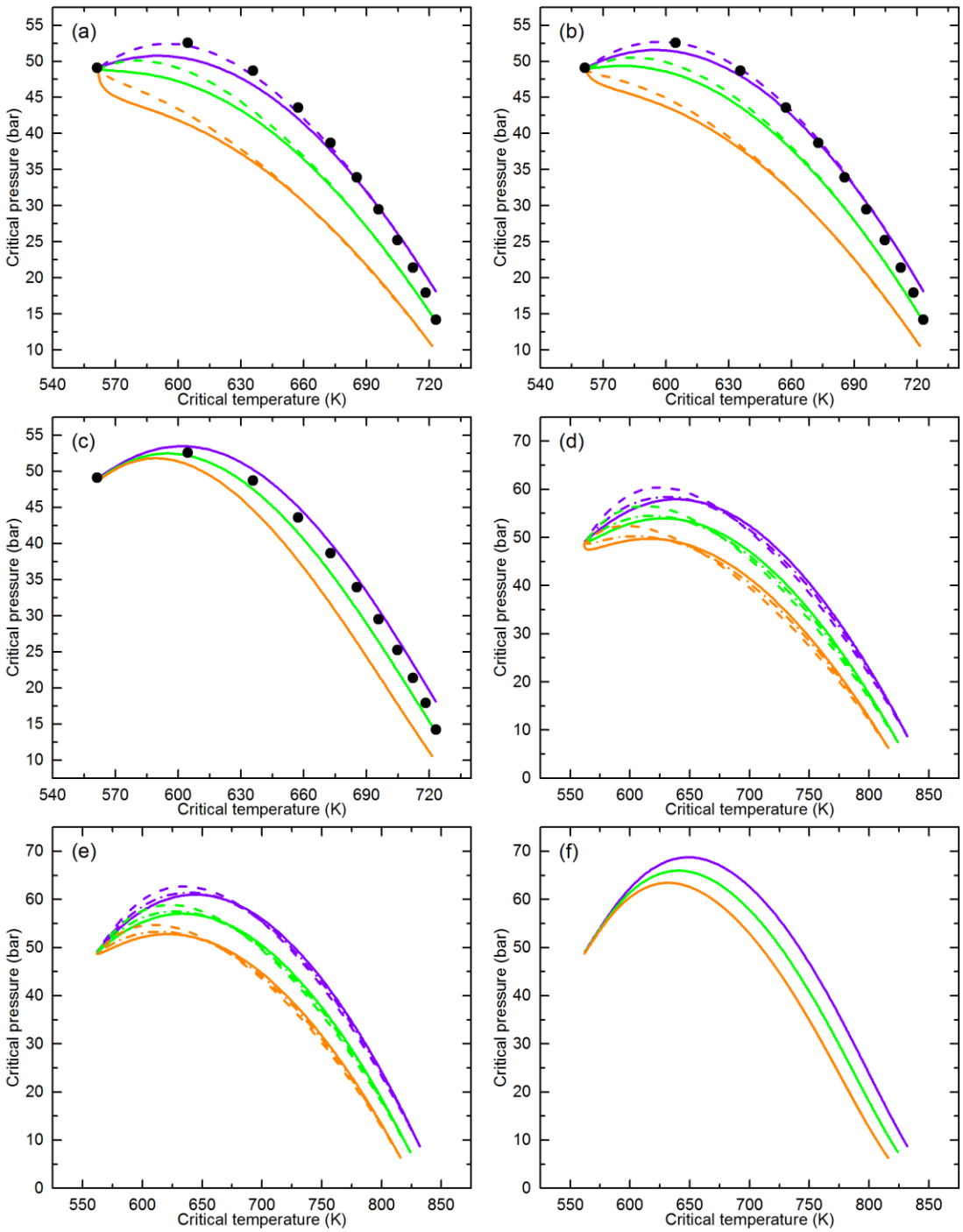

Figure 4.11 Critical loci for (a-c) benzene + n-C_{16} and (d-f) benzene + n-C_{28} using the (a, d) PR, (b, e) the SRK and (c, f) the PC SAFT EOS. Black dots (●) represent experimental values [15]. Calculation outcomes using upper, mean and lower bound pure compound critical properties are shown using violet, green and orange curves respectively. k_{ij} values used in calculations: (——) k_{ij} = 0; (– – –) k_{ij} = Set II; (. . . .) k_{ij} = Set III (Table 4.1).

4.5 Conclusions

Quantitative prediction of phase equilibria, the numbers and natures of phases as well as their compositions and densities, are cornerstones of engineering calculations for

hydrocarbon process design and process optimization. Equations of state are relied upon to deliver quality computed outcomes for diverse fluids over broad ranges of conditions. With the trend toward molecular based speciation of middle distillates and crude oils the demands on these models are intensifying, and the need for scrutiny of underlying assumptions has become apparent. Such mixtures include a broad range of aromatic, naphthenic, and paraffinic, and branched chain compounds. Irreducible uncertainty linked to the quality of critical temperature and pressure data or estimates is increasingly understood. For example, the PC-SAFT EOS provides qualitatively correct phase behaviors for such mixtures and quantitatively correct phase behaviors, for benzene + n-alkane mixtures as illustrated in this work, if the pure component parameters appearing in the equation are scaled relative to known or estimated critical properties. No mixture specific coefficients are required. By contrast, the PR and SRK (cubic) EOS predict qualitatively incorrect phase behaviors unless non-standard mixture-specific interaction parameter values are used. With the cubic EOS, quantitative outcomes are sensitive to binary interaction parameter values and to the uncertainties of pure component properties, as illustrated for benxene + n-alkane mixtures. New bubble pressure data for benzene + n-C_{20}, n-C_{24}, n-C_{28}, n-C_{36} were obtained to test hypotheses related to interaction parameter estimation for cubic EOS, with the goal of providing general guidelines for molecularly speciated middle distillates and crude oils, and to further examine the predictive quality of the PC-SAFT EOS. Generalized correlations for estimating interaction parameters for cubic EOS provide values of the wrong sign. While we show that interpolation and extrapolation of fitted interaction parameter values (k_{ij} set II) for related mixtures is preferred over choosing values of zero or the maximum interaction parameter values that yield the correct phase behavior (k_{ij} set III), selection of interaction parameters

for cubic EOS that most closely mimic bubble pressures predicted by the scaled PC-SAFT EOS is recommended. Further testing based on different families of mixtures is in progress.

4.6 Nomenclature

EOS	equation of state
k_{ij}	binary interaction parameter
m	shape parameter
σ	segment diameter
ε/k	segment energy parameter
L	liquid
LL	liquid-liquid
LV	liquid-vapor
LLV	liquid-liquid-vapor
ω	acentric factor
P	pressure (bar)
P_c	critical pressure
T_c	critical temperature
T	temperature (K)

4.7 References

(1) Gross, J.; Sadowski, G. Perturbed-chain SAFT: An equation of state based on a perturbation theory for chain molecules. *Ind. Eng. Chem. Res.* **2001**, 40, 1244-1260.

(2) Van Konynenburg, P. H.; Scott, R. L. Critical lines and phase equilibria in binary van der Waals mixtures. *Philos. Trans. R. Soc. London, Ser. A* **1980**, 298, 495-540.

(3) Peng, D. -Y; Robinson, D. B. A new two-constant equation of state. *Ind. Eng. Chem. Fundament.* **1976**, 15, 59-64.

(4) Soave, G. Equilibrium constants from a modified Redlich-Kwong equation of state. *Chem. Eng. Sci.* **1972**, 27, 1197-1203.

(5) Ahitan, S.; Satyro, M. A.; Shaw, J. M. Systematic Misprediction of n-Alkane + Aromatic and Naphthenic Hydrocarbon Phase Behavior Using Common Equations of State. *J. Chem. Eng. Data* **2015**, 60, 3300-3318.

(6) Kim, S. H.; Kang, J. W.; Kroenlein, K.; Magee, J. W.; Diky, V.; Muzny, C. D.; Kazakov, A. F.; Chirico, R. D.; Frenkel, M. Online data resources in chemical engineering education: Impact of the uncertainty concept for thermophysical properties. *Chem. Eng. Educ.* **2013**, 47, 48-57.

(7) Reed, M. E.; Whiting, W. B. Sensitivity and uncertainty of process designs to thermodynamic model parameters: a Monte Carlo approach. *Chem. Eng. Commun.* **1993**, 124, 39-48.

(8) Macchietto, S.; Maduabeuke, G.; Szczepanski, R. Exact determination of process sensitivity to physical properties. *Fluid Phase Equilib.* **1986**, 29, 59-67.

(9) Mathias, P. M. Sensitivity of process design to phase equilibrium-A new perturbation method based upon the Margules equation. *J. Chem. Eng. Data* **2014**, 59, 1006-1015.

(10) Hajipour, S.; Satyro, M. A. Uncertainty analysis applied to thermodynamic models and process design – 1. Pure components. *Fluid Phase Equilib.* **2011**, 307, 78-94.

(11) Hajipour, S.; Satyro, M. A.; Foley, M. W. Uncertainty analysis applied to thermodynamic models and process design—2. Binary mixtures. *Fluid Phase Equilib.* **2014**, 364, 15-30.

(12) Amani, M. J.; Gray, M. R.; Shaw, J. M. Phase behavior of Athabasca bitumen + water mixtures at high temperature and pressure. *J. Supercrit. Fluids* **2013**, 77, 142-152.

(13) Amani, M. J.; Gray, M. R.; Shaw, J. M. The phase behavior of Athabasca bitumen + toluene + water ternary mixtures. *Fluid Phase Equilib.* **2014**, 370, 75-84.

(14) Dini, Y.; Becerra, M.; Shaw, J. M. Phase behavior and thermophysical properties of Peace River bitumen + propane mixtures from 303 K to 393 K. submitted to the Journal of Chemical and Engineering Data (January, 2016). **2016**.

(15) *NIST Standard Reference Database 103b: NIST ThermoData Engine*, Version 7.1, accessed from Aspen Plus.

(16) *VMGSim Process Simulator*, Version 8.0; Virtual Materials Group Inc.: Calgary, AB 2013.

(17) *Aspen Plus*, Version 8.4; Aspen Technology, Inc.: Burlington, MA, 2013.

(18) Cismondi, M.; Nuñez, D. N.; Zabaloy, M. S.; Brignole, E. A.; Michelsen, M. L.; Mollerup, J. M. In *GPEC: A Program for Global Phase Equilibrium Calculations in Binary Systems*, Proceedings of Equifase 2006: VII Iberoamerican Conference on Phase Equilibria and Fluid Properties for Process Design, Morelia, Michoacán, México, 2006.

(19) Cismondi, M.; Brignole, E. A.; Mollerup, J. Rescaling of three-parameter equations of state: PC-SAFT and SPHCT. *Fluid Phase Equilib.* **2005**, 234, 108-121.

(20) Alfradique, M. F.; Castier, M. Critical points of hydrocarbon mixtures with the Peng–Robinson, SAFT, and PC-SAFT equations of state. *Fluid Phase Equilib.* **2007**, 257, 78-101.

(21) Blanco, S. T.; Gil, L.; Garcla-Gimenez, P.; Artal, M.; Otin, S.; Velasco, I. Critical properties and high-pressure volumetric behavior of the carbon dioxide

+ propane system at T = 308.15 K. Krichevskii function and related thermodynamic properties. *J. Phys. Chem. B* **2009**, 113, 7243–7256.

(22) Gil, L.; Martínez-López, J. F.; Artal, M.; Blanco, S. T.; Embid, J. M.; Fernández, J.; Otín, S.; Velasco, I. Volumetric behavior of the {CO_2 (1) + C_2H_6 (2)} system in the subcritical (T = 293.15 K), critical, and supercritical (T = 308.15 K) regions. *J. Phys. Chem. B* **2010***,* 114, 5447-5469.

(23) Gil, L.; Blanco, S. T.; Rivas, C.; Laga, E.; Fernández, J.; Artal, M.; Velasco, I. Experimental determination of the critical loci for {n-C_6H_{14} or CO_2 + alkan-1-ol} mixtures. Evaluation of their critical and subcritical behavior using PC-SAFT EoS. *J. Supercrit. Fluids* **2012***,* 71, 26-44.

(24) Frenkel, M.; Chirico, R. D.; Diky, V.; Yan, X.; Dong, Q.; Muzny, C. ThermoData Engine (TDE): Software implementation of the dynamic data evaluation concept. *J. Chem. Inf. Model.* **2005***,* 45, 816-838.

(25) Wang, L.; Tan, Z.; Meng, S.; Liang, D. Low-temperature heat capacity and phase transition of n-hexatriacontane. *Thermochim. Acta* **1999***,* 342, 59-65.

(26) *VMGSim User's Manual,* version 8.0; Virtual Materials Group Inc.: Calgary, AB 2013.

Chapter 5. Conclusions and Recommendations

5.1 Conclusions

Phase behavior of binary aromatic + n-alkane and naphthenic + n-alkane hydrocarbon mixtures was evaluated using the Peng-Robinson (PR), Soave-Redlich-Kwong (SRK) and Perturbed-Chain Statistical Associating Fluid Theory (PC-SAFT) equations of state. The computed outcomes were validated against experimental results, where available. Measurements were also made as part of this work to generate additional experimental data for the benzene + n-C_{20}, n-C_{24}, n-C_{28} and n-C_{36} binary mixtures to validate calculations. The disagreement observed between the predicted and experimental results was reported. The potential causes of errors were investigated and identified using sensitivity analyses. Recommendations were proposed that can significantly improve the quality of predictions by cubic equations of state for the above-mentioned families of binary mixtures. The key findings and recommendations of this work are as follows:

1. The Peng-Robinson and Soave-Redlich-Kwong equations of state predict incorrect phase behavior for binary aromatic + large n-alkane and naphthenic + large n-alkane hydrocarbon mixtures. Not only quantitatively but also qualitatively inaccurate results are obtained, if standard pure component and binary interaction parameter values are used. The cubic equations of state overestimate the non-ideality of these two classes of binary mixture; thereby predicting non-physical liquid-liquid phase behavior (Type II) instead of Type I phase behaviour. As a result, significantly higher bubble pressure values are predicted than arise

experimentally, well above the UCEP for the mixtures. The models also fail to reproduce the shape of experimental critical loci for these mixtures.

2. The systematic misprediction of phase behavior by the cubic equations of state is not due to errors arising during numerical computations or inappropriate selection of correlations used to estimate input pure component parameters (T_c, P_c, ω). Although, the outcomes are sensitive to the uncertainty in T_c, P_c, and ω of pure components, it is not the main cause of misprediction.
3. The dissonance in the predicted phase behaviors in the sub-critical region can be corrected if non-standard mixture-specific values for binary interaction parameters (k_{ij}) are used. The magnitude of k_{ij} values is dependent on the molecular size of compounds constituting the mixture - the greater the difference in the size of the molecules, the greater the magnitude of the k_{ij} required in order to get accurate predictions. In the near-critical and critical regions, negative k_{ij} values along with adjusted pure component parameters need to be used to fit experimental results.
4. The PC-SAFT EOS, with standard parameter values correctly predicts Type I phase behavior for binary aromatic + heavy n-alkane and naphthenic + heavy n-alkane hydrocarbon mixtures. It underestimates the bubble pressure values for binary mixtures of these families, but predicts values close to experimental measurements. It also yields better results than the cubic equations of state in the critical region, if the pure component parameters are scaled appropriately.
5. Generalized correlations for estimating interaction parameters for cubic EOS provide values of the wrong sign. Non-zero k_{ij} values required for the cubic equations of state in order to get both qualitatively and quantitatively correct results can be estimated using experimental data and/or outcomes from the PC-SAFT EOS, if there are no data available. Interpolation and extrapolation of fitted

interaction parameter values (k_{ij} set II) for related mixtures provide more accurate results than values of zero or the maximum interaction parameter values that yield the correct phase behavior (k_{ij} set III). Selection of interaction paramaters for cubic EOS that most closely mimic bubble pressures predicted by the scaled PC-SAFT EOS is recommended based on outcomes for benzene + n-alkane binary mixtures.

5.2 Recommendations for Future Work

1. Generalization of the recommendation related to interaction parameter estimation for cubic EOS must be tested for other families of binary mixtures (for e.g., toluene + n-alkanes, cycohexane + n-alkanes etc.) and eventually for multicomponent mixtures to validate the robustness of the recommendation.
2. Experimental data for relevant families of binary mixtures, though industrially very important, are scarce. Experiments need to be performed to generate vapor-liquid equilibrium data required to test the generalization of the recommendation regarding interaction parameter estimation.

Bibliography

Abrams, D. S.; Prausnitz, J. M. Statistical thermodynamics of liquid mixtures: a new expression for the excess Gibbs energy of partly or completely miscible systems. *AIChE J.* **1975**, 21, 116-128.

Afidick, D.; Kaczorowski, N. J.; Bette, S. In Production performance of a retrograde gas reservoir: a case study of the Arun Field; SPE - Asia Pacific Oil & Gas Conference; Society of Petroleum Engineers: Melbourne, Australia, **1994**.

Ahitan, S.; Satyro, M. A.; Shaw, J. M. Systematic Misprediction of n-Alkane + Aromatic and Naphthenic Hydrocarbon Phase Behavior Using Common Equations of State. *J. Chem. Eng. Data* **2015***,* 60, 3300-3318.

Aladwani, H. A.; Riazi, M. R. Some guidelines for choosing a characterization method for petroleum fractions in process simulators. *Chem. Eng. Res. Des.* **2005**, 83, 160-166.

Alfradique, M. F.; Castier, M. Critical points of hydrocarbon mixtures with the Peng–Robinson, SAFT, and PC-SAFT equations of state. *Fluid Phase Equilib.* **2007***,* 257, 78-101.

Altgelt, K. H.; Boduszynski, M. M. *Composition and analysis of heavy petroleum fractions;* M. Dekker: New York, 1994.

Altgelt, K. H.; Boduszynski, M. M. Composition of heavy petroleums. 3. An improved boiling point-molecular weight relation. *Energy Fuels* **1992**, 6, 68-72.

Amani, M. J.; Gray, M. R.; Shaw, J. M. Phase behavior of Athabasca bitumen + water mixtures at high temperature and pressure. *J. Supercrit. Fluids* **2013***,* 77, 142-152.

Amani, M. J.; Gray, M. R.; Shaw, J. M. The phase behavior of Athabasca bitumen + toluene + water ternary mixtures. *Fluid Phase Equilib.* **2014***,* 370, 75-84.

Aspen HYSYS, Version 8.4; Aspen Technology, Inc.: Burlington, MA 2013.

Aspen Plus, Version 8.4; Aspen Technology, Inc.: Burlington, MA, 2013.

Ba, A.; Eckert, E.; Vanek, T. Procedures for the selection of real components to characterize petroleum mixtures. *Chem. Pap.* **2003**, 57, 53-62.

Baker, L. E.; Pierce, A. C.; Luks, K. D. Gibbs energy analysis of phase equilibria. *Soc. Pet. Eng. J.* **1982**, 22, 731-742.

Balogh, J.; Csendes, T.; Stateva, R. P. Application of a stochastic method to the solution of the phase stability problem: Cubic equations of state. *Fluid Phase Equilib.* **2003**, 212, 257-267.

Blanco, S. T.; Gil, L.; Garcla-Gimenez, P.; Artal, M.; Otin, S.; Velasco, I. Critical properties and high-pressure volumetric behavior of the carbon dioxide + propane system at T = 308.15 K. Krichevskii function and related thermodynamic properties. *J. Phys. Chem. B* **2009**, 113, 7243–7256.

Blas, F. J.; Vega, L. F. Critical behavior and partial miscibility phenomena in binary mixtures of hydrocarbons by the statistical associating fluid theory. *J. Chem. Phys.* **1998**, 109, 7405-7413.

Blas, F. J.; Vega, L. F. Thermodynamic behaviour of homonuclear and heteronuclear Lennard-Jones chains with association sites from simulation and theory. *Mol. Phys*. **1997**, 92, 135-150.

Boduszynski, M. M. Composition of heavy petroleums. 1. Molecular weight, hydrogen deficiency, and heteroatom concentration as a function of atmospheric equivalent boiling point up to 1400 °F (760 °C). *Energy Fuels* **1987**, 1, 2-11.

Boduszynski, M. M. Composition of heavy petroleums. 2. Molecular characterization. *Energy Fuels* **1988**, 2, 597-613.

Boduszynski, M. M.; Altgelt, K. H. Composition of heavy petroleums. 4. Significance of the extended Atmospheric Equivalent Boiling Point (AEBP) scale. *Energy Fuels* **1992**, 6, 72-76.

Boukouvalas, C.; Spiliotis, N.; Coutsikos, P.; Tzouvaras, N.; Tassios, D. Prediction of vapor-liquid equilibrium with the LCVM model: a linear combination of the Vidal and Michelsen mixing rules coupled with the original UNIFAC and the t-mPR equation of state. *Fluid Phase Equilib*. **1994**, 92, 75-106.

Brunner, E. Fluid mixtures at high pressures II. Phase separation and critical phenomena of (ethane + an n-alkanol) and of (ethane + methanol) and (propane + methanol). *J. Chem. Thermodyn.* **1985**, 17, 871-885.

Cañas-Marín, W. A.; Ortiz-Arango, J. D.; Guerrero-Aconcha, U. E.; Soto-Tavera, C. P. Thermodynamic derivative properties and densities for hyperbaric gas condensates: SRK equation of state predictions versus Monte Carlo data. *Fluid Phase Equilib*. **2007**, 253, 147-154.

Castier, M.; Sandler, S. I. Critical points with the Wong-Sandler mixing rule - II. Calculations with a modified Peng-Robinson equation of state. *Chem. Eng. Sci.* **1997**, 52, 3579-3588.

Chang, H. L.; Hurt, L. J.; Kobayashi, R. Vapor-liquid equilibria of light hydrocarbons at low temperatures and high pressures: The methane-n-heptane system. *AIChE J.* **1966**, 12, 1212-1216.

Chapman, W. G.; Gubbins, K. E.; Jackson, G.; Radosz, M. New reference equation of state for associating liquids. *Ind. Eng. Chem. Res*. **1990**, 29, 1709-1721.

Chapman, W. G.; Gubbins, K. E.; Jackson, G.; Radosz, M. SAFT: Equation-of-state solution model for associating fluids. *Fluid Phase Equilib.* **1989**, 52, 31-38.

Cismondi Duarte, M.; Cruz Doblas, J.; Gomez, M. J.; Montoya, G. F. Modelling the phase behavior of alkane mixtures in wide ranges of conditions: New parameterization and predictive correlations of binary interactions for the RKPR EOS. *Fluid Phase Equilib.* **2015**, 403, 49-59.

Cismondi Duarte, M.; Galdo, M. V.; Gomez, M. J.; Tassin, N. G.; Yanes, M. High pressure phase behavior modeling of asymmetric alkane + alkane binary systems with the RKPR EOS. *Fluid Phase Equilib.* **2014**, 362, 125-135.

Cismondi, M.; Brignole, E. A.; Mollerup, J. Rescaling of three-parameter equations of state: PC-SAFT and SPHCT. *Fluid Phase Equilib.* **2005***,* 234, 108-121.

Cismondi, M.; Nuñez, D. N.; Zabaloy, M. S.; Brignole, E. A.; Michelsen, M. L.; Mollerup, J. M. In *GPEC: A Program for Global Phase Equilibrium Calculations in Binary Systems*, Proceedings of Equifase 2006: VII Iberoamerican Conference on Phase Equilibria and Fluid Properties for Process Design, Morelia, Michoacán, México, 2006.

Cismondi, M.; Nuñez, D. N.; Zabaloy, M. S.; Brignole, E. A.; Michelsen, M. L.; Mollerup, J. M. In *GPEC: A Program for Global Phase Equilibrium Calculations in Binary Systems*, Proceedings of Equifase 2006: VII Iberoamerican Conference on Phase Equilibria and Fluid Properties for Process Design, Morelia, Michoacán, México, 2006.

Constantinou, L.; Gani, R. New group contribution method for estimating properties of pure compounds. *AIChE J.* **1994**, 40, 1697-1709.

Dadgostar, N.; Shaw, J. M. On the use of departure function correlations for hydrocarbon isobaric liquid phase heat capacity calculation. *Fluid Phase Equilib*. **2015**, 385, 182-195.

Dahl, S.; Michelsen, M. L. High-pressure vapor-liquid equilibrium with a UNIFAC-based equation of state. *AIChE J*. **1990**, 36, 1829-1836.

Davenport, A. J.; Rowlinson, J. S. The solubility of hydrocarbons in liquid methane. *Trans. Faraday Soc.* **1963***,* 59, 78-84.

De Goede, R.; Peters, C. J.; Van Der Kooi, H. J.; Lichtenthaler, R. N. Phase equilibria in binary mixtures of ethane and hexadecane. *Fluid Phase Equilib.* **1989**, 50, 305-314.

Dini, Y.; Becerra, M.; Shaw, J. M. Phase behavior and thermophysical properties of Peace River bitumen + propane mixtures from 303 K to 393 K. submitted to the Journal of Chemical and Engineering Data (January, 2016). **2016**.

Domanska, U.; Hofman, T.; Rolinska, J. Solubility and vapour pressures in saturated solutions of high-molecular-weight hydrocarbons. *Fluid Phase Equilib.* **1987**, 32, 273-293.

Domanska, U.; Kniaz, K. Solid-liquid equilibrium. cyclopentane-octacosane system. *Int. DATA Ser., Sel. Data Mixtures, Ser. A* **1990**, 206.

Domanska, U.; Rolinska, J.; Szafranski, A. M. Solid-liquid equilibrium. cyclohexane-octacosane system. *Int. DATA Ser., Sel. Data Mixtures, Ser. A* **1987***,* 276.

Eckert, E. Do we need pseudocomponents? *Chem. Listy* **2001**, 95, 368-373.

Eckert, E.; Vanek, T. Improvements in the selection of real components forming a substitute mixture for petroleum fractions. *Chem. Pap.* **2009**, 63, 399-405.

Eckert, E.; Vanek, T. New approach to the characterisation of petroleum mixtures used in the modelling of separation processes. *Comput. Chem. Eng.* **2005**, 30, 343-356.

Elhassan, A. E.; Barrufet, M. A.; Eubank, P. T. Correlation of the critical properties of normal alkanes and alkanols. *Fluid Phase Equilib.* **1992**, 78, 139-155.

Fernandez-Lima, F.; Becker, C.; McKenna, A. M.; Rodgers, R. P.; Marshall, A. G.; Russell, D. H. Petroleum crude oil characterization by IMS-MS and FTICR MS. *Anal. Chem.* **2009**, 9941-9947.

Frenkel, M.; Chirico, R. D.; Diky, V.; Yan, X.; Dong, Q.; Muzny, C. ThermoData Engine (TDE): Software implementation of the dynamic data evaluation concept. *J. Chem. Inf. Model.* **2005***,* 45, 816-838.

Fu, Y. H.; Sandler, S. I. A simplified SAFT equation of state for associating compounds and mixtures. *Ind. Eng. Chem. Res*. **1995**, 34, 1897-1909.

Gao, G.; Daridon, J. L.; Saint-Guirons, H.; Xans, P.; Montel, F. A simple correlation to evaluate binary interaction parameters of the Peng-Robinson equation of state : Binary light hydrocarbon systems. *Fluid Phase Equilib.* **1992**, 74, 85–93.

Gil-Villegas, A.; Galindo, A.; Whitehead, P. J.; Mills, S. J.; Jackson, G.; Burgess, A. N. Statistical associating fluid theory for chain molecules with attractive potentials of variable range. *J. Chem. Phys*. **1996**, 106, 4168-4186.

Gil, L.; Blanco, S. T.; Rivas, C.; Laga, E.; Fernández, J.; Artal, M.; Velasco, I. Experimental determination of the critical loci for {n-C_6H_{14} or CO_2 + alkan-1-ol} mixtures. Evaluation of their critical and subcritical behavior using PC-SAFT EoS. *J. Supercrit. Fluids* **2012***,* 71, 26-44.

Gil, L.; Martínez-López, J. F.; Artal, M.; Blanco, S. T.; Embid, J. M.; Fernández, J.; Otín, S.; Velasco, I. Volumetric behavior of the {CO_2 (1) + C_2H_6 (2)} system in the subcritical (T = 293.15 K), critical, and supercritical (T = 308.15 K) regions. *J. Phys. Chem. B* **2010***,* 114, 5447-5469.

Gonzalez, D. L.; Hirasaki, G. J.; Creek, J.; Chapman, W. G. Modeling of asphaltene precipitation due to changes in composition using the perturbed chain statistical associating fluid theory equation of state. *Energy Fuels* **2007**, 213, 1231-1242.

Gonzalez, D. L.; Vargas, F. M.; Hirasaki, G. J.; Chapman, W. G. Modeling study of CO2-induced asphaltene precipitation. *Energy Fuels* **2008**, 22, 757-762.

Gross, J.; Sadowski, G. Modeling polymer systems using the perturbed-chain statistical associating fluid theory equation of state. *Ind. Eng. Chem. Res.* **2002**, 41, 1084-1093.

Gross, J.; Sadowski, G. Perturbed-chain SAFT: An equation of state based on a perturbation theory for chain molecules. *Ind. Eng. Chem*. Res. **2001**, 40, 1244-1260.

Hajipour, S.; Satyro, M. A. Uncertainty analysis applied to thermodynamic models and process design – 1. Pure components. *Fluid Phase Equilib*. **2011**, 307, 78-94.

Hajipour, S.; Satyro, M. A.; Foley, M. W. Uncertainty analysis applied to thermodynamic models and process design—2. Binary mixtures. *Fluid Phase Equilib.* **2014**, 364, 15-30.

Holderbaum, T.; Gmehling, J. PSRK: A group contribution equation of state based on UNIFAC. *Fluid Phase Equilib*. **1991**, 70, 251-265.

Hua, J. Z.; Maier, R. W.; Tessier, S. R.; Brennecke, J. F.; Stadtherr, M. A. Interval analysis for thermodynamic calculations in process design: A novel and completely reliable approach. *Fluid Phase Equilib.* **1999**, 158, 607-615.

Huron, M.; Vidal, J. New mixing rules in simple equations of state for representing vapour-liquid equilibria of strongly non-ideal mixtures. *Fluid Phase Equilib*. **1979**, 3, 255-271.

J.D. van der Waals. On the continuity of the gaseous and liquid State. Ph.D. Thesis, University of Leiden, Netherlands, 1873.

Jaubert, J.; Mutelet, F. VLE predictions with the Peng–Robinson equation of state and temperature dependent kij calculated through a group contribution method. *Fluid Phase Equilib.* **2004**, 224, 285-304.

Jaubert, J.; Vitu, S.; Mutelet, F.; Corriou, J. Extension of the PPR78 model (predictive 1978, Peng–Robinson EOS with temperature dependent kij calculated through a group contribution method) to systems containing aromatic compounds. *Fluid Phase Equilib.* **2005**, 237, 193-211.

Jennings, D. W.; Weispfennig, K. Experimental solubility data of various n-alkane waxes: Effects of alkane chain length, alkane odd versus even carbon number structures, and solvent chemistry on solubility. *Fluid Phase Equilib.* **2005**, 227, 27-35.

Joback, K. G.; Reid, R. C. Estimation of pure-component properties from group-contributions. *Chem. Eng. Commun.* **1987**, 57, 233-243.

Jones, D. R.; Perttunen, C. D.; Stuckman, B. E. Lipschitzian optimization without the Lipschitz constant. *J. Optimiz. Theory Appl.* **1993**, 79, 157-181.

Kariznovi, M.; Nourozieh, H.; Abedi, J. (Vapor + liquid) equilibrium properties of (ethane + ethanol) system at (295, 303, and 313) K. *J. Chem. Thermodyn.* **2011**, 43, 1719-1722.

Kim, S. H.; Kang, J. W.; Kroenlein, K.; Magee, J. W.; Diky, V.; Muzny, C. D.; Kazakov, A. F.; Chirico, R. D.; Frenkel, M. Online data resources in chemical engineering education: Impact of the uncertainty concept for thermophysical properties. *Chem. Eng. Educ.* **2013***,* 47, 48-57.

Kontogeorgis, G. M.; Tassios, D. P. Critical constants and acentric factors for long-chain alkanes suitable for corresponding states applications. A critical review. *Chem. Eng. J.* **1997**, 66, 35-49.

Konynenburg, v., P. H.; Scott, R. L. Critical lines and phase-equilibria in binary van der Waals mixtures. *Philos. Trans. R. Soc*. **1980**, 298, 495-540.

Kordas, A.; Magoulas, K.; Stamataki, S.; Tassios, D. Methane-hydrocarbon interaction parameters correlation for the Peng-Robinson and the t-mPR equation of state. *Fluid Phase Equilib.* **1995**, 112, 33-44.

Kraska, T.; Gubbins, K. E. Phase equilibria calculations with a modified SAFT equation of state. 1. Pure alkanes, alkanols, and water. *Ind. Eng. Chem. Res*. **1996**, 35, 4727-4737.

Lam, D. H.; Jangkamolkulchai, A.; Luks, K. D. Liquid-liquid-vapor phase equilibrium behavior of certain binary ethane + n-alkanol mixtures. *Fluid Phase Equilib.* **1990**, 59, 263-277.

Leekumjorn, S.; Krejbjerg, K. Phase behavior of reservoir fluids: Comparisons of PC-SAFT and cubic EOS simulations. *Fluid Phase Equilib.* **2013**, 359, 17-23.

Lin, Y. N.; Chen, R. J. J.; Chappelear, P. S.; Kobayashi, R. Vapor-liquid equilibrium of the methane-n-hexane system at low temperature. *J. Chem. Eng. Data* **1977**, 22, 402-408.

Macchietto, S.; Maduabeuke, G.; Szczepanski, R. Exact determination of process sensitivity to physical properties. *Fluid Phase Equilib.* **1986***,* 29, 59-67.

Marrero-Morejón, J.; Pardillo-Fontdevila, E. Estimation of pure compound properties using group-interaction contributions. *AIChE J.* **1999**, 45, 615-621.

Marrero, J.; Gani, R. Group-contribution based estimation of pure component properties. *Fluid Phase Equilib.* **2001**, 183, 183-208.

Mathias, P. M. Sensitivity of process design to phase equilibrium-A new perturbation method based upon the Margules equation. *J. Chem. Eng. Data* **2014**, 59, 1006-1015.

McCabe, C.; Gil-Villegas, A.; Jackson, G. Predicting the high-pressure phase equilibria of methane + n-hexane using the SAFT-VR approach. *J. Phys. Chem. B* **1998**, 102, 4183-4188.

McDonald, C. M.; Floudas, C. A. Global optimization for the phase stability problem. *AIChE J.* **1995**, 41, 1798-1814.

McKenna, A. M.; Blakney, G. T.; Xian, F.; Glaser, P. B.; Rodgers, R. P.; Marshall, A. G. Heavy petroleum composition. 2. Progression of the Boduszynski model to the limit of distillation by ultrahigh-resolution FT-ICR mass spectrometry. *Energy Fuels* **2010**, 24, 2939-2946.

McKenna, A. M.; Donald, L. J.; Fitzsimmons, J. E.; Juyal, P.; Spicer, V.; Standing, K. G.; Marshall, A. G.; Rodgers, R. P. Heavy petroleum composition. 3. Asphaltene aggregation. *Energy Fuels* **2013**, 27, 1246-1256.

McKenna, A. M.; Marshall, A. G.; Rodgers, R. P. Heavy petroleum composition. 4. Asphaltene compositional space. *Energy Fuels* **2013**, 27, 1257-1267.

McKenna, A. M.; Purcell, J. M.; Rodgers, R. P.; Marshall, A. G. Heavy petroleum composition. 1. Exhaustive compositional analysis of Athabasca bitumen HVGO distillates by Fourier Transform Ion Cyclotron Resonance Mass Spectrometry: A definitive test of the Boduszynski model. *Energy Fuels* **2010**, 24, 2929-2938.

Meindersma, G. W.; de Haan, A. B. Conceptual process design for aromatic/aliphatic separation with ionic liquids. *Chem. Eng. Res. Design* **2008**, 86, 745-752.

Meindersma, G. W.; Hansmeier, A. R.; De Haan, A. B. Ionic liquids for aromatics extraction. Present status and future outlook. *Ind. Eng. Chem. Res.* **2010**, 49, 7530-7540.

Michelsen, M. L. The isothermal flash problem. Part II. Phase-split calculation. *Fluid Phase Equilib.* **1982**, 9, 21-40.

Minicucci, D.; Zou, X.-Y.; Shaw, J. M. The impact of liquid–liquid–vapour phase behaviour on coke formation from model coke precursors. *Fluid Phase Equilib.* **2002**, 194–197, 353-360.

Mushrif, S. H.; Phoenix, A. V. Effect of Peng-Robinson binary interaction parameters on the predicted multiphase behavior of selected binary systems. *Ind. Eng. Chem. Res.* **2008**, 47, 6280-6288.

Nichita, D. V.; Gomez, S.; Luna E. Phase stability analysis with cubic equations of state by using a global optimization method. *Fluid Phase Equilib.* **2002**, 194, 411-437.

Nichita, D. V.; Gomez, S.; Luna, E. Multiphase equilibria calculation by direct minimization of Gibbs free energy with a global optimization method. *Comput. Chem. Eng.* **2002**, 26, 1703-1724.

Nishiumi, H.; Arai, T.; Takeuchi, K. Generalization of the binary interaction parameter of the Peng-Robinson equation of state by component family. *Fluid Phase Equilib.* **1988**, 42, 43-62.

NIST Standard Reference Database 103b: NIST ThermoData Engine, Version 7.1, accessed from Aspen Plus.

Peng, D. -Y; Robinson, D. B. A new two-constant equation of state. *Ind. Eng. Chem. Fundament*. **1976**, 15, 59-64.

Peters, C. J.; De Roo, J. L.; De Swaan Arons, J. Phase equilibria in binary mixtures of propane and triphenylmethane. *Fluid Phase Equilib.* **1995**, 109, 99-111.

Peters, C. J.; De Roo, J. L.; De Swaan Arons, J. Three-phase equilibria in (ethane + pentacosane). *J. Chem. Thermodyn.* **1987**, 19, 265-272.

Peters, C. J.; De Roo, J. L.; Lichtenthaler, R. N. Measurements and calculations of phase equilibria in binary mixtures of ethane + eicosane. *Fluid Phase Equilib.* **1991**, 69, 51-66.

Peters, C. J.; De Roo, J. L.; Lichtenthaler, R. N. Measurements and calculations of phase equilibria of binary mixtures of ethane + eicosane. Part I: vapour + liquid equilibria. *Fluid Phase Equilib.* **1987**, 34, 287-308.

Peters, C. J.; Lichtenthaler, R. N.; De Swaan Arons, J. Three phase equilibria in binary mixtures of ethane and higher n-alkanes. *Fluid Phase Equilib.* **1986**, 29, 495-504.

Peters, C. J.; Rijkers, M. P. W. M.; De Roo, J. L.; De Swaan Arons, J. Phase equilibria in binary mixtures of near-critical propane and poly-aromatic hydrocarbons. *Fluid Phase Equilib.* **1989**, 52, 373-387.

Peters, C. J.; Spiegelaar, J.; De Swaan Arons, J. Phase equilibria in binary mixtures of ethane + docosane and molar volumes of liquid docosane. *Fluid Phase Equilib.* **1988**, 41, 245-256.

Peters, C. J.; Van Der Kooi, H. J.; De Swaan Arons, J. Measurements and calculations of phase equilibria for (ethane + tetracosane) and (p, Vm′∗, T) of liquid tetracosane. *J. Chem. Thermodyn.* **1987**, 19, 395-405.

Podgorski, D. C.; Corilo, Y. E.; Nyadong, L.; Lobodin, V. V.; Bythell, B. J.; Robbins, W. K.; McKenna, A. M.; Marshall, A. G.; Rodgers, R. P. Heavy petroleum composition. 5. Compositional and structural continuum of petroleum revealed. *Energy Fuels* **2013**, 27, 1268-1276.

Polishuk, I.; Wisniak, J.; Segura, H. Prediction of the critical locus in binary mixtures using equation of state: I. Cubic equations of state, classical mixing rules, mixtures of methane–alkanes. *Fluid Phase Equilib.* **1999**, 164, 13-47.

Privat, R.; Conte, E.; Jaubert, J.; Gani, R. Are safe results obtained when SAFT equations are applied to ordinary chemicals? Part 2: Study of solid–liquid equilibria in binary systems. *Fluid Phase Equilib*. **2012**, 318, 61-76.

Privat, R.; Gani, R; Jaubert, J. Are safe results obtained when the PC-SAFT equation of state is applied to ordinary pure chemicals? *Fluid Phase Equilib.* **2010**, 295, 76-92.

Quann, R. J.; Jaffe, S. B. Structure-oriented lumping: describing the chemistry of complex hydrocarbon mixtures. *Ind. Eng. Chem. Res.* **1993**, 32, 1800-1800.

Redlich, O.; Kwong, J. N. S. On the thermodynamics of solutions. V: An equation of state. Fugacities of gaseous solutions. *Chem. Rev*. **1949**, 44, 233-244.

Reed, M. E.; Whiting, W. B. Sensitivity and uncertainty of process designs to thermodynamic model parameters: a Monte Carlo approach. *Chem. Eng. Commun.* **1993***,* 124, 39-48.

Renon, H.; Prausnitz, J. M. Local compositions in thermodynamic excess functions for liquid mixtures. *AIChE J*. **1968**, 14, 135-144.

Stamataki, S.; Tassios, D. Performance of cubic eos at high pressures. *Rev. Inst. Fr. Pet.* **1998**, 53, 367–378.

Saber, N. Phase Behaviour Prediction for Ill-Defined Hydrocarbon Mixtures. Ph.D. Thesis, University of Alberta, AB, 2011.

Saber, N.; Shaw, J. M. Rapid and robust phase behaviour stability analysis using global optimization. *Fluid Phase Equilib*. **2008**, 264, 137-146.

Saber, N.; Shaw, J. M. Toward multiphase equilibrium prediction for ill-defined asymmetric hydrocarbon mixtures. *Fluid Phase Equilib.* **2009**, 285, 73-82.

Shaw, J. M.; Satyro, M. A.; Yarranton, H. W. Chapter 7-The phase behaviour and properties of heavy oils. In *Practical Advances in Petroleum Production and Processing*; Hsu, C. S., Robinson, P. R., Eds.; Springer: New York, 2015.

Soave, G. Equilibrium constants from a modified Redlich-Kwong equation of state. *Chem. Eng. Sci*. **1972**, 27, 1197-1203.

Sun, A. C.; Seider, W. D. Homotopy-continuation method for stability analysis in the global minimization of the Gibbs Free energy. *Fluid Phase Equilib.* **1995**, 103, 213-249.

Thermo Explorer User's Manual, version 1.0; Virtual Materials Group Inc.: Calgary, AB 2009.

Tihic, A.; Kontogeorgis, G. M.; Solms, von, N.; Michelsen, M. L. Applications of the simplified perturbed-chain SAFT equation of state using an extended parameter table. *Fluid Phase Equilib.* **2006**, 248, 29-43.

Ting, P. D.; Gonzalez, D. L.; Hirasaki, G. J.; Chapman, W. G. Application of the PC-SAFT equation of state to asphaltene phase behavior. In *Asphaltenes, Heavy Oils, and Petroleomics*; Mullins, O.C., Sheu, E.Y., Hammami, A., Marshall, A.G., Eds.; Springer: New York, **2007**; 301-327.

Van Konynenburg, P. H.; Scott, R. L. Critical lines and phase equilibria in binary van der Waals mixtures. *Philos. Trans. R. Soc. London, Ser. A* **1980***,* 298, 495-540.

Vargas, F. M.; Gonzalez, D. L.; Hirasaki, G. J.; Chapman, W. G. Modeling asphaltene phase behavior in crude oil systems using the perturbed chain form of the statistical associating fluid theory (PC-SAFT) equation of state. *Energy Fuels* **2009**, 23, 1140-1146.

VMGSim Process Simulator, Version 8.0; Virtual Materials Group Inc.: Calgary, AB 2013.

VMGSim User's Manual, version 8.0; Virtual Materials Group Inc.: Calgary, AB 2013.

Von Solms, N.; Michelsen, M. L.; Kontogeorgis, G. M. Computational and physical performance of a modified PC-SAFT equation of state for highly asymmetric and associating mixtures. *Ind. Eng. Chem. Res*. **2003**, 42, 1098-1105.

Vostrikov, S. V.; Nesterova, T. N.; Nesterov, I. A.; Sosin, S. E.; Nazmutdinov, A. G. III. Study of critical and maximum temperatures of coexistence of liquid and gas phase in hydrocarbons binary mixtures of aromatic hydrocarbons with alkanes and cycloalkanes. *Fluid Phase Equilib.* **2014**, 377, 56-75.

Wang, L.; Tan, Z.; Meng, S.; Liang, D. Low-temperature heat capacity and phase transition of n-hexatriacontane. *Thermochim. Acta* **1999***,* 342, 59-65.

Wertheim, M. S. Fluids with highly directional attractive forces. I. Statistical thermodynamics. *J. Stat. Phys*. **1984**, 35, 19-34.

Wertheim, M. S. Fluids with highly directional attractive forces. II. Thermodynamic perturbation theory and integral equations. *J. Stat. Phys*. **1984**, 35, 35-47.

Wertheim, M. S. Fluids with highly directional attractive forces. III. Multiple attraction sites. *J. Stat. Phys*. **1986**, 42, 459-476.

Wertheim, M. S. Fluids with highly directional attractive forces. IV. Equilibrium polymerization. *J. Stat. Phys*. **1986**, 42, 477-492.

Wong, D. S. H.; Orbey, H.; Sandler, S. I. Equation of state mixing rule for nonideal mixtures using available activity coefficient model parameters and that allows extrapolation over large ranges of temperature and pressure. *Ind. Eng. Chem. Res*. **1992**, 31, 2033-2039.

Yelash, L.; Müller, M.; Paul, W.; Binder, K. A global investigation of phase equilibria using the perturbed-chain statistical-associating-fluid-theory approach. *J. Chem. Phys.* **2005**, 123, 014908.

Yelash, L.; Müller, M.; Paul, W.; Binder, K. Artificial multiple criticality and phase equilibria: An investigation of the PC-SAFT approach. *Phys. Chem. Chem. Phys.* **2005**, 7, 3728-3732.

Yushan, Z.; Zhihong, X. Lipschitz optimization for phase stability analysis: Application to Soave-Redlich-Kwong equation of state. *Fluid Phase Equilib.* **1999**, 162, 19-29.

Appendix 1. Supplementary data*

Pure component properties and parameters used for calculations, and binary interaction parameters used in the simulation software. Please refer main article for cited references.

Table S1. Binary interaction parameters for the PR equation of state in VMGSim

	n-C_{10}	n-C_{15}	n-C_{17}	n-C_{20}	n-C_{24}	n-C_{28}	n-C_{30}	n-C_{36}	n-C_{40}	n-C_{50}
Benzene	0.0003	0.0018	0.0024	0.0032	0.0043	0.0054	0.0059	0.0073	0.0081	0.0099
Toluene	0.0001	0.0011	0.0015	0.0022	0.0032	0.0041	0.0045	0.0058	0.0065	0.0082
Ethylbenzene	0.0000	0.0006	0.0010	0.0015	0.0024	0.0032	0.0036	0.0047	0.0053	0.0069
n-Propylbenzene	0.0000	0.0003	0.0006	0.0011	0.0018	0.0025	0.0029	0.0039	0.0045	0.0059
Naphthalene	0.0012	0.0001	0.0000	0.0000	0.0002	0.0004	0.0006	0.0011	0.0014	0.0023
1-Methylnaphthalene	0.0017	0.0003	0.0001	0.0000	0.0001	0.0002	0.0004	0.0008	0.0010	0.0018
Phenanthrene	0.0039	0.0014	0.0010	0.0006	0.0002	0.0000	0.0000	0.0000	0.0001	0.0004
Cyclopentane	0.0012	0.0035	0.0043	0.0054	0.0068	0.0082	0.0088	0.0104	0.0114	0.0136
Cyclohexane	0.0004	0.0020	0.0027	0.0035	0.0047	0.0058	0.0063	0.0077	0.0086	0.0105
Methylcyclohexane	0.0002	0.0015	0.0021	0.0028	0.0039	0.0049	0.0054	0.0067	0.0075	0.0093
Ethylcyclohexane	0.0000	0.0007	0.0012	0.0017	0.0026	0.0035	0.0039	0.0050	0.0057	0.0073
n-Propycyclohexane	0.0000	0.0003	0.0006	0.0011	0.0018	0.0025	0.0028	0.0038	0.0045	0.0059
Bicyclohexyl	0.0009	0.0000	0.0000	0.0001	0.0004	0.0007	0.0009	0.0015	0.0019	0.0028
cis-Decahydronaphthalene	0.0001	0.0003	0.0006	0.0010	0.0016	0.0023	0.0027	0.0036	0.0042	0.0056
Perhydrophenanthrene	0.0020	0.0004	0.0002	0.0000	0.0000	0.0001	0.0002	0.0006	0.0008	0.0015

* Refer Chapter-3 for the cited references in Appendix-1.

Table S2. Binary interaction parameters for the PR equation of state in Aspen HYSYS

	n-C_{10}	n-C_{15}	n-C_{17}	n-C_{20}	n-C_{24}	n-C_{28}	n-C_{30}	n-C_{36}	n-C_{40} [a]	n-C_{50} [a]
Benzene	0.0097	0.0203	0.0249	0.0313	0.0385	0.0448	0.0477	0.0574	-	-
Toluene	0.0057	0.0144	0.0183	0.0239	0.0303	0.0360	0.0387	0.0476	-	-
Ethylbenzene	0.0031	0.0101	0.0134	0.0183	0.0240	0.0292	0.0316	0.0398	-	-
n-Propylbenzene	0.0014	0.0066	0.0094	0.0136	0.0186	0.0232	0.0253	0.0328	-	-
Naphthalene	0.0020	0.0080	0.0111	0.0156	0.0208	0.0257	0.0280	0.0357	-	-
1-Methylnaphthalene	0.0003	0.0037	0.0059	0.0093	0.0135	0.0175	0.0194	0.0261	-	-
Phenanthrene	0.0001	0.0030	0.0049	0.0081	0.0120	0.0158	0.0176	0.0240	-	-
Cyclopentane	0.0097	0.0203	0.0249	0.0313	0.0385	0.0448	0.0477	0.0574	-	-
Cyclohexane	0.0062	0.0151	0.0191	0.0248	0.0313	0.0372	0.0398	0.0489	-	-
Methylcyclohexane [a]	-	-	-	-	-	-	-	-	-	-
Ethylcyclohexane [a]	-	-	-	-	-	-	-	-	-	-
n-Propycyclohexane	0.0008	0.0052	0.0077	0.0115	0.0161	0.0205	0.0225	0.0296	-	-
Bicyclohexyl	0.0000	0.0021	0.0037	0.0065	0.0102	0.0137	0.0154	0.0214	-	-
cis-Decahydronaphthalene	0.0007	0.0052	0.0077	0.0115	0.0161	0.0204	0.0225	0.0295	-	-
Perhydrophenanthrene [a]	-	-	-	-	-	-	-	-	-	-

[a] compound not available in compound library of the software

Table S3. Pure component parameters for the PC-SAFT equation of state

Compound	m	σ [Å]	ε/k (K)	Reference
n-C_{10}	4.6627	3.8384	243.8700	[3]
n-C_{15}	6.2855	3.9531	254.1400	[3]
n-C_{17}	6.9809	3.9675	255.6500	[3]
n-C_{20}	7.9849	3.9869	257.7500	[3]
n-C_{24}	9.4034	3.9896	254.6100	[39]

n-C_{28}	10.8004	4.0019	255.6700	[39]
n-C_{30}*	11.4996	4.0070	256.1117	[39]
n-C_{36}	13.5946	4.0189	257.1500	[39]
n-C_{40}*	14.9923	4.0249	257.6781	[39]
n-C_{50}*	18.4850	4.0360	258.6525	[39]
benzene	2.4653	3.6478	287.3500	[3]
toluene	2.8149	3.7169	285.6900	[3]
ethylbenzene	3.0799	3.7974	287.3500	[3]
n-propylbenzene	3.3438	3.8438	288.1300	[3]
naphthalene	3.0047	3.9133	353.6300	[39]
1-methylnaphthalene	3.5975	3.8173	335.5700	[39]
phenanthrene	3.4890	4.1053	403.0600	[40]
cyclopentane	2.3655	3.7114	265.8300	[3]
cyclohexane	2.5303	3.8499	278.1100	[3]
methylcyclohexane	2.6637	3.9993	282.3300	[3]
ethylcyclohexane	2.8256	4.1039	294.0400	[3]
n-propycyclohexyl	3.2779	4.0499	285.9100	[39]
bicyclohexyl*	4.3733	4.0309	279.6842	[39]
cis-decahydronaphthalene	2.9850	4.1803	331.1800	[39]
perhydrophenanthrene*	4.9540	4.0575	280.8965	[39]

* calculated using correlations in Tihic et al. [39]

Table S4. Pure component properties from NIST/TDE [37].

Compounds	T_C (K)	P_C (bar)	Z_C	ω	T_B (K)	T_F (K)
n-C_{10}	618.05	21.02	0.254	0.485	447.27	243.53
n-C_{15}	706.88	14.44	0.230	0.684	543.79	283.10
n-C_{17}	735.71	13.22	0.235	0.750	575.87	295.12
n-C_{20}	768.22	10.77	0.221	0.868	617.23	309.63
n-C_{24}	799.55	8.69	0.207	1.057	664.23	323.53
n-C_{28}	824.00	7.51	0.210	1.264	707.20	334.43
n-C_{30}	843.00	6.45	0.189	1.182	725.70	339.01
n-C_{36}	872.00	4.72	0.168	1.419	775.40	348.96
n-C_{40}	867.00	3.82	0.157	1.769	786.60	354.58
n-C_{50}	1016.00	4.20	0.190	1.395	938.10	364.89
benzene	562.02	48.94	0.269	0.210	353.22	278.67
toluene	591.89	41.27	0.266	0.265	383.73	178.08
ethylbenzene	617.12	36.16	0.263	0.304	409.32	178.20
n-propylbenzene	638.29	32.01	0.266	0.345	432.35	173.63
naphthalene	748.33	40.40	0.265	0.303	491.13	353.32
1-methylnaphthalene	770.71	35.41	0.265	0.347	517.78	242.71
phenanthrene	866.00	24.89	0.190	0.434	611.62	372.20
cyclopentane	511.74	45.15	0.276	0.195	322.39	179.46
cyclohexane	553.40	40.70	0.272	0.210	353.84	279.71
methylcyclohexane	572.31	34.81	0.269	0.235	374.04	146.76
ethylcyclohexane	606.90	32.86	0.284	0.294	404.91	161.85

n-propycyclohexyl	630.80	28.69	0.266	0.327	429.85	178.29
bicyclohexyl	742.00	29.18	0.290	0.382	510.85	276.86
cis-decahydronaphthalene	702.22	32.02	0.269	0.286	468.94	230.16
perhydrophenanthrene	795.00	26.34	0.274	0.409	555.80	283.00

Table S5. Pure component properties selected for joint property variation sensitivity analysis.

Compounds	Lower bound			Upper bound		
	T_C (K)	P_C (bar)	ω	T_C (K)	P_C (bar)	ω
n-C_{10}	618.05	21.02	0.485	618.05	21.02	0.485
n-C_{15}	706.88	14.44	0.684	706.88	14.44	0.684
n-C_{17}	735.71	13.22	0.750	735.71	13.22	0.750
n-C_{20}	768.22	10.77	0.868	768.22	10.77	0.868
n-C_{24}	788.52	8.83	0.995	808.82	10.36	1.070
n-C_{28}	818.07	7.15	1.138	835.40	8.70	1.188
n-C_{30}	830.09	6.49	1.194	848.33	8.12	1.277
n-C_{36}	863.73	4.82	1.374	880.82	6.87	1.506
n-C_{40}	882.06	3.93	1.487	898.87	6.00	1.701
n-C_{50}	907.81	2.39	1.748	936.43	5.09	2.132
benzene	562.02	48.94	0.210	562.02	48.94	0.210
toluene	591.89	41.27	0.265	591.89	41.27	0.265
ethylbenzene	617.12	36.16	0.304	617.12	36.16	0.304
n-propylbenzene	638.29	32.01	0.345	638.29	32.01	0.345
naphthalene	748.33	40.40	0.303	748.33	40.40	0.303
1-methylnaphthalene	770.71	35.41	0.347	770.71	35.41	0.347
phenanthrene	866.00	24.89	0.434	866.00	24.89	0.434
cyclopentane	511.74	45.15	0.195	511.74	45.15	0.195
cyclohexane	553.40	40.70	0.210	553.40	40.70	0.210
methylcyclohexane	572.31	34.81	0.235	572.31	34.81	0.235
ethylcyclohexane	606.90	32.86	0.294	606.90	32.86	0.294
n-propycyclohexyl	630.80	28.69	0.327	630.80	28.69	0.327
bicyclohexyl	742.00	29.18	0.382	742.00	29.18	0.382
cis-decahydronaphthalene	702.22	32.02	0.286	702.22	32.02	0.286
perhydrophenanthrene	795.00	26.34	0.409	795.00	26.34	0.409